VOLUME 55 [J. CELL. AND COMP. PHYSIOL.] NUMBER 1

JOURNAL OF CELLULAR AND COMPARATIVE PHYSIOLOGY

FEBRUARY 1960

PUBLISHED BIMONTHLY BY
THE WISTAR INSTITUTE OF ANATOMY AND BIOLOGY
THIRTY-SIXTH STREET AT SPRUCE, PHILADELPHIA 4, PA.

Second class postage paid at Philadelphia, Pa.

Publications of The Wistar Institute

THE JOURNAL OF MORPHOLOGY

Devoted to the publication of original research on animal morphology, including cytology, protozoology, and the embryology of vertebrates and invertebrates. Articles do not usually exceed 50 pages in length.

Issued bimonthly, 2 vols. annually: $20.00 Domestic, $21.00 Foreign, per year.

THE JOURNAL OF COMPARATIVE NEUROLOGY

Publishes the results of original investigations on the comparative anatomy and physiology of the nervous system.

Issued bimonthly, 2 vols. annually: $20.00 Domestic, $21.00 Foreign, per year.

THE AMERICAN JOURNAL OF ANATOMY

Publishes the results of comprehensive investigations in vertebrate anatomy — descriptive, analytical, experimental.

Issued bimonthly, 2 vols. annually: $20.00 Domestic, $21.00 Foreign, per year.

THE ANATOMICAL RECORD

Organ of the American Association of Anatomists and the American Society of Zoologists

For the prompt publication of concise original articles on vertebrate anatomy, preliminary reports; technical notes; critical notes of interest to anatomists and short reviews of noteworthy publications.

Issued monthly, 3 vols. annually: $30.00 Domestic, $32.00 Foreign, per year.

THE JOURNAL OF EXPERIMENTAL ZOOLOGY

Publishes papers embodying the results of original researches of an experimental or analytical nature in the field of zoology.

Issued 9 times a year, 3 vols. annually: $30.00 Domestic, $32.00 Foreign, per year.

AMERICAN JOURNAL OF PHYSICAL ANTHROPOLOGY

Official Organ of the American Association of Physical Anthropologists

Publishes original articles on comparative human morphology and physiology as well as on the history of this branch of science and the techniques used therein. In addition, it gives comprehensive reviews of books and papers, a bibliography of current publications, abstracts and proceedings of the American Association of Physical Anthropologists, and informal communications.

Issued quarterly, 1 vol. annually: $10.00 Domestic, $11.00 Foreign, per year.

JOURNAL OF CELLULAR AND COMPARATIVE PHYSIOLOGY

Publishes papers which embody the results of original research of a quantitative or analytical nature in general and comparative physiology, including both their physical and chemical aspects.

Issued bimonthly, 2 vols. annually: $20.00 Domestic, $21.00 Foreign, per year.

THE JOURNAL OF NUTRITION

Official Organ of the American Institute of Nutrition

Publishes original research bearing on the nutrition of any organism. Supplements to the regular monthly issues are published irregularly as required by the editorial board.

Issued monthly, 3 vols. annually: $22.50 Domestic, $24.00 Foreign, per year.

THE AMERICAN ANATOMICAL MEMOIRS

Publishes original monographs based on experimental or descriptive investigations in the field of anatomy which are too extensive to appear in the current periodicals. Each number contains only one monograph. List of monographs already published, with prices, sent on application.

These publications enjoy the largest circulation of any similar journals published.

Send Subscriptions and Business Correspondence to

THE WISTAR INSTITUTE OF ANATOMY AND BIOLOGY

THIRTY-SIXTH STREET AT SPRUCE, PHILADELPHIA 4, PA.

SYMPOSIUM ON ENZYME REACTION MECHANISMS

Sponsored by

THE BIOLOGY DIVISION

OAK RIDGE NATIONAL LABORATORY

The papers originating from this Symposium are made available to scientific circles for the first time as a Supplement issue to the JOURNAL OF CELLULAR AND COMPARATIVE PHYSIOLOGY. The publication is identified as *Supplement 1, volume 54, Journal of Cellular and Comparative Physiology,* is available without added cost to subscribers for 1959 volumes 53–54 and if requested with new subscription orders for the 1960 volumes 55–56. Single copies of Supplement issues are not for sale but are available only to subscribers of the journal. *Information concerning reprints may be obtained by addressing The Biology Division, Oak Ridge National Laboratory.*

CONTENTS

Edition limited, no single copy sales — Subscribe now

THE PRESS OF THE WISTAR INSTITUTE
3631 SPRUCE STREET
PHILADELPHIA 4, PA.

Please send copy of Supplement 1 to volume 54 and enter my subscription to JOURNAL OF CELLULAR AND COMPARATIVE PHYSIOLOGY, 1959 volumes 53–54 and/or 1960 volumes 55–56 to include other supplements as published in 1960.

NAME

STREET

CITY ZONE STATE

Annual subscription price in U.S., $20.00; all other countries, $21.00

Original first edition back issues of

Journal of Cellular and Comparative PHYSIOLOGY

Complete volumes	*Year*	*Each volume*
1	1932	$15.00
2	1932–33	15.00
4	1933–34	10.00
5	1934–35	10.00
6	1935	10.00
7	1935–36	10.00
8	1936	10.00
30	1947	5.00
34	1948	7.50
40	1952	7.50
41	1953	7.50
42	1953	7.50
44	1954	7.50
46	1955	7.50
48	1956	7.50
50	1957	7.50
51	1958	10.00
52	1958	10.00

Incomplete volumes	*Year*	*Each number*
3, Nos. 1, 3, 4	1933	$5.00
11, No. 1	1938	2.75
12, Nos. 2, 3	1938	3.50
14, Nos. 2, 3	1939	2.75
18, No. 3	1941	2.00
28, No. 3	1946	2.00
29, Nos. 2, 3	1947	2.00
36, No. 1	1950	3.00
39, No. 1	1952	3.00
43, No. 1	1954	3.00
45, No. 3	1955	3.00
47, No. 1	1956	3.00
49, No. 3	1957	3.00

Note: Unlisted volumes and single numbers are now out of print.

1959 volumes 53–54
6 issues, $20.00

Prices subject to change without notice. Availability depends upon prior sales (issued October 15, 1959)

THE PRESS OF THE WISTAR INSTITUTE
3631 SPRUCE STREET
PHILADELPHIA 4, PA.

You may send the following issues from above listing. Complete volumes

_____

Incomplete volumes _____

_____

NAME

_____

STREET

_____

CITY ZONE STATE

Physiology of Induced Catalase Synthesis in Rhodopseudomonas spheroides

RODERICK K. CLAYTON
Biology Division, Oak Ridge National Laboratory,[1] Oak Ridge, Tennessee

Synthesis of catalase is induced in *Rhodopseudomonas spheroides* by aeration (Clayton, '60a). It will be shown in this paper that H_2O_2 is a more effective inducer than O_2, and that induction by air involves H_2O_2 as an intermediate. Some aspects of the kinetics of induction will be described. Evidence will be presented that strong illumination causes a conversion of O_2 to H_2O_2 in *Rps. spheroides;* this phenomenon will be discussed in relation to the photodynamic killing of the blue-green mutant of *Rps. spheroides* (Sistrom et al., '56).

METHODS

Rps. spheroides, strain 2.4.1, was grown anaerobically in the light in a synthetic medium described earlier (Clayton, '60a). Cultures in exponential growth [0.3–1.4 mg (dry mass)/ml] were used directly for induction experiments. Stationary cultures, limited by depletion of carbon sources, were diluted fourfold with distilled water before use (final density 0.5 mg/ml) to improve their optical transmission. These will henceforth be called young and mature cultures, respectively. The generation time of a young culture was about 5 hours, so that in an experiment lasting 1 hour the cell density did not increase greatly.

To begin an experiment the suspensions were dispensed into 30-ml test tubes, illuminated, and bubbled with oxygen-free nitrogen. Chemicals could then be added and samples withdrawn for assay at intervals. Oxygen generated by the addition of H_2O_2 was swept out rapidly by the nitrogen in this arrangement. A trace of air did enter the open test tubes, but its effect could be eliminated or taken into account (see the section *"Light as a variable in the system"*). Illumination was altered by changing the voltage applied to two 150-watt, 115-volt lamps situated 4 inches apart and 6 inches from the test tubes. Unless otherwise specified, the lamps were operated at 22 volts with mature cultures and at 70 volts with young cultures. Temperatures of the suspensions ranged from 25° to 28°C during an experiment.

Catalase was assayed by the iodometric titration described earlier (Clayton, '59). Peroxidase-like activity (Clayton, '60b), which becomes important at H_2O_2 concentrations less than about 100 μM, was measured by the luminol assay as described by Dolin ('59). No other peroxide-destroying agents are found in *Rps. spheroides* (Clayton, '60b).

Cell suspension density was measured turbidimetrically at 680 mμ.

RESULTS

Effectiveness of several inducers

It was noted in an earlier paper (Clayton, '60a) that air is a much more effective inducer of catalase synthesis in mature cultures of *Rps. spheroides* than in young cultures. The responses of young and mature cultures to aeration and also to the addition of H_2O_2 are shown in figure 1, in which catalase content is plotted against time. "Air" denotes continuous aeration; H_2O_2 was added as a single dose to an initial concentration of 40 μM. This amount was established to be saturating for induced catalase synthesis when given as a single addition.

Aeration produced an O_2 concentration of about 240 μM in the suspension. H_2O_2, present initially at a concentration of 40 μM, had a measured half life of less than 1 minute in the suspension. H_2O_2 is therefore a much more effective inducer than O_2.

[1] Operated by Union Carbide Corporation for the United States Atomic Energy Commission.

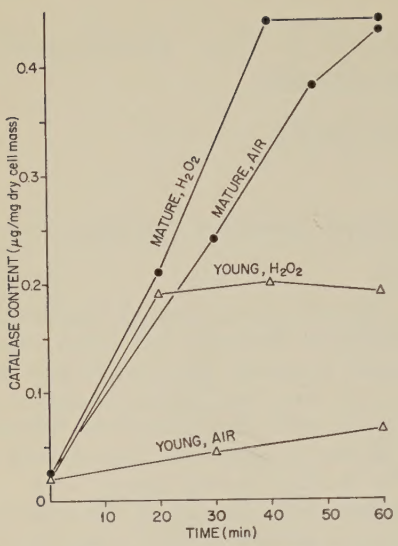

Fig. 1 Induced catalase synthesis in young and mature cultures of *Rps. spheroides*, using air and H_2O_2 as inducers. "Air" denotes continuous aeration from $t = 0$. H_2O_2 was added to a concentration of 40 μM at $t = 0$.

The relatively poor inducibility of young cultures is striking when air is the inducer. With H_2O_2 as the inducer, the difference between young and mature cultures is much less pronounced.

Succinic peroxyacid,[2] one of the most effective radiomimetic organoperoxides, is not a substrate of catalase and is ineffective as an inducer. Methyl hydrogen peroxide at a concentration of 700 μM induced the same amount of catalase synthesis as 40 μM H_2O_2. This could easily have been caused, however, by H_2O_2 present as an impurity in the CH_3OOH.

Light as a variable in the system

The induced synthesis of catalase in *Rps. spheroides* involves *de novo* synthesis of protein (Clayton, '60c) and hence requires energy. Under vigorous aeration this energy can be provided through respiration, but a more rapid induced synthesis can be attained when light furnishes the energy through photosynthesis. Within limits, the rates of induced catalase synthesis and growth show the same sort of light-saturation curve. Departures from this parallelism were found, however, under certain conditions of illumination and exposure to air. Experiments illustrating these departures were performed with mature cultures; several inducing regimes were used at various light intensities. For measurement of growth rate, the cultures were diluted with growth medium instead of water.

Results are shown in figure 2, where the catalase synthesized during 1 hour is plotted against light intensity (the successive lamp voltages on the abscissa correspond very roughly to threefold increases in illumination). Maximal catalase synthesis was attained by adding H_2O_2 continuously at a rate of 12.5 μM/minute (curve A); the rate of synthesis was then nearly independent of light intensity over

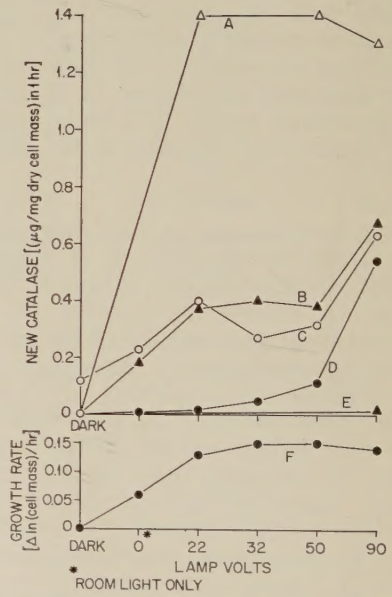

Fig. 2 Effect of light intensity on induced catalase synthesis in mature *Rps. spheroides*. Each step of the abscissa represents crudely a threefold increase in illumination. For curves A-E the ordinate is new catalase synthesized in one hour. Curve A, H_2O_2 added at a rate of 12.5 μM/minute to a suspension bubbled with N_2; B, H_2O_2 added in a single dose to a concentration of 20 μM; C, suspension bubbled with air instead of N_2; D, suspension bubbled with N_2 + about 1% air; E, suspension kept in a sealed tube for strict anaerobicity. The ordinate of curve F is growth rate measured as the increase in ln (cell mass) during one hour. For measurement of growth the mature culture was diluted with growth medium and bubbled with N_2.

[2] Donated by Dr. P. Demerseman.

the range 22–90 volt (lamp voltage). Growth rate (curve F) was correspondingly light-saturated over this range. Suspensions bubbled with N_2 or with N_2 + 1% air (curve D) showed negligible induced catalase synthesis at a light intensity that was just saturating for growth (22 volts) but considerable induction under strong illumination (90 volts). In a rigorously anaerobic suspension[3] (curve E), there was no induction at the highest light intensity. Strong light therefore potentiates the inducing effect of traces of O_2 (entering at the top of a tube bubbled with N_2), but does not act by itself as an inducer. The inducing effect of H_2O_2 added in a single 20 μM dose (curve B) parallels the growth curve, with the potentiating action ofstrong light superimposed. The response to continuous aeration (curve C) is somewhat different. In the dark, respiration provides energy for some induced catalase synthesis. As the light intensity is raised, induced synthesis increases and then declines as the saturating intensity for growth is exceeded. The curve rises again when the potentiating action of strong light becomes effective. The decline in the effectiveness of air at an intermediate light intensity can be related to the fact that light in this range suppresses respiration in *Rps. spheroides* (Clayton, '55, '60a). Thus, if O_2 acts as an inducer by generating intracellular H_2O_2 (see the next section), its effectiveness will be reduced when respiration is retarded.

On the basis of these results, the inducing effects of H_2O_2 and air could be studied in mature cultures, without interference from the potentiating action of strong light, at a lamp setting of 22 volts. The "trace-O_2 plus strong light" effect could be studied in N_2-bubbled suspensions with the lamp at 90 volts. The foregoing applies to cultures adjusted to a cell suspension density of 0.5 mg/ml.

Essentially similar results were obtained with young cultures of density 0.5 mg/ml, except that the responses to aeration and to "trace-O_2 plus strong light" were relatively much smaller. These differences will be discussed in a later section. In the young cultures, growth rate was saturated at a lamp setting of 70 volts.

Light absorbed by bacteriochlorophyll is effective in potentiating the induction by traces of O_2. This was demonstrated with filtered light ranging from 710 to 1150 mμ (Corning no. 2600 filter) and also with sodium light of wave length 589 mμ.

Peroxide as an intermediate in the induction by oxygen

Since inducers of enzyme synthesis are usually substrates of the corresponding enzymes, it is plausible to suppose that air induces catalase synthesis in *Rps. spheroides* through its intracellular conversion to H_2O_2. This view is strengthened by the fact that H_2O_2 is a much more effective inducer, mole for mole, than O_2. The reduced effectiveness of air at a light intensity that inhibits respiration is also suggestive. In the light of this hypothesis the inducing action of air should be enhanced by substances that interfere with the destruction of intracellular peroxide. Chantrenne ('55) has shown that sodium azide, which inhibits catalase, augments the effectiveness of air as an inducer of catalase synthesis in yeast.

At pH 7, 3 μM azide inhibits the catalase of *Rps. spheroides* more than 90%, but growth over a period of three hours is not affected. Azide at this concentration should therefore potentiate the inducing action of H_2O_2 to the extent that inactivating the catalase prolongs the presence of the H_2O_2. The same potentiation should occur when O_2 is the inducer if O_2 acts through its conversion to H_2O_2.

Rps. spheroides contains, in addition to catalase, a peroxidase-like activity insensitive to 3 μM azide (Clayton, '60b). This "peroxidase" activity obeys Michaelis-Menten kinetics: the rate at which it destroys H_2O_2 is proportional to peroxide concentration up to about 10 μM, is half-maximal at 28 μM H_2O_2, and is nearly independent of H_2O_2 concentration above about 100 μM. The "peroxidase" activity of *Rps. spheroides* is not changed by exposure to O_2 or H_2O_2, in contrast to the in-

[3] Rigorous anaerobicity was achieved by growing, diluting, and illuminating a culture in a sealed tube having no gas phase. The growing culture and the diluting water were separated by a Saran membrane that was ruptured at the start of the experiment.

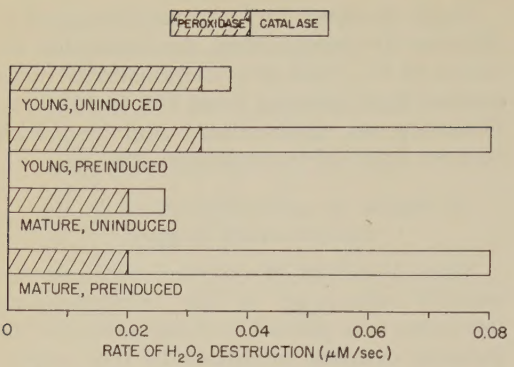

Fig. 3 Relative importance of catalase and a peroxidase-like activity in *Rps. spheroides* for the destruction of H_2O_2, at concentrations of H_2O_2 less than 10 μM. The abscissa is the rate of peroxide destruction in a cell suspension of density 1 mg (dry cell mass)/ml containing 1 μM H_2O_2. Preinduced cultures had been treated with H_2O_2 sufficient to induce a tenfold increase in catalase content.

ducible catalase. The relative importance of "peroxidase" and catalase in dealing with H_2O_2 can therefore be altered by inducing catalase synthesis to different degrees. The relative contributions of "peroxidase" and catalase activities to the destruction of peroxide, at H_2O_2 concentrations less than 10 μM, are shown in figure 3 for young and mature cultures uninduced and induced to a tenfold increase in catalase content. In uninduced cultures, catalase contributes relatively little to the destruction of H_2O_2; any effect of azide should therefore be correspondingly slight.

During exploration of the effect of azide on the induction of catalase synthesis in *Rps. spheroides*, cultures were treated with 3 μM NaN_3 and the inducer (air or peroxide) was introduced 10 minutes later. After one hour the cultures were washed twice to remove the azide, and their catalase content was assayed. Control cultures received no azide. Preinduced cultures, of higher initial catalase content, were obtained by adding small amounts of H_2O_2 5 hours before the start of the experiment. In every case the catalase and "peroxidase" activities were assayed at the start of the experiment. Results of these experiments are shown in table 1. The second column gives the ratio of catalase activity to total H_2O_2-destroying activity, and the third column gives the corresponding effect of azide in prolonging the presence of H_2O_2 by inactivating the catalase. The last column gives the ratio of newly synthesized catalase in the presence of azide to that in the absence of azide.

Regardless of the inducer (H_2O_2, air, or trace-O_2 plus strong light), azide enhances the induced synthesis of catalase. The ex-

TABLE 1

Effect of sodium azide (3 μM) on the induced synthesis of catalase in Rhodopseudomonas spheroides[1]

Type of culture	Ratio: Catalase activity/ total activity[2]	Ratio: Half life of H_2O_2 (with azide)/ half life of H_2O_2 (without azide)	Inducer	Ratio: New catalase (with azide)/ new catalase (without azide)
Young, uninduced	0.135	1.16	Continuous aeration	1.14
Young, preinduced	0.43	1.75	Continuous aeration	1.36
			20 μM H_2O_2	1.38
Mature, uninduced	0.23	1.30	None	No induced catalase
			5 minutes aeration	1.37
			6 μM H_2O_2	1.17
			Trace-O_2; lamp at 70 volts	1.35
Mature, preinduced slightly	0.39	1.64	10 minutes aeration	1.67
Mature, preinduced	0.69	3.23	10 minutes aeration	2.38
			6 μM H_2O_2	2.44
			Trace-O_2; lamp at 70 volts	1.79

[1] NaN_3 (3 μM) was added to young and mature cultures of *Rps. spheroides*, uninduced or preinduced to a higher catalase content. After 10 minutes, the inducer was added; catalase was assayed initially and after one hour. The second column shows the ratio of catalase activity to total peroxide-destroying activity (catalase plus a peroxidase-like activity) in cells without azide. The third column shows the corresponding effect of 3 μM azide (which inactivates catalase selectively) on the rate of peroxide destruction.

[2] Catalase plus "peroxidase."

tent of this enhancement is in good agreement with the extent to which azide prolongs the presence of H_2O_2 by inactivating catalase. This correlation provides sound evidence that H_2O_2 is an intermediate in the induction of catalase synthesis in *Rps. spheroides* when air, or trace-O_2 plus strong light, is the inducer.

On the basis of this conclusion, strong light potentiates the inducing action of traces of O_2 by accelerating the conversion of O_2 to H_2O_2. Light absorbed by bacteriochlorophyll is effective in this respect (see "*Light as a variable in the system*").

Sodium azide is not itself an inducer of catalase synthesis in *Rps. spheroides* (see row 4, table 1).

Steady-state kinetics of induced catalase synthesis

When H_2O_2 is added continuously to a suspension of *Rps. spheroides*, an approximation to a steady state is achieved in which the H_2O_2 concentration is nearly constant. The rate of induced catalase synthesis can then be measured as a function of H_2O_2 concentration.

At concentrations of H_2O_2 less than about 10 μM, the rate of destruction of H_2O_2 by *Rps. spheroides* is proportional to the peroxide concentration; it is equal to $(k_c + k_p)$ $[H_2O_2]$, where k_c and k_p represent the activities of catalase and "peroxidase," respectively (Clayton, '60b). If H_2O_2 is added continuously at a rate k_0 μM sec^{-1}, and is destroyed as rapidly as it is added (steady state), then

$$k_0 = (k_c + k_p)\,[H_2O_2], \text{ or } [H_2O_2] = \frac{k_0}{k_c + k_p}. \quad (1)$$

In this equation k_c and k_p are expressed in sec^{-1}, the units of k_0 are μM sec^{-1}, and so $[H_2O_2]$ is in μM. For a true steady state, k_0 and $k_c + k_p$ should be constant. In these experiments k_0 and k_p were constant, but k_c increased gradually as new catalase was synthesized. At the start of an experiment, however, k_p was three to 10 times as great as k_c. Consequently, the sum of k_c and k_p varied so slowly that, for all practical purposes, a steady state was attained.

These experiments were performed, then, by adding H_2O_2 to an illuminated suspension of *Rps. spheroides* at a constant rate and assaying the activities of catalase and "peroxidase" over a period of about two hours. The rate of peroxide addition ranged from 0.001 to 3 μM/sec, producing steady-state H_2O_2 concentrations from about 0.05 to 30 μM. The data were processed to yield rate of induced catalase synthesis as a function of H_2O_2 concentration; results are shown in figure 4 (the meaning of the lines marked "A" and "L" will be discussed later in this section).

Both young and mature cultures attained a maximum rate of catalase synthesis at 1–2 μM H_2O_2; higher concentrations were inhibitory. The maximum rate of synthesis amounted to about 6 molecules of new catalase per cell per minute. The maximum response of a young culture is somewhat greater than that of a mature culture.

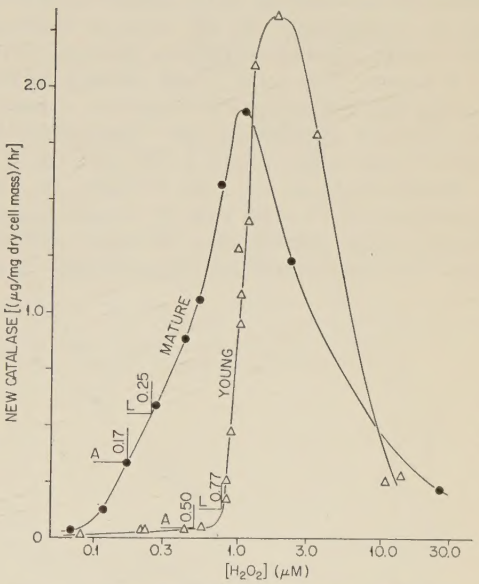

Fig. 4 Rate of catalase synthesis induced by H_2O_2 in young and mature cultures of *Rps. spheroides*, as a function of H_2O_2 concentration. H_2O_2 was added continuously to an illuminated cell suspension to establish a steady state. H_2O_2 concentration is plotted logarithmically. Rates of catalase synthesis induced by aeration are shown by the horizontal lines labeled A. The H_2O_2 concentration which is equivalent to continuous aeration is obtained from the intersection of line "A" with the appropriate curve ("mature" or "young"). This equivalent H_2O_2 concentration is written along a vertical line meeting line "A" at the curve. The inducing effect of a trace of O_2 plus strong illumination is shown similarly, the horizontal lines being labeled "L."

The relative insensitivity of young cultures to aeration and to small single doses of H_2O_2 therefore has nothing to do with the cells' inability to make enzyme. The difference between young and mature cultures is related, rather, to the kinetics of catalase synthesis at low peroxide concentrations: the response declines abruptly below 1 μM H_2O_2 in young cultures but not in mature ones.

The mature cultures in all these experiments had been diluted fourfold with H_2O; the possibility must therefore be considered that, in a prolonged experiment, the rate of catalase synthesis became limited through exhaustion of endogenous reserves of amino acids. Figure 5 shows that this limitation did not actually become serious. Here the time course of catalase synthesis is plotted for mature and young cultures exposed to H_2O_2 added at a rate of 15 μM/minute. In the mature culture, the rate of catalase synthesis declined little in 6 hours. The more rapid decline in the young culture occurred when, as a result of catalase synthesis, the concentration of H_2O_2 fell below about 1 μM (see fig. 4).

Since H_2O_2 is an intermediate in the induction by O_2, the rate of catalase synthesis under continuous aeration will reflect the corresponding intracellular H_2O_2 concentration. This concentration will depend on the rate at which H_2O_2 is generated and destroyed and hence on the enzymic constitution of the cells. For the cultures used in these experiments, the rates of catalase synthesis after 30 minutes of aeration are shown by horizontal lines marked "A" in figure 4. The corresponding intracellular H_2O_2 concentrations, deduced from the curves, are 0.17 μM for a mature culture and 0.50 μM for a young culture. The values of $k_c + k_p$ [see eq. (1)] were 0.050 and 0.021 for the mature and young cultures, respectively. Then from equation (1) the rate at which H_2O_2 was generated, k_0, was 0.050×0.17 or 0.0085 μM/sec in the mature culture and 0.0105 μM/sec in the young culture. Cell suspension densities were 0.5 mg/ml. For the reaction $O_2 + 2H_2O \rightarrow 2H_2O_2$, the rates of oxygen uptake corresponding to these rates of peroxide formation were 0.68 and 0.84 μl mg^{-1} $hour^{-1}$ (mature and young cultures, respectively). The Q_{O_2} observed manometrically in such cultures ranged from about 50 to 100 μl mg^{-1} $hour^{-1}$; on the basis of these calculations about 1% of the assimilated O_2 appeared as free H_2O_2.

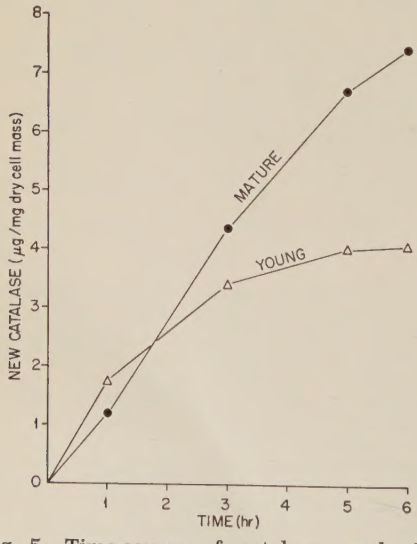

Fig. 5 Time-course of catalase synthesis in young and mature cultures of *Rps. spheroides*, induced by continuous addition of H_2O_2 at a rate of 15 μM/minute.

The response to a trace of O_2 plus strong light is shown by the lines marked "L" in figure 4; the corresponding H_2O_2 concentrations for mature and young cultures are 0.25 and 0.77 μM. This accelerated formation of H_2O_2 is fully saturated at an O_2 concentration of about 3 μM, corresponding to saturation with $N_2 + 1\%$ air.

DISCUSSION

The foregoing data have indicated that, in strong light, O_2 is converted with high efficiency to H_2O_2 in *Rps. spheroides*. Light absorbed by bacteriochlorophyll is effective; the phenomenon appears at an intensity somewhat higher than that which is saturating for growth (i.e., for photosynthesis). This process is by definition a photooxidation sensitized by bacteriochlorophyll. Another photooxidative effect mediated by bacteriochlorophyll, is the killing of the blue-green mutant of *Rps. spheroides* (Sistrom et al., '56). These two phenomena may well be different manifestations of the same process; there is considerable evidence (Blum, '41) that

photosensitized oxidations of biological materials involve an efficient conversion of O_2 to H_2O_2. Comparative studies of the blue-green mutant and wild type *Rps. spheroides* should reveal whatever relation exists between photooxidative killing and H_2O_2 formation.

The data of this paper indicate that H_2O_2 is a highly effective inducer of catalase synthesis in *Rps. spheroides*, whereas organic peroxides (e.g., methyl hydrogen peroxide and succinic peroxy-acid) are nearly or completely ineffective. Induction of catalase synthesis in *Rps. spheroides* seems therefore to be a sensitive and highly specific test for H_2O_2. This biological assay may prove useful in distinguishing between H_2O_2 and organic peroxides formed when organic systems are exposed to ionizing radiations.

SUMMARY

In growing and in stationary cultures of *Rps. spheroides*, synthesis of catalase is induced at a maximal rate (about 6 molecules/cell/minute) by H_2O_2 at a steady-state concentration of 1–2 μM. In growing cultures the rate of induced synthesis declines abruptly as the steady-state H_2O_2 concentration falls below 1 μM; the decline in rate is more gradual in stationary cultures. The effect of NaN_3 shows that H_2O_2 is an intermediate when O_2 is the inducer. Saturation with air [$(O_2) = 240$ μM] produces the same effect as a sustained H_2O_2 concentration of 0.17–0.5 μM. Methyl hydrogen peroxide and succinic peroxyacid have little or no effect as inducers.

Strong light potentiates the inducing effect of traces of O_2; 3 μM O_2 in strong light is equivalent to 0.25–0.77 μM H_2O_2. This effect is mediated by bacteriochlorophyll-absorbed light and involves H_2O_2 as an intermediate.

LITERATURE CITED

Blum, H. 1941 Photodynamic Action and Diseases Caused by Light. Reinhold Publishing Corp., New York, pp. 95–97.

Chantrenne, H. 1955 Effets d'un inhibiteur de la catalase sur la formation induite de cet enzyme chez la levure. Biochim. et Biophys. Acta, *16:* 410–417.

Clayton, R. K. 1955 Photosynthesis and respiration in Rhodospirillum rubrum. Arch. Mikrobiol., *22:* 180–194.

——— 1959 Permeability barriers and the assay of catalase in intact cells. Biochim. et Biophys. Acta, *36:* 35–39.

——— 1960a The induced synthesis of catalase in *Rhodopseudomonas spheroides*. Ibid., *37:* 502–512.

——— 1960b Kinetics of H_2O_2 destruction in *Rhodopseudomonas spheroides*: roles of catalase and other enzymes. Ibid., *40:* 165–167.

——— 1960c Protein synthesis in the induced formation of catalase in *Rhodopseudomonas spheroides*. J. Biol. Chem., *235:* 405–407.

Dolin, M. I. 1959 Oxidation of reduced diphosphopyridine nucleotide by *Clostridium perfringens*. J. Bacteriol., *77:* 383–392.

Sistrom, W. R., M. Griffiths and R. Y. Stanier 1956 The biology of a photosynthetic bacterium which lacks colored carotenoids. J. Cell. and Comp. Physiol., *48:* 473–515.

An Intermediate Stage in the H_2O_2-Induced Synthesis of Catalase in Rhodopseudomonas spheroides

RODERICK K. CLAYTON
Biology Division, Oak Ridge National Laboratory,[1] Oak Ridge, Tennessee

Catalase synthesis is induced by H_2O_2 in *Rhodopseudomonas spheroides*. Some aspects of the kinetics of this phenomenon have been described in a recent paper (Clayton, '60c); it was shown that H_2O_2 is also an intermediate when O_2 is used as the inducer. Evidence will be presented here that H_2O_2 generates, in *Rps. spheroides*, an internal substance or condition that promotes catalase synthesis. The formation and stability of this internal inducer will be described.

METHODS

Rps. spheroides, strain 2.4.1, was cultivated anaerobically in the light as described earlier (Clayton, '60a). Stationary-phase cultures, of density 2 mg (dry cell mass)/ml, were used for all experiments unless otherwise specified. The cultures were placed in vessels that could be illuminated (to provide energy through photosynthesis) and bubbled with O_2-free N_2. H_2O_2 was added to a suitable initial concentration and the time course of catalase synthesis was observed.

Cell suspension density, catalase content, and a peroxidase-like activity were assayed as described in earlier papers (Clayton, '60a,b,c). The assays for catalase and "peroxidase" involved measurement of H_2O_2 destruction in cell suspensions over a wide range (3–10 mM) of H_2O_2 concentration. On the basis of these assays, the rate of destruction of H_2O_2 in the actual experimental situations could be computed with a precision of about $\pm 10\%$.

RESULTS

The time course of catalase synthesis after a single addition of H_2O_2

The time course of catalase synthesis in *Rps. spheroides*, after addition of H_2O_2 to an initial concentration of 4–40 μM, is shown in figure 1. The cultures, some undiluted and others diluted fourfold with H_2O, were illuminated and bubbled with N_2 throughout the experiment. The essential features of the curves in figure 1 are a lag of 7 minutes followed by a period of catalase synthesis lasting about 30 minutes. The time course was independent of the initial H_2O_2 concentration in the range 4–40 μM, and unaltered by a fourfold change in cell suspension density.

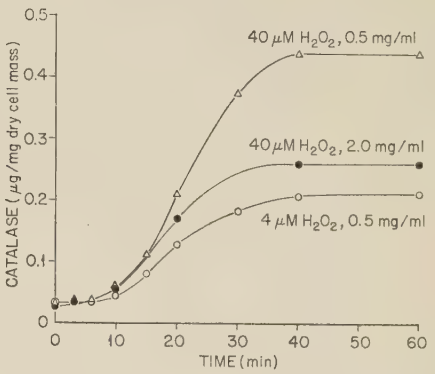

Fig. 1 Time-course of catalase synthesis in *Rps. spheroides*, induced by H_2O_2 added as a single dose. The doses (initial H_2O_2 concentration) and cell suspension densities (mg dry cell mass per ml) are written along the curves. Suspensions were illuminated and bubbled with N_2 during the experiment.

Since, in the undiluted cultures, the half life of H_2O_2 was 12 sec[1], after about two minutes the H_2O_2 concentration was 0.04 μM or less. A sustained H_2O_2 concentration of 0.04 μM causes no measurable induction (Clayton, '60c); the H_2O_2 was therefore effectively destroyed within two minutes. The response, then, is initiated by H_2O_2 but is consummated largely after the H_2O_2 has been destroyed. Exposure to H_2O_2 has generated in the cells a state or a substance

[1] Operated by Union Carbide Corporation for the United States Atomic Energy Commission.

("internal inducer," to be denoted I_i) that promotes the synthesis of catalase. After about 30 minutes, I_i is no longer effective. A larger initial dose of H_2O_2 produces more I_i, or more effective I_i. But, the *time* during which I_i can promote catalase synthesis does not depend on the amount or on the lifetime of the H_2O_2 added initially.

The stability of internal inducer at 0°C

The inducible state that follows the addition of H_2O_2 to *Rps. spheroides* can be preserved for many hours by placing the cells in darkness at 0°C. At room temperature (25°C), I_i is dissipated more quickly. The stability of I_i was investigated as follows: A cell suspension was illuminated and bubbled with N_2. H_2O_2 was added, at the start of the experiment, to a concentration of 60 μM. After 5 minutes in the light at 25°C under N_2, the suspension was dispensed into 3-ml glass-stoppered tubes leaving no air inside. The 5 minutes of illumination was designed to permit nearly complete generation of I_i (as we shall see, this process requires energy) and to flush out most of the O_2 evolved by the destruction of H_2O_2. Some of the tubes were placed immediately in the light at 25°C; others were placed in darkness, at 25°C or in ice-water. After some minutes or hours, the tubes kept in darkness were placed in the light at 25°C. At appropriate times, tubes were opened and assayed for catalase.

Results of a typical experiment are shown in figure 2. In the tubes placed directly in the light at 25°C (curve A), catalase synthesis proceeded as described earlier (cf. fig. 1). In suspensions kept in darkness at 25°C after the first 5 minutes (curve B), the time course was similar but the response was much smaller. Synthesis of catalase in these suspensions was limited because energy was not entering the system. If the initial 5 minutes of illumination was omitted, synthesis of catalase was negligible in darkened suspensions at 25°C. Curve C shows that some synthesis of catalase occurs in suspensions returned to the light after 25 minutes of darkness. The magnitude of this response defines the amount[2] of I_i remaining at the end of the 25 minutes of darkness; on this basis the ratio of *b* to *a* (see figure 2) gives the relative amounts of I_i after and before the dark period. Curve D shows that almost no catalase is formed in the suspen-

[2] For convenience, I_i will be referred to as a substance whose amount determines, under specified conditions, the amount of subsequent catalase synthesis. I_i may represent a change in configuration of the system rather than a substance. Its amount or extent may govern the amount of new catalase in a very indirect way.

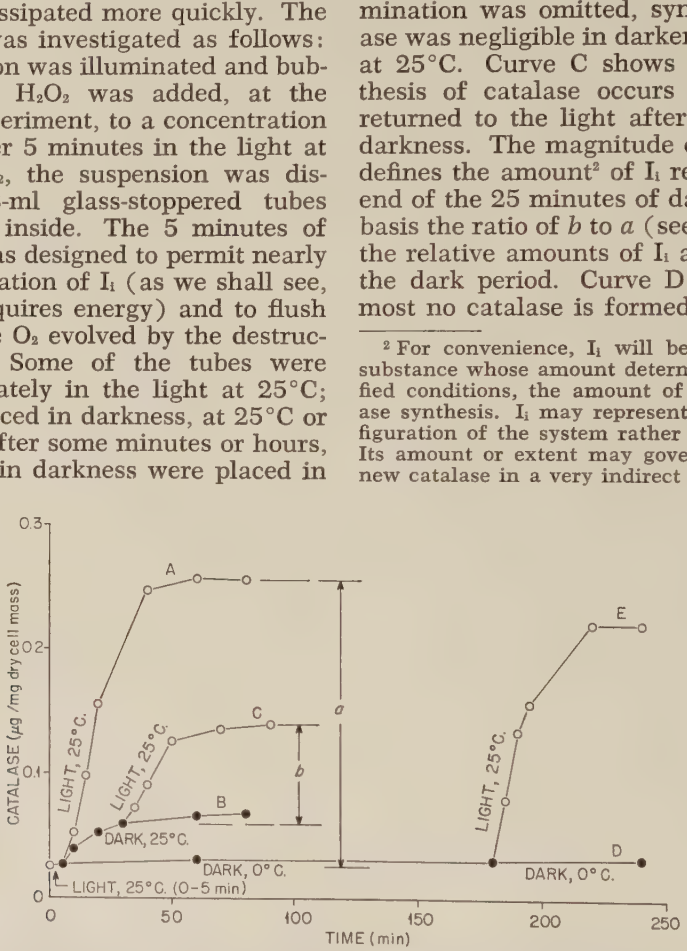

Fig. 2 Persistence of the induced state for catalase synthesis in *Rps. spheroides* after addition of H_2O_2. Cultures were treated with H_2O_2 (60 μM) at t = 0; induced synthesis of catalase then required light as a source of energy. All suspensions were illuminated at 25°C for the first 5 minutes. Some were then left in the light at 25°C (curve A); others were placed in darkness at 25° (curve B) or at 0° (curve D). Of these darkened samples, some were later returned to the light at 25° (curves C and E). Increments of catalase content, upon illumination, are shown by the intervals *a* and *b* for the samples of curves A and C, respectively.

sions kept in darkness at 0°C. When these suspensions are restored to light at 25°C (curve E), a synthesis of catalase occurs that nearly equals the response of suspensions illuminated from the start. In this example the amount of I_1 was about 80% of its initial value after three hours of darkness at 0°C.

The experiment exemplified by curves A, D, and E of figure 2 was repeated to determine the amount of I_1 remaining after various intervals of darkness at 0°C. Results are shown in table 1 under the heading of "mature cultures." Even after 24 hours, almost half of the original amount of I_1 remained. Control suspensions, that received no H_2O_2, synthesized negligible amounts of catalase.

TABLE 1

Stability of the induced state for catalase synthesis in Rps. spheroides maintained at 0°C in darkness after exposure to H_2O_2

Dark period	Relative magnitude of I_1	
	Mature cultures	Young cultures
0	100	100
20 minutes	77	95
1 hour	73	90
3 hours	80	93
5 hours	80	80
24 hours	43	50

Cell suspensions were treated with H_2O_2, illuminated and bubbled with N_2 for 5 minutes, and then placed in darkness at 0°C. Later the suspensions were returned to light at 25°C, and the ensuing catalase synthesis was measured. The amount of internal inducer (I_1) remaining at the end of the dark period was measured by the amount of catalase subsequently formed. See text and figure 2 for further experimental details.

At 0°C the stability of I_1 is reduced by illumination. An experiment demonstrating this was performed in the same way as the foregoing experiment, except that the tubes containing cell suspensions were placed at 0° in bright light, in dim light, or in darkness. "Bright" light (from a tungsten lamp) was saturating as a source of energy for growth and enzyme synthesis. "Dim" light was about one-fourth as intense. Results are shown in figure 3. Samples placed immediately in bright light (curve A) made twice as much catalase as those placed immediately in dim light (curve B). In the latter case the rate of enzyme synthesis was lower because insufficient energy was available. Samples kept in darkness at 0°C for 110 minutes and then illuminated at 25° (curve C) were almost as responsive as those tested immediately. In contrast, samples kept at 0°C in dim or bright light synthesized little new catalase when brought to 25° in bright light (curves D and E). This attenuation of I_1 can be caused by bacteriochlorophyll-absorbed light. The effect was just as great if filtered light (710–1150 mμ) or sodium light (589 mμ) was used in place of white light during the "cold period"; these wave lengths are absorbed almost exclusively by bacteriochlorophyll in *Rps. spheroides*.

The stability of internal inducer at 25°C

Before proceeding further let us consider the way in which the amount of I_1 has been defined operationally. Once I_1 has been

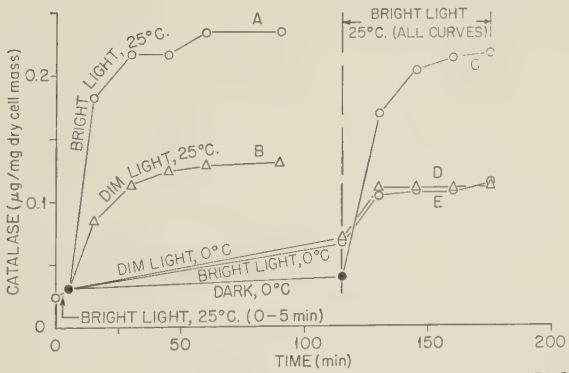

Fig. 3 Same as figure 2, with samples placed in bright light, dim light, or darkness at 25° or at 0°C after the first 5 minutes. After 115 minutes, the refrigerated samples were placed in bright light at 25°. "Bright" light was about 4 times as intense as "dim" light.

fully formed, its amount at any instant is measured by the amount of catalase that can be synthesized subsequently under standard, near-optimum conditions (at 25°C in bright light). This definition cannot apply, of course, to the period during which I_i is being formed and H_2O_2 is disappearing. With this exception, the time course of catalase synthesis in the light at 25°C (fig. 1) is by definition a description of the disappearance of I_i. At any instant the amount of I_i equals the amount of catalase yet to be synthesized. Graphically, inverting the curves of figure 1 gives the amounts of I_i versus time. The latter are not valid during the first few minutes, when I_i is being formed.

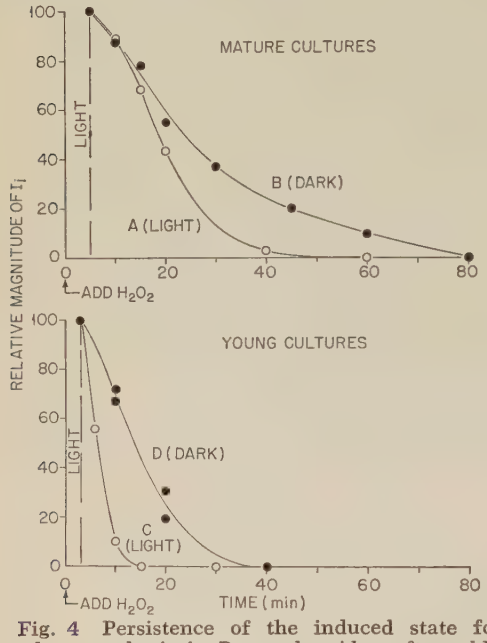

Fig. 4 Persistence of the induced state for catalase synthesis in *Rps. spheroides*, after addition of H_2O_2. H_2O_2 (60 μM for mature cultures; 30 μM for young) was added at $t = 0$ and the suspensions were illuminated under N_2 for 5 minutes (mature cultures) or three minutes (young cultures). Some samples were then kept in the light; others were placed in darkness and later returned to the light. Catalase was assayed at intervals, as in figure 2. The temperature was 25°C throughout the experiment. Curves A and C: suspensions illuminated continuously. For any time t, the ordinate is the amount of catalase synthesized after that time. This defines the amount of internal inducer (I_i) present at the time t. Units of I_i are relative, referred to a maximum of 100. Curves B and D: suspensions placed in darkness at 5 minutes and returned to the light at t. The ordinate, amount of I_i remaining at t, is again measured by the amount of catalase synthesized after t, during the period of reillumination.

Curve A of figure 2 shows the time course of catalase synthesis in the light at 25°C. An inverted plot of this curve, with the ordinate expressed in arbitrary units, is shown in figure 4 as curve A and represents the dissipation of I_i in the light at 25°C. The disappearance of I_i in darkness at 25° was measured in the same way as at 0°C (see, for example, curves B and C of fig. 2); this is shown by curve B of figure 4. It appears that at 25°C, as well as at 0°, illumination accelerates the destruction of I_i.

Curves C and D of figure 4 show the corresponding results with cultures in exponential growth, of density 0.5 mg/ml, given 30 μM H_2O_2 at $t = 0$. In the young cultures the lifetime of I_i is less than in the mature cultures, and correspondingly less new catalase is formed. At 0°C in darkness, I_i was found to be as stable in young cultures as in mature ones (see table 1).

Further aspects of the sequence $H_2O_2 \rightarrow I_i \rightarrow$ catalase synthesis

The time course of catalase synthesis upon addition of H_2O_2 involves a lag of several minutes; this period is also the time during which H_2O_2 disappears and I_i is generated. If a preparation containing I_i is transferred from darkness to light, catalase synthesis begins without measurable delay (see, for example, curves C and E of fig. 2).

The formation I_i from H_2O_2 does not require a reaction of H_2O_2 with catalase. If the catalase already present in uninduced *Rps. spheroides* is inactivated with sodium azide, H_2O_2 becomes a more efficient inducer (Clayton, '60c). The efficiency of H_2O_2 as an inducer is less in cells that have been preinduced to a higher initial catalase content. Catalatic destruction of H_2O_2 therefore detracts from the formation of I_i.

The disappearance of I_i is not related stoichiometrically to the formation of new catalase. At 0°C in the light, for example, I_i is destroyed rapidly but the synthesis of catalase is very slow. Moreover, a comparison of curves A and B of figure 3 shows a large difference in the rates of catalase

synthesis but no difference in the time-course and hence in the rate of dissipation of I_i.

The formation of I_i requires energy. If H_2O_2 is added to a suspension of *Rps. spheroides* and the first few minutes, when H_2O_2 is still present, are spent in darkness, relatively little I_i is formed. This was demonstrated as follows: Illuminated suspensions, bubbled with N_2, were treated with H_2O_2 and placed immediately in darkness at 25°C. After an interval of 1–75 minutes, the suspensions were returned to the light at 25°, and the ensuing synthesis of catalase was measured. This measure of I_i is plotted against the duration of the dark interval in figure 5. The curves of figure 5 fall abruptly in the range 0–5 minutes of darkness, and then decline gradually. The abrupt drop coincides with the time the I_i could be formed from H_2O_2 and shows that relatively little I_i was formed in darkness. If the dark interval was terminated while H_2O_2 was still present (e.g., after one minute), some I_i was formed during the subsequent period of illumination. In interpreting figure 5, one must appreciate that the ordinate represents not only the amount of I_i present at the time t (end of dark period) but also the I_i that was formed subsequently, in the light.

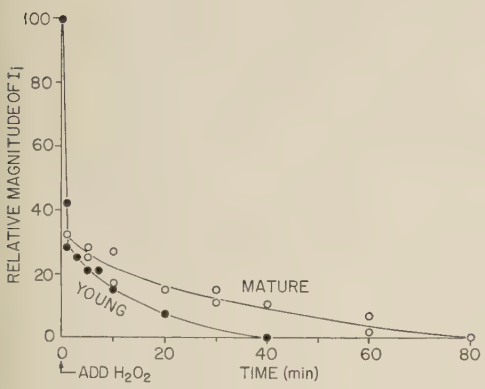

Fig. 5 Experimental details as in figure 4, except that all samples were placed in darkness at $t = 0$, immediately after H_2O_2 was added. Samples were returned to the light after time t; the ordinate is the amount of catalase synthesized (in relative units) during the period of illumination after t.

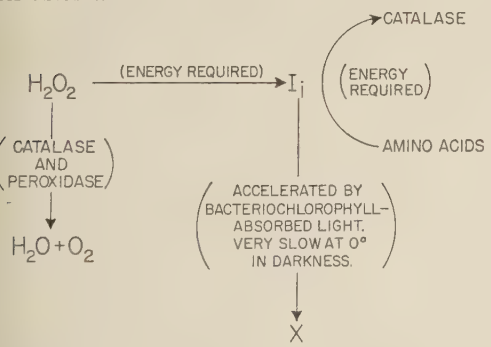

Fig. 6 Scheme representing the formation and dissipation of the induced state, or internal inducer (I_i), in the H_2O_2-induced synthesis of catalase in *Rps. spheroides*.

DISCUSSION

The foregoing results are summarized by the scheme shown in figure 6. H_2O_2 is destroyed rapidly by catalase and a peroxidase-like activity; while present it promotes an energy-dependent formation of I_i. In turn, I_i promotes an energy-dependent synthesis of catalase from amino acids [*de novo* synthesis of the catalase-protein has demonstrated; (Clayton, '60d)]. I_i is destroyed at a rate independent of the rate of induced catalase synthesis. The process of destruction of I_i is probably enzymatic, since it is blocked at 0°C. At 0° in darkness, I_i can be preserved for many hours. The destruction of I_i is accelerated by bacteriochlorophyll-absorbed light, and may therefore require energy. Mole for mole, H_2O_2 is not an efficient inducer of catalase synthesis; about 30,000 molecules of H_2O_2 must be added for each molecule of catalase formed. Thus, if $H_2O_2 \rightarrow I_i$ represents a chemical reaction, the destruction of H_2O_2 by catalase and "peroxidase" is far more probable. The imbalance is even greater if one molecule of I_i can catalyze the formation of many molecules of catalase.

In stability or detectability of an internal inducer [in Pollock's terminology, an organizer (Pollock, '53)], this system is intermediate between the induction of β-galactosidase in *Escherichia coli*, where synthesis of the enzyme stops as soon as the external inducer is withdrawn (Cohn, '57), and the induction of penicillinase in *Bacillus cereus* where synthesis continues for many cell generations in the absence of external inducer (Pollock, '59).

Whether I_i represents an inducer or the antagonist of a repressor is an open ques-

tion. If I_i is the antagonist of a repressor, the dissipation of I_i can be identified as the formation of more repressor. In these terms some aspects of the kinetics of disappearance of I_i are more easily understood. The faster disappearance of I_i in young cultures can reflect the more vigorous synthesis of repressor in these cultures. At 0°C in darkness the formation of new repressor ceases and I_i remains effective for hours. Illumination at 0° provides energy for a slow synthesis of new repressor, and I_i loses its effectiveness.

In conclusion, I_i is not necessarily a substance, but if it is, one can hope to isolate it, demonstrate its effectiveness as an inducer, and identify it.

SUMMARY

When H_2O_2 (4–60 μM) is added to a moderately dense suspension (0.5–2.0 mg dry cell mass/ml) of *Rps. spheroides*, the H_2O_2 is destroyed within a few minutes by catalase and peroxidase-like activities. While H_2O_2 is present, it generates an induced state or an inducing substance (I_i) that promotes catalase synthesis for 15–40 minutes. Formation of I_i requires energy. I_i is preserved for many hours at 0°C in darkness; light accelerates its dissipation. The formation of I_i does not require a reaction between H_2O_2 and catalase, and its destruction is not related stoichiometrically to the synthesis of new catalase. The time course of induced catalase synthesis appears to reflect the formation and dissipation of I_i.

LITERATURE CITED

Clayton, R. K. 1960a The induced synthesis of catalase in *Rhodopseudomonas spheroides*. Biochim. et Biophys. Acta, *37:* 502–512.

——— 1960b Kinetics of H_2O_2 destruction in *Rhodopseudomonas spheroides*: roles of catalase and other enzymes. Ibid., *40:* 165–167.

——— 1960c Physiology of induced catalase synthesis in *Rhodopseudomonas spheroides*. J. Cell. and Comp. Physiol., *55:* 1–8.

——— 1960d Protein synthesis in the induced formation of catalase in *Rhodopseudomonas spheroides*. J. Biol. Chem., *235:* 405–407.

Cohn, M. 1957 Contributions of studies on the β-galactosidase of *Escherichia coli* to our understanding of enzyme synthesis. Bacteriol. Rev., *21:* 140–168.

Pollock, M. R. 1953 Stages in enzyme adaptation. Symposium Soc. Gen. Microbiol., *3:* 150–175.

——— 1959 Induced formation of enzymes. In: The Enzymes, 2nd ed., Vol. 1, ed., P. D. Boyer, H. Lardy and K. Myrbäck. Academic Press Inc., New York, pp. 619–680.

Electrical Properties and Activities of Single Sympathetic Neurons in Frogs[1]

S. NISHI AND K. KOKETSU
Research Laboratories, Department of Psychiatry, University of Illinois College of Medicine, Chicago, Illinois

The electrical properties and the activities of single sympathetic neurons have not previously been explored intracellularly in detail because of the tough connective tissue dispersed throughout the ganglion and because of the smallness of the neuron. In spite of the technical difficulties in inserting the microelectrode into the cell, Eccles ('55) has succeeded in recording intracellularly the electrical responses of ganglion cells in the isolated superior cervical ganglion of rabbits. As far as the microelectrode technique is concerned, the frog's sympathetic ganglion has some advantages. Since the connective tissue covering the ganglion can be easily removed, the individual cells located on the surface of the ganglion are clearly seen so that the insertion of a microelectrode can be carried out under visual control.

The histological feature of the frog's sympathetic neuron has been examined and compared to those in the different classes of vertebrates by Huber (1899). According to his description, each cell is surrounded by a thin fibrous capsule in which the presynaptic fibers present a pericellular nest after losing their myelination and terminate with their free endings on the neuron soma (see fig. 1, C).

A large number of the post-ganglionic fibers have no myelin sheath. A marked difference, which exists between the neurons in frog's and mammalian sympathetic chains, is that the former is a unipolar cell while the latter is multipolar having several dendrites as well as the axon (De Castro, '32).

The purpose of the present study was to explore the electrical membrane characteristics, the activities of single sympathetic neurons, and the mode of synaptic transmission. A preliminary account of this experiment has been published (Nishi and Koketsu, '59).

MATERIAL AND METHODS

The sympathetic chain together with the lumbar spinal nerves of a frog (*Rana pipiens*) was carefully dissected out. The chain was cut at the level of the third or 4th spinal nerve and freed from the aorta which is intimately associated with the chain. The *rami communicantes* were cut except for those of the 8th to the 10th ganglia to maintain connection between the ganglia and corresponding spinal nerves intact. The lumbar spinal nerves were freed by cutting them at their entry into the spinal vertebrae and at the level where the 9th and 10th spinal nerves were joined. A typical isolated preparation is shown schematically in figure 1, A. The connective tissue covering the surface of the sympathetic ganglia was removed under the binocular microscope. Individual cells were then easily seen with a magnification of 100 × (fig. 1, B).

The preparation was placed in a small lucite chamber divided into three compartments. The 8th to 10th ganglia were placed in the middle compartment and covered with a thin layer of Ringer's solution. The upper part of the sympathetic chain and the peripheral part of the lumbar spinal nerves were lifted from the Ringer's bath and led separately into the lateral compartments and mounted on the stimulating electrodes. The lateral compartments were covered with glass plates to prevent the nerve tissues from drying. It was unnecessary to add oxygen to the Ringer's solution, since the electrical activity as well as the synaptic transmission of the sympa-

[1] This research was supported by the Institute of Neurological Diseases and Blindness, National Institute of Health grant B-1650.

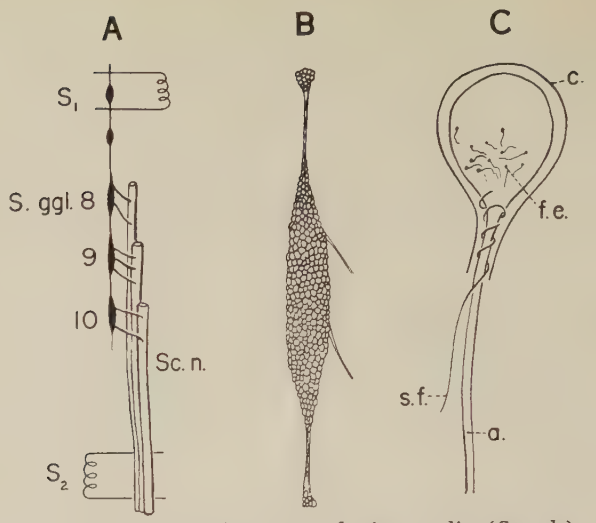

Fig. 1 A, Schematic drawing of lumbar sympathetic ganglia (S. ggl.) and sciatic nerve plexus (Sc. n.). S_1 and S_2 indicate locations of electrodes for orthodromic and antidromic stimulation. B, View of sympathetic ganglion under dissecting microscope. Individual cells located on surface are clearly recognizable. C, Simplified histological features of a sympathetic ganglion cell to illustrate the general relationship of preganglionic fiber and axon to soma. a, axon. c, thin fibrous capsule surrounding cell. f.e., free endings of presynaptic terminal fibers. s.f., spiral fiber which is the unmedullated peripheral part of presynaptic fiber.

thetic neurons were sufficiently maintained under such conditions.

Antidromic, orthodromic, and intracellular direct stimulation were used in the present experiments. For antidromic stimulation, a square pulse of 1 msec. duration was applied to the peripheral end of the lumbar spinal nerves, since a large number of cells in the 8th to 10th ganglia send their axons into these nerves. The orthodromic stimulation was applied through the sympathetic chain at the level of the 5th or 6th ganglion (fig. 1, A), since these parts consist of many preganglionic fibers which form synapses in the 8th to 10th ganglia. For direct stimulation of the soma membrane, stimulating currents were applied intracellularly through the recording microelectrode connected to a Wheatstone bridge device. The current sent through the electrode was measured by the method previously described (Koketsu and Nishi, '57).

The Wheatstone bridge used in the present experiment was almost identical to that used in the experiments on frog's intrafusal muscle fibers (Koketsu and Nishi, '57) and spinal ganglion cells (Koketsu et al., '59). The current due to the cell's resting potential when the bridge circuit was used, was compensated by a dry cell and a variable resistor. For calibration of the obtained potential a 50 mv. pulse was applied to both ends of the 100 Ω resistor inserted between the cathode and ground.

Microelectrodes were made of pyrex tubing filled with 3 M KCl. Only those with a resistance between 20–40 MΩ were chosen. High frequency distortion caused by stray capacity of the microelectrode and input lead was minimized by using a positive feed-back circuit incorporated in the cathode follower input amplifier.

Frog Ringer's solution of the following composition was used: NaCl, 112 mM; KCl, 2.0 mM; $CaCl_2$, 1.8 mM; $NaHCO_3$, 2.4 mM. All experiments were carried out at room temperature (24–26°C).

RESULTS

Resting membrane characteristics

Resting membrane potential. Individual cells have either a spherical or oval shape with a maximum diameter of 20–35 μ (mean of 50 cells, 26.8 μ). The tip of the microelectrode was placed at the center

of a cell, then gradually pushed until a negative potential appeared. The condition of the impaled neuron was judged by the shape of the antidromic responses and of the electrotonic potentials of the cell membrane. Some cells showed steady potentials for over 30 minutes, although the majority showed a progressive decrease or a sudden disappearance of the potentials 5–10 minutes after insertion. The values of the resting membrane potential given in table 1 were recorded from cells in which the microelectrode was satisfactorily inserted. The mean value for the measured resting potential was approximately 65 mv.

Electrical constants of the resting membrane. To determine the electrical constants of the resting membrane, anodal and cathodal square pulses of various intensities were applied through the recording electrode by means of the bridge device. Typical potential changes are illustrated in figure 2. When the applied current was less than approximately 5×10^{-10}A, the magnitude and time course of the anelectrotonic potentials were practically identical to those of the catelectrotonic potentials. The effective resistance and time constant of the resting membrane were calculated from these potentials, the mean values (for 7 cells) being approximately 20 MΩ and 10.6 msec., respectively. With the mean neuronal surface area of 2282×10^{-8} cm², this effective resistance yields a specific membrane resistance of 456 Ω·cm². The specific membrane capacitance calculated from the values of the specific membrane resistance and time constant was 24.4 μf/cm². The values of the electrical constants obtained from individual sympathetic neurons are summarized in table 1.

Voltage-current relation. Figure 3 shows the relationship between the magnitude of the passive potential changes and the intensity of the applied currents. The V–I relation in either direction was almost linear when the current was less than approximately 1×10^{-9}A (curve A of fig. 3). When the depolarization exceeded about 20 mv., there was a gradual increase of the slope and an appearance of local and eventually spike action potentials. In many cases, when the hyperpolarizations exceeded 30 mv., the slope had a tendency to become slightly steeper than that obtained by smaller current intensities.

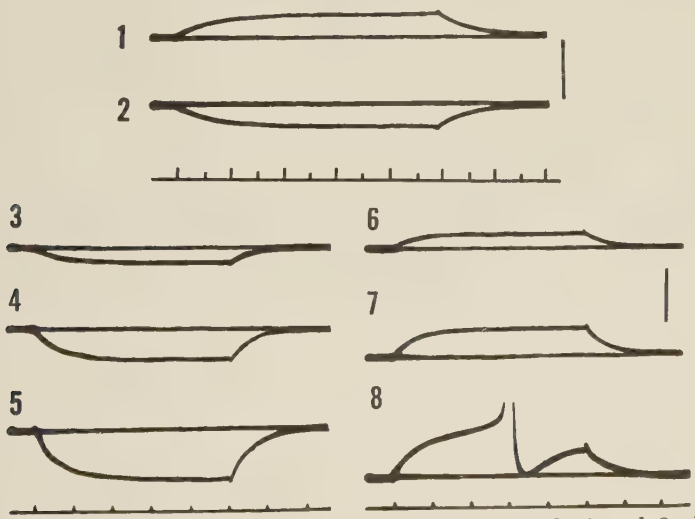

Fig. 2 Electrotonic potentials of neuronal membrane. Records 1 and 2 obtained from same cell. They were generated by rectangular current pulses of 5×10^{-10}A which are in depolarizing and hyperpolarizing directions, respectively. Records 3–8 recorded from another cell. Records 3 and 6, 4 and 7, and 5 and 8 generated by depolarizing and hyperpolarizing current pulses of 2.5×10^{-10}A, 5.8×10^{-10}A and 9.5×10^{-10}A, respectively. Calibration: 20 mv. Time mark: 5 and 10 msec. for records 1 and 2, and 10 msec. for records 3–8.

TABLE 1

No.	Diameter	Surface area	Resting potential	Effective resistance	Rm	Tm	Cm
	μ	$\times 10^{-8}$ cm^2	mv	MΩ	Ω·cm^2	msec	μf/cm^2
1	26	2123	62	21	445.8	10.5	23.3
2	22	1517	60	16	242.7	9.6	39.6
3	28	2458	75	26	639.1	13.0	20.3
4	30	2822	67	21	592.6	11.5	19.4
5	26	2123	73	24	509.5	12.2	23.9
6	32	3210	63	23	738.3	10.3	13.9
7	25	1956	55	12	234.7	7.2	30.7
Mean	27	2282	65	20	456.4	10.6	24.4

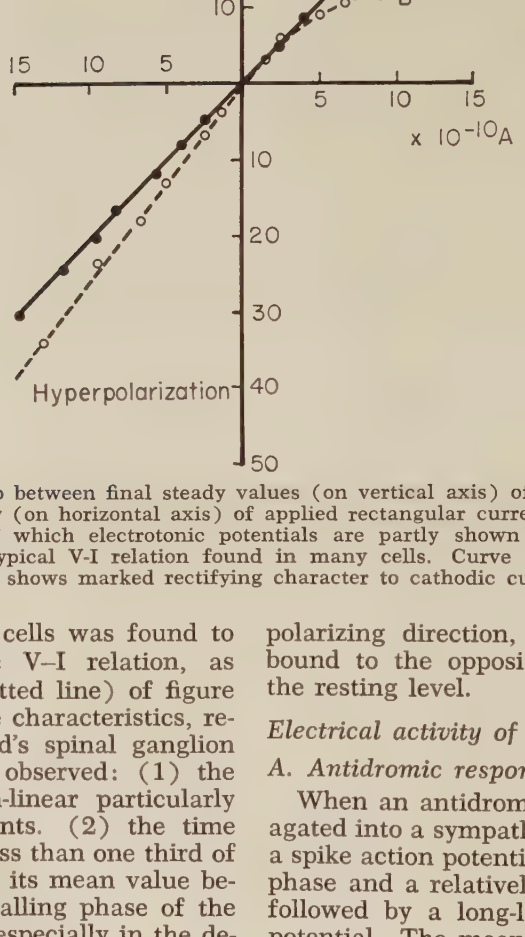

Fig. 3 Relationship between final steady values (on vertical axis) of altered membrane potential and intensity (on horizontal axis) of applied rectangular current pulse. Curve A, obtained from cell of which electrotonic potentials are partly shown in records 3–8 in figure 2; represents typical V-I relation found in many cells. Curve B obtained from a small number of cells shows marked rectifying character to cathodic current.

A small number of cells was found to show a characteristic V–I relation, as shown in curve B (dotted line) of figure 3. The following three characteristics, resembling those of toad's spinal ganglion cells (Ito, '57), were observed: (1) the V–I relation was non-linear particularly for depolarizing currents. (2) the time constant was always less than one third of that of the other cells; its mean value being 3 msec. (3) the falling phase of the electrotonic potential, especially in the depolarizing direction, showed a slight rebound to the opposite direction crossing the resting level.

Electrical activity of sympathetic neurons

A. Antidromic response

When an antidromic impulse was propagated into a sympathetic neuron, it set up a spike action potential with a sharp rising phase and a relatively slow falling phase, followed by a long-lasting positive after-potential. The mean height of the action

otentials was 90 mv. (maximum, 113 mv., epresenting an overshoot of about 25 nv.). The mean value of the spike dura- on in 25 cells was 3 msec. (range 2.2–4 nsec.). Typical examples of antidromic esponses are shown in figure 4. By re- ording with a fast time base the action otentials of many cells revealed an in- ection on the rising phase at approxi- nately 40 mv. (ranging from 32–45 mv. in 8 cells) from the resting potential. The ise time to the inflection ranged from ap- roximately 0.2–0.7 msec. and that to the pike peak from 0.6–1.2 msec. Frequently, he falling phase of the spike showed a hort slow phase immediately after the pike crest, which lasted for about 0.5 nsec. with a slope of 10–20 v/sec. The naximum slopes of the rising and falling hases obtained were 140–160 v/sec. and 5–80 v/sec., respectively. The after-po- ential reached its maximum amplitude bout 1.5 msec. after its initiation, and asted for 150–500 msec.; the maximum mplitude (measured from the resting po- ential) ranged from 14–35 mv. (the

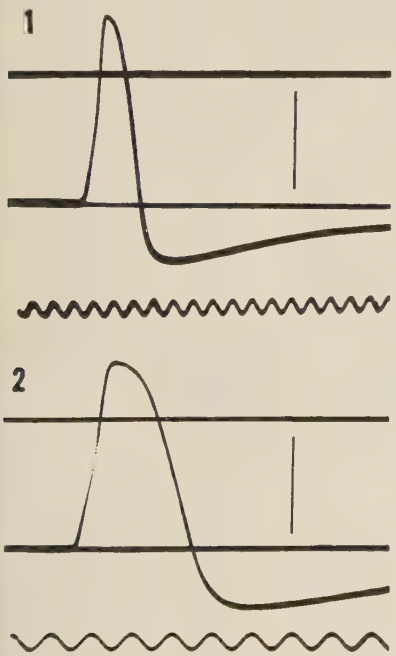

Fig. 4 Spike potentials induced by antidromic mulation. Recorded from same cell at different eep speeds. Calibration: 50 mv. Time mark: 00 cycles/sec.

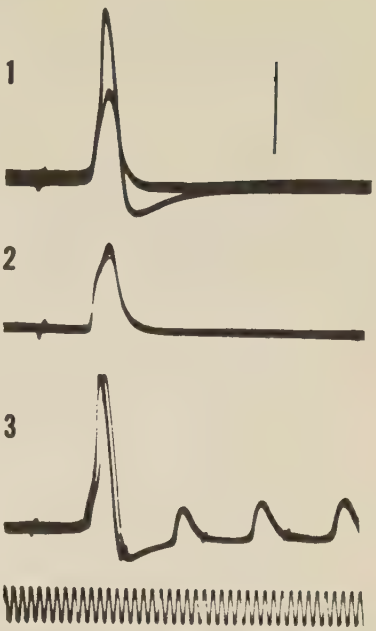

Fig. 5 Record 1 shows spontaneous separation of antidromic response and record 2 isolated small spike only. Separation of antidromic response by repetitive stimulation with frequency of 100/sec. is shown in record 3. Calibration: 50 mv. Time mark: 1000 cycles/sec.

mean of 15 cells, 24.7 mv.), which was about 30% of the spike potential.

In some cases the antidromic responses spontaneously fractionated in an all-or-nothing manner at the point of inflection, leaving a small spike (fig. 5, 1 and 2). The falling phase of the small spike usually returned to the resting membrane potential without any hyperpolarizing after-potential, although it sometimes showed a very small one. A similar small-spike potential was occasionally detected when an antidromic response was evoked a few msec. after a conditioning one or when repetitive antidromic responses were elicited (fig. 5, 3).

Separation of antidromic response by hyperpolarization. An analysis of the mode of propagation of the antidromic impulse was made by changing the resting membrane potential by passing a hyperpolarizing current through the recording electrode. The antidromic response shown in figure 6, A1 revealed an inflection (marked by arrow in record A3) when the

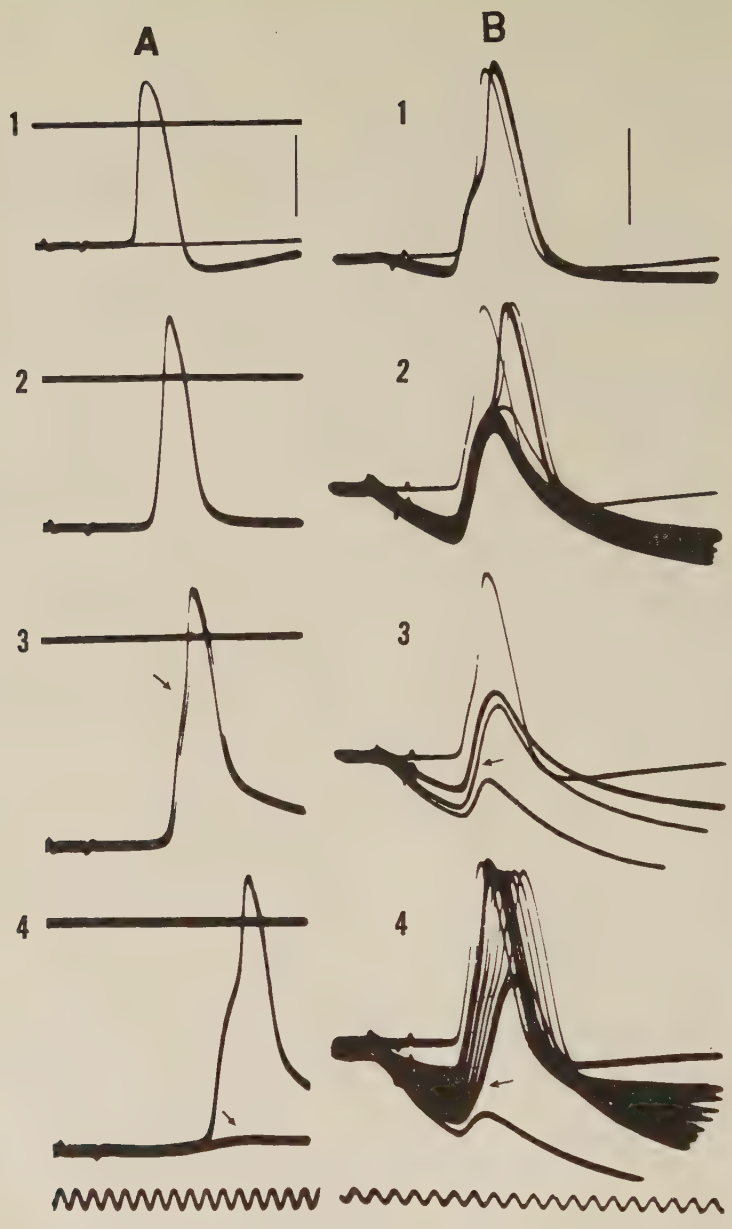

Fig. 6 Two series of antidromic responses evoked on plateau (left column) and rising phase (right column) of hyperpolarizations of various magnitudes. Each series recorded from different cells. In left-side series, antidromic responses were evoked at membrane potentials of approximately 73 (normal value), 87, 122, and 135 mv. In each record of right-side series, control response was always recorded before applying hyperpolarization. Intensity of applied current was increased stepwise from B1–B3 and also changed progressively to some extent in each record. Record B4 shows whole course of alteration of antidromic response under steeply rising hyperpolarization of which magnitude varied to the same extent as those in B1–B3. Calibration: 50 mv. Time mark: 1000 cycles/sec.

hyperpolarization of the cell membrane was sufficiently large. At a critical membrane potential (about 60 mv. from the resting level) the antidromic response failed at the foot of the response, leaving a very small potential of only a few millivolts (marked by arrow in record A4). During steady hyperpolarizations, such blockage of the antidromic conduction was commonly observed. If, however, the antidromic response was elicited on the rising phase of the hyperpolarization, conduction was blocked at the inflection of the response as illustrated in figure 6, B. The small spike, which remained after blockage at the inflection had occurred, also revealed an inflection (marked by arrows in records B3 and B4) on its rising phase and eventually failed at this inflection by applying stronger hyperpolarization.

It was interesting to notice that steady hyperpolarizations markedly lengthened the latency for spike initiation; while the spike, evoked on the rising phase of a hyperpolarization, was very slightly delayed even when strong hyperpolarization was applied.

Other effects of hyperpolarization. The potential level of the peak and inflection remained unchanged regardless of the increase of the applied hyperpolarization; only when relatively small inward currents were applied, the increment in spike height exceeded the displacement of the membrane potential. The maximum rate of rise and fall increased practically in proportion to the increase of hyperpolarization. A slow falling phase, which was frequently observed shortly after the crest (fig. 4, 2 and fig. 6, A1), disappeared with hyperpolarization. The after-positivity diminished by increasing the membrane potential and reversed polarity when the applied polarization exceeded a certain level. There was a linear relationship between the magnitude of the after-potential and the membrane potential, with a slope slightly smaller than unity (the mean value of 12 cells was 0.9). Reversal of the after-positivity was observed when the membrane potential was between −82 and −97 mv. (mean value −90 mv.).

B. Spike elicited by intracellular direct stimulation

The size and time course of spike potentials (fig. 7, 1 and 2) evoked by intracellular direct stimulation were similar to those elicited by an antidromic impulse. In figure 7, 3, the direct response and the antidromic response obtained from the same cell are traced and superimposed upon each other for comparison. The direct response did not exhibit any appreciable step on its rising phase even when recorded with a fast sweep speed (fig. 7, 2). The threshold depolarization for spike initiation ranged from 16–31 mv. (mean of 22 cells, 25.3 mv.). This value was apparently smaller than that of the height of the inflection (40 mv.) on the rising phase of antidromic responses. This suggested that direct intracellular stimulation may initially evoke the action potential of the membrane adjacent to the soma, where the threshold is lower, as was suggested in spinal motoneurons (Araki and Otani, '55; Fatt, '57; Fuortes et al., '57; Coombs et al., '57a,b). If a strong hyperpolarizing current was applied immediately after the initiation of a direct response, the direct response sometimes revealed an inflection on its rising phase about 10–15 mv. higher than the level of the threshold depolarization (fig. 8, 2). In some instances, the full-size direct response was blocked leaving a small spike potential (record 3).

C. Orthodromic response

The orthodromic responses were preceded by an initial depolarization phase (synaptic potential) which formed a step at approximately 25 mv. from the resting membrane potential (fig. 9, 1 and 2). The mean value of the step height was 26.1 mv. (18–35 mv. in 20 cells) and that of the spike height was 85 mv. (75–105 mv. in 20 cells). The descending phase of the spike reached the resting membrane potential within 3 msec., and was followed by a long-lasting "positive" after-potential (undershoot). The maximum magnitude of the positive after-potential was smaller than that of the antidromic response, being approximately −10 mv. from the resting membrane potential. In some cells with a large resting potential, there was

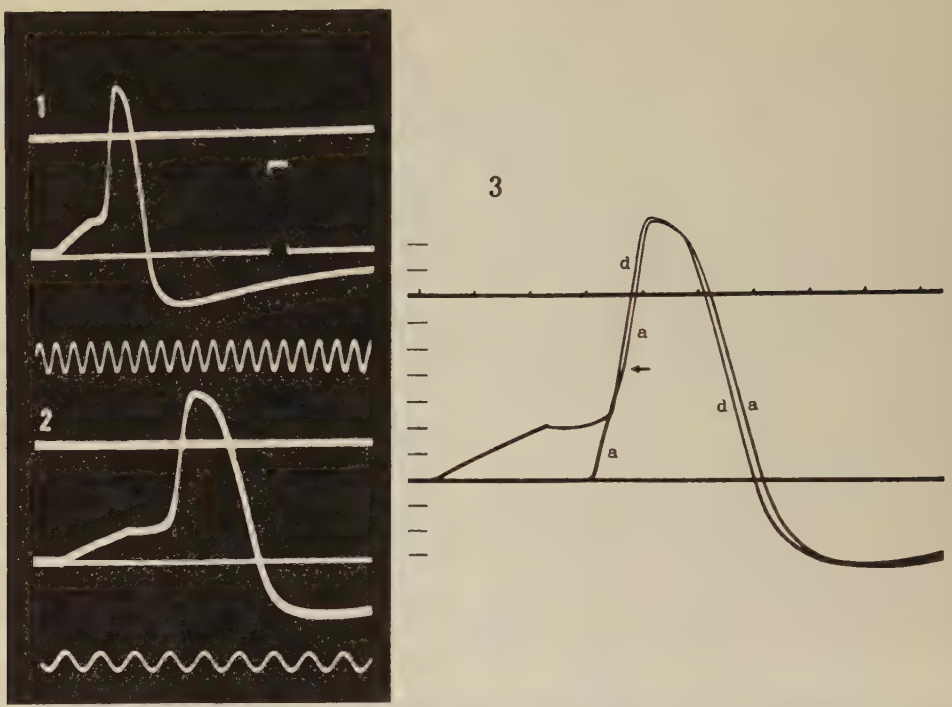

Fig. 7 Responses to intracellular direct stimulation (1 and 2) and comparison of direct and antidromic spikes (3). Action potentials in 1 and 2 elicited by cathodic current pulses (2 msec.) with different sweep velocities. In both records, intensity of applied current was just sufficient to elicit spike response so that spike occurred at a certain time after cessation of rectangular current pulse. Square pulse in record 1 is 50 mv. in height, which is also applicable to record 2 for calibration. Time mark: 1000 cycles/sec. Record 3 shows tracings of antidromic (a) and direct (d) responses. Arrow indicates height of inflection on rising phase of antidromic response. Time mark on zero line indicates 1 msec. Each division of left column equal to 10 mv.

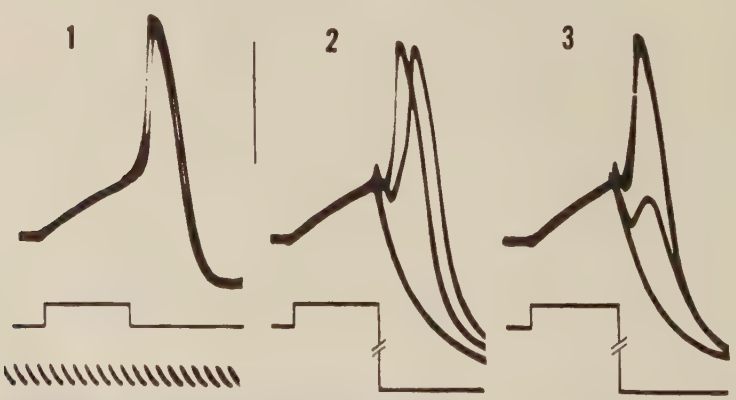

Fig. 8 Effect of hyperpolarization applied immediately after initiation of direct response. Record 1 shows control responses elicited by cathodic current pulse slightly larger than threshold intensity with duration of about 7 msec. In record 2, responses clearly revealed an inflection on rising phase under the effect of applied hyperpolarization. In record 3 response intermittently failed to develop fully, leaving a small spike. Line under each record indicates time course of applied cathodic and anodic currents. Calibration: 50 mv. Time mark: 1000 cycles/sec.

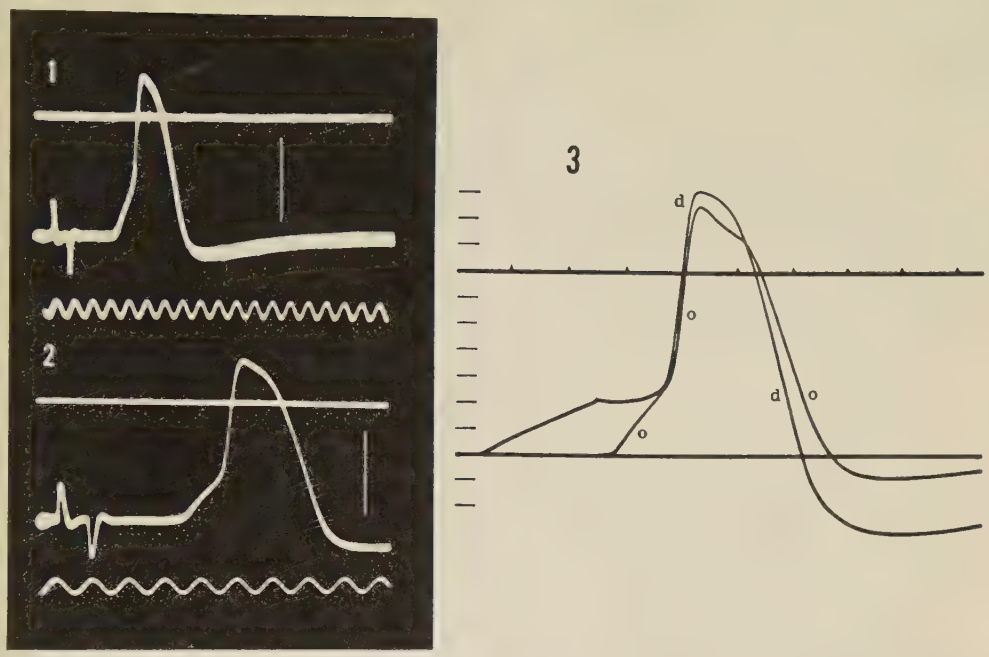

Fig. 9 Orthodromic responses and comparison of orthodromic and direct responses. Records 1 and 2 show responses of cell to orthodromic stimulation recorded with different sweep velocities. Calibration: 50 mv. Time mark: 1000 cycles/sec. Record 3 shows tracings of orthodromic and direct responses of same cell. Time mark on zero line indicates 1 msec. Each division of left column is equal to 10 mv.

first a small "negative" after-potential which lasted for about 5–20 msec. and then, in turn, a positive after-potential. The smallness of the positive after-potential and the occasional appearance of the negative after-potential were apparently due to the synaptic potential. The entire duration of the positive after-potential was practically the same as those observed in antidromic and direct responses, the value being 150–500 msec.

Comparison of the orthodromic response and direct response obtained from the same cell is shown in figure 9, 3. The initial part of the falling phase of the orthodromic response characteristically differed from that of the direct response; the peak of the orthodromic response was about 7 mv. lower than that of the direct response and the initial falling phase frequently showed a small dip immediately after the spike crest, forming a hump on the falling phase of the spike. There were some exceptional cases in which the magnitude of both orthodromic and direct responses were almost equal, but a difference of approximately 5 mv. was commonly observed (the largest difference so far obtained was 12 mv.). The threshold level for the initiation of the orthodromic responses was practically identical with that of the direct response (approximately 25 mv.).

The orthodromic response usually did not show any inflection on its rising phase as was also observed in direct responses. In some cases, however, the orthodromic response showed an inflection on its rising phase at about 30—40 mv. from the resting potential, or only local responses appeared on the synaptic potential (fig. 10, A1 and A2). Such evidence suggests that the spike responses evoked by a synaptic potential and a directly applied current are identical in their initiation process.

In most cases, it was very difficult to obtain the synaptic potential alone by weakening the stimulus strength. A spontaneous variation in the time from the onset of the synaptic potential to the spike initiation was sometimes observed during

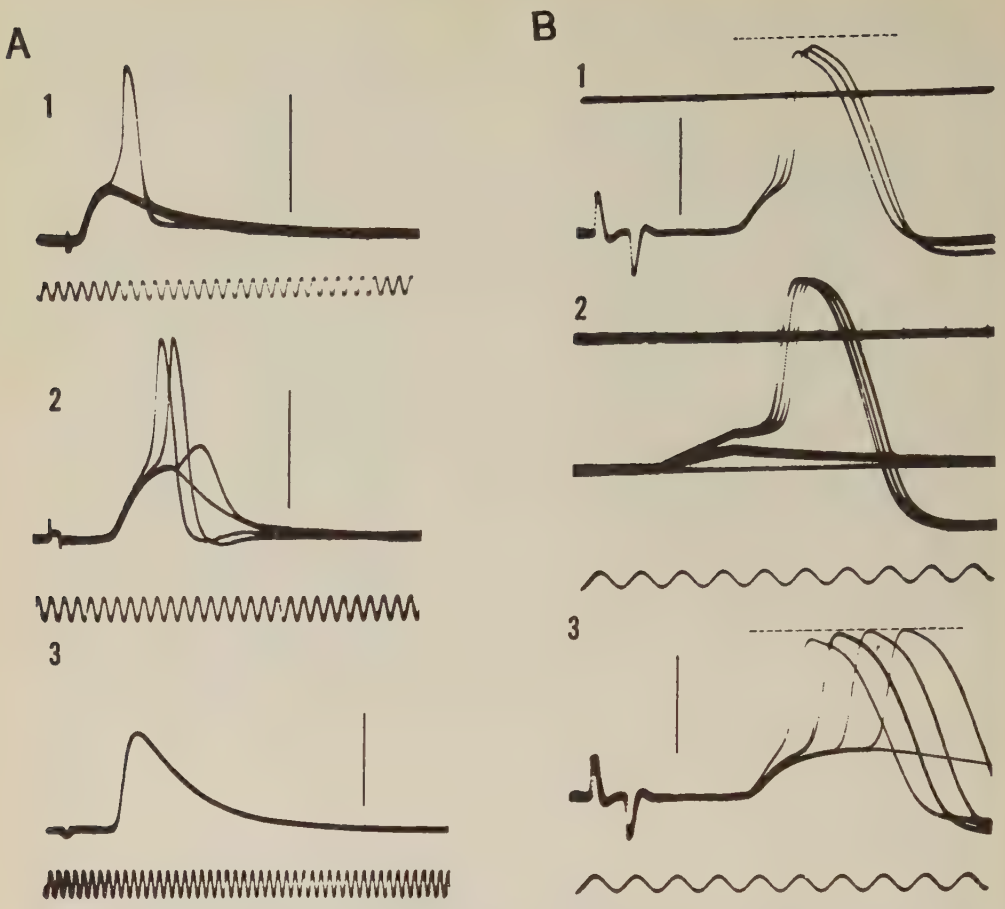

Fig. 10 A, Orthodromic responses which showed inflection on rising phase of spike potential (1) and small spike on synaptic potential (2). Record 3 shows time course of synaptic potential. B, Spontaneous variations in critical depolarization time for spike initiation. Records 1 (orthodromic response) and 2 (direct response) obtained from same cell, while record 3 is from a different neuron. Dotted lines in records 1 and 3 show height of direct response of each cell. Note difference in height of each orthodromic response recorded from single cell. Calibration: 50 mv. except 20 mv. in A3. Time mark: 1000 cycles/sec.

application of stimulation of the same intensity (fig. 10, B1 and B3). An interesting phenomenon observed in figure 10, B was that the height of the spike response increased when initiation was delayed. In record B1, the difference between the earliest spike (1.38 msec. from initiation of synaptic potential to spike peak) and the last one (1.75 msec.) was approximately 2.3 mv. Direct responses of the same cell (B2) was 6.9 mv. higher than that of the earliest spike. In record B3, the amplitude of the orthodromic spikes increased gradually according to the delay, the last spike (3.75 msec.) having an amplitude almost the same as that of direct responses.

Synaptic potential

The synaptic potential reaches a summit about 2.5–3 msec. after initiation, and declines slowly in an approximately exponential time course (fig. 10, A3). The mean time constant of decay was 12 msec. (range, 8–15.5 msec. in 25 cells). The total duration of the synaptic potential was about 40 msec., and there was no subsequent hyperpolarization (fig. 10). The

maximum rate of rise of the synaptic potential ranged between 25–32 v/sec. (mean of 25 cells was 30 v/sec.).

In order to produce the synaptic potential, the activated synapses must cause a current which depolarizes the post-synaptic membrane. It is of interest to analyze the time course of such a current (subsynaptic current) which may be comparable with that of the synaptic transmitter action (Fatt and Katz, '51; Coombs et al., '56). It might be important to clarify whether or not the repolarization phase of the synaptic potential is determined by the passive decay of the charge that has been placed on the membrane capacity during the transmitter action. Actually, this could be observed by comparing the time constant of the cell membrane and that of the synaptic potential decay (table 2). In some cases the values were almost the same, but the majority of the synaptic potentials had a much longer time constant than those of the cell membrane. The mean difference was found to be 2.4 msec. (table 2, col. 5) which suggests that the repolarization phase of the synaptic potential does not decay simply in accordance with the membrane time constant. In most cases, there should be some residual flow of an inward current through the subsynaptic membrane after the synaptic potential reaches its crest. To test this possibility, the approximate time course of the synaptic current was calculated by analyzing the synaptic potential using the value of the time constant of the same cell. Two examples of the calculated time course of the synaptic current are illustrated in figure 11, which resemble the results obtained from motoneurons by Coombs et al. ('56) except for a slight difference in the time factor. The time course shown in A was commonly observed, while the one shown in B rather seldom.

Spontaneous miniature synaptic potentials, similar to those described by Brock et al. ('52), were observed in some cells. The size of single units of these potentials was about 1 mv. with a frequency that varied in different cells. Presumably these potentials are attributable to the random synaptic activation of presynaptic impulses from injured tissues (Brock et al., '52).

Effect of membrane potential on the synaptic potential. At the neuromuscular junction, it has been suggested that the chemical transmitter (acetylcholine) "short-circuits" the end-plate membrane, i.e., produces a relatively nonselective increase in the ionic permeability. Consequently, the membrane potential of the end-plate is driven towards the "equilibrium potential" for free diffusion (Fatt and Katz, '51; del Castillo and Katz, '54). To determine whether the same type of process existed in the sympathetic neuron, the effect of displacement of the resting potential on the synaptic potential was studied.

An example of the synaptic potential set up at various levels of membrane potential is shown in figure 12. The amplitude of the synaptic potential was increased by increasing the membrane potential. When the membrane was progressively depolarized, the synaptic potential was reduced accordingly and finally reversed

TABLE 2

Comparison of membrane time constant and time constant of synaptic potential decay

Cell no.	S. height[1]	S.t.c.[2]	M.t.c.[3]	M.t.c.-S.t.c.
	mv	*msec.*	*msec.*	*msec.*
1	20	11.2	9.2	2.0
2	15	9.5	7.5	2.0
3	18	9.5	8.0	1.5
4	30	15.5	11.3	4.2
5	23	12.5	10.2	2.3
6	25	11.8	9.8	2.0
7	24	14.5	12.0	2.5
Mean		12.1	9.7	2.4

[1] S. height, height of synaptic potential.
[2] S.t.c., time constant of synaptic potential decay.
[3] M.t.c., membrane time constant.

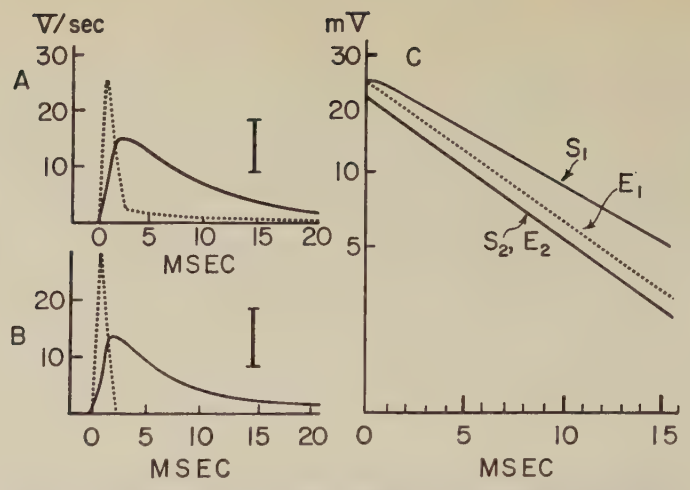

Fig. 11 A and B, Continuous lines are tracings of synaptic potentials, while broken lines show time course of subsynaptic current required to generate potential changes. C, S_1 and S_2 are time courses of falling phase of synaptic potentials shown in A and B plotted on semi-logarithmic scale. E_1 and E_2 are relative time courses of falling phase of electronic potentials obtained from cells from which synaptic potentials in A and B were recorded. Initial heights of E_1 and E_2 adjusted to maximum heights of corresponding synaptic potentials. Note deviation from exponential line at top of S_1 and difference in time course of S_1 and E_1. Voltage calibration in A and B is 10 mv.

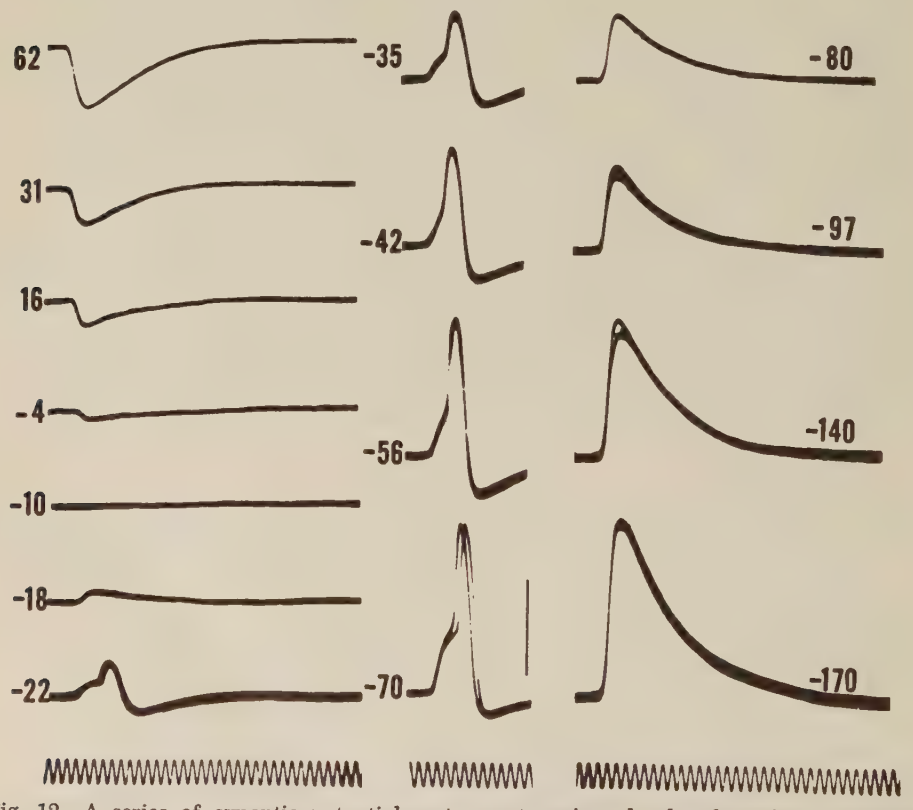

Fig. 12 A series of synaptic potentials set up at various levels of resting membrane potential. Membrane potentials indicated in mv. in each record. Resting membrane potential was —70 mv.; other potentials obtained by application of current through recording electrode. Spike potentials evoked by synaptic potential at membrane potentials between —22 and —70 mv. Calibration: 50 mv. Time mark: 1000 cycles/sec.

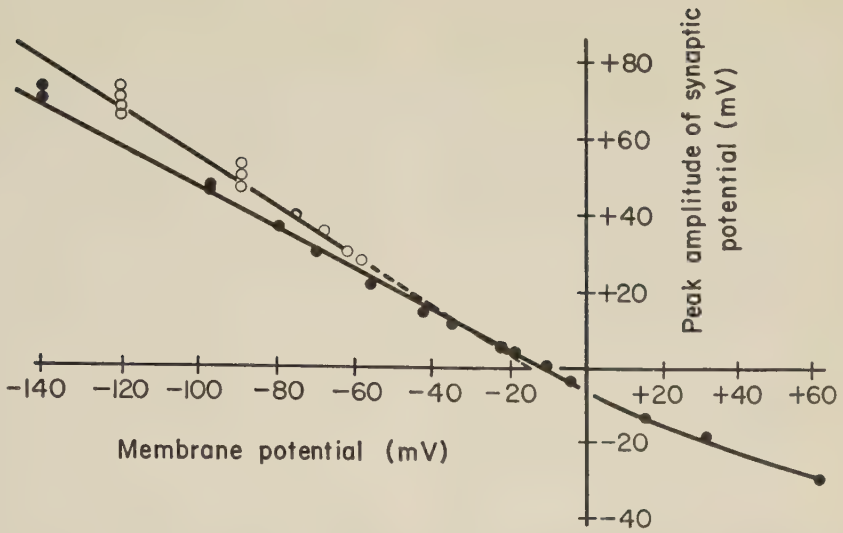

Fig. 13 Two examples showing relationship between peak amplitude of synaptic potential and initial level of membrane potential. Closed circles plotted from records shown in figure 12, while open circles obtained from another cell. Records in which spike potentials were initiated on synaptic potential, point of maximum curvature at start of spike was plotted instead of peak amplitude of synaptic potential.

when depolarization exceeded a certain level. The relation between the amplitude of the synaptic potential and the displacement of the membrane potential is almost linear over a wide extent (fig. 13). When depolarization exceeded the zero level, however, the size of the synaptic potential became smaller than expected for a linear relationship. A slight deviation from linearity also occurred when a strong hyperpolarizing current was applied; the synaptic potential slightly exceeded the expected value. Generally, the amplitude of the synaptic potential was proportional to the displacement of the membrane potential from a critical level, and its deflection was always directed towards this level. In the case shown in figure 12, the reversal level of the synaptic potential was −10 mv. In this particular case, the electrode resistance was almost independent of the applied current in both the depolarizing and hyperpolarizing directions (+62 to −170 mv.). But, in many cases it was seen from the height of the test square pulse (applied between cathode and ground) that the electrode resistance became unstable and markedly increased during application of strong depolarization. On the other hand, the electrode resistance was not appreciably altered by passing an anodic current within the satisfactory range. The reversal values found by extrapolation of the plotted curve for hyperpolarizations (see fig. 13) were ranged between −8 and −20 mv. (the mean being −14.3 mv.). These values, however, may not be accurate since the membranes of many cells, as mentioned before, show slight rectification when hyperpolarization exceeded 30 mv.

The time course of the synaptic potential did not show appreciable change with the change of the membrane potential over a wide range, especially in hyperpolarization. But, the reversed synaptic potentials, accompanying a strong depolarization, decayed much faster than the others, apparently due to rectification of the membrane. For instance, the reversed synaptic potentials in the upper 4 records of the left column decayed with time constants of 6.5–7 msec., which amounts to about 25% decrease of the normal value (9 msec.).

DISCUSSION

On the basis that sympathetic neurons have no dendritic process and a majority

of their axons are free of a myelin sheath, the most difficult point for antidromic propagation would presumably be the axon-soma junction provided the membrane does not change its properties. In the present experiments, the tip of the microelectrode was inserted into the neuron soma under visual control. The fully developed spike must represent a potential change of the membrane immediately adjacent to the microelectrode, since it is large enough to dismiss the possibility that the potential change occurring in some other region is recorded electrotonically. The inflection on the rising phase of the full spike, therefore, would be attributed to the delay in the invasion process at the axon-soma junction. Thus, the isolation of the small spike would indicate the blockage of antidromic conduction at the axon-soma junction, and the small spike would be the rapid depolarization of the soma membrane produced by the current flowing into the proximal axon. Evidence that the full spike occurs when the small spike reaches the level of inflection indicates that the threshold level for the firing of the soma membrane is equal to the height of the inflection (approximately 40 mv.). It might, therefore, be reasonable to call the fully developed spike the soma- or S-spike and the isolated small spike the initial segment or IS-spike, according to Eccles' terminology (cf. Coombs et al., '57a) without strictly referring to the boundary of the respective zones.

From the morphological standpoint there seems to be no particular zone to hinder the antidromic invasion in the axon close to the axon-soma junction, since most of the post-ganglionic fibers have no myelin sheath and the proximal part of the axon continues smoothly into the peripheral part of the axon. Nevertheless, the antidromic response evoked on an intense continuous hyperpolarization of the cell membrane, separated at its foot, but not at the inflection. Furthermore, the isolated small spike induced by a steeply rising hyperpolarization showed a distinct inflection on its ascent and failed from the point of inflection. A similar inflection sometimes appeared in the normal response without applying hyperpolarization. Such evidence indicates that there is another difficult point for propagation, presumably located in the axon in the vicinity of the axon-soma junction. The isolated very small spike, therefore, would be attributed to some region of the axon adjacent to the axon-soma junction. It would be feasible to call such a spike an axon- or A-spike. The height of this spike varies in different cells, and also in the same cell, probably due to the different lengths of the proximal part of the axon responsible for the IS-spike generation and the difference in distances between the tip of the electrode and the position where the blockage occurred. Continuous hyperpolarization of the cell membrane markedly lengthened the latent time for initiation of the antidromic response, while the steeply rising hyperpolarization did not. This may be due to the possibility that the electrotonic potentials would spread further from the soma into the axon, in the former case, according to the cable properties of the membrane.

It is clear from experimental evidence that direct intracellular stimulation and orthodromic stimulation first evoke the IS-spike, indicating that the IS membrane has a lower threshold (25 mv.) for firing than that of the soma membrane (40 mv.). This suggests that the mode of spike production in the sympathetic neuron by direct and orthodromic stimulation is basically similar to that of the spinal motoneuron (Coombs et al., '57a, b). In direct and orthodromic responses, the transition of the impulse from the IS to the S membrane is aided by the electronic depolarization or the post-synaptic potential of the soma, thus tending to obscure the inflection, whereas, the antidromically generated IS-spike is not thus aided. It has been reported that with a fast sweep speed, direct and orthodromic responses of spinal motoneurons frequently reveal an inflection on their rising phase (Araki and Otani, '55; Frank and Fuortes, '55; Fuortes et al., '57; Fatt, '57; Coombs et al., '57a,b), but the sympathetic neuron very seldom reveals such an inflection. In this respect, the latter may have a much closer coupling of the IS-S components than the spinal motoneuron. In fact, the continuous hyperpolarization required for the separation of the IS and S component is much greater

than that required in the spinal motoneuron (cf. Coombs et al., '55; Eccles, '55).

It has been found that the peak of the orthodromic spike response was significantly reduced when it was initiated near the peak of the synaptic potential. By comparing the time courses of the reduction (fig. 10, B3) and of the synaptic potential, it can be seen that reduction is most prominent at the middle part of the rising phase of the synaptic potential where the transmitter action is strongest (fig. 11). Furthermore, the formation of the dip and hump immediately after the spike crest (fig. 9, 3) seems to correspond with that observed in the end-plate potential of skeletal muscles (Fatt and Katz, '51). This evidence suggests that during the rising phase of the synaptic potential the synaptic membrane briefly and intensively increases its permeability to certain ions and "short-circuits" the active neuronal membrane.

The synaptic potential changed almost in proportion to the displacement of the membrane potential and reversed its polarity when the membrane potential shifted to a certain level (about −14.3 mv.). This suggests that the action of the synaptic transmitter (Ach) on the sympathetic neuron is quite similar to that on skeletal muscle (Fatt and Katz, '51; del Castillo and Katz, '54). When the cell membrane was strongly depolarized by an applied current, the synaptic potential was reduced in height from that expected on the basis of a linear relationship and its falling phase decayed more rapidly. This may have been because the membrane resistance was reduced by such a strong depolarization while the shunting effect of the transmitter action was constant.

SUMMARY

1. The electrical membrane characteristics and activity of the frog's sympathetic neuron and the mode of its synaptic transmission have been studied with intracellular microelectrodes.

2. Resting potentials of the sympathetic neurons ranged from 50–80 mv. The specific resistance and capacitance of the cell membrane were 456.4 $\Omega \cdot cm^2$ and 24.4 $\mu f/cm^2$, respectively.

3. The voltage-current relation of the cell membrane is approximately linear. Only a small number of cells showed a rectifying characteristic.

4. The antidromic volley set up an action potential of approximately 90 mv. (overshoot of 25 mv.) with a duration of 2.2–4 msec., being followed by a long-lasting hyperpolarizing after-potential.

5. The antidromic responses often had an inflection on the rising phase and were separated by the hyperpolarization of the cell membrane into three component spikes which had different sites of origin (axon, initial segment, and soma spikes).

6. Intracellular direct stimulation evoked an action potential similar to the antidromic response. The direct response revealed an inflection on its rising phase during experimentally applied hyperpolarizations, and could also be separated at this inflection. The latter occurred earlier in the rising phase of the spike than in the antidromic case, indicating that the proximal part of the axon (IS segment) was first excited and the soma activated later.

7. The orthodromic volley set up a response of 85 mv. which was always preceded by an initial depolarizing phase (synaptic potential), forming a step at approximately 25 mv. from the resting membrane potential. The orthodromic response often had a small hump immediately after its crest, also a relatively longer falling phase and smaller after-potential. The mode of spike production is supposed to be similar to that of directly evoked action potentials by intracellular stimulation.

8. The synaptic potential reached a summit in 3 msec. and lasted for approximately 40 msec. Its time constant was usually slightly larger than that of the cell membrane.

9. When the membrane was depolarized to a particular level, the synaptic potential was annulled. At any other level the amplitude of the synaptic potential was proportional to the displacement from the reversal level; its deflection being directed towards this level (−14.3 mv.).

ACKNOWLEDGMENT

The authors wish to thank Miss Y. Kimura for assistance in preparing the manuscript for publication.

LITERATURE CITED

Araki, T., and T. Otani 1955 Response of single motoneurones to direct stimulation in toad's spinal cord. J. Neurophysiol., *18:* 472–485.

Brock, L. G., J. S. Coombs and J. C. Eccles 1952 The recording of potentials from motoneurones with an intracellular electrode. J. Physiol., *117:* 431–460.

Coombs, J. S., J. C. Eccles and P. Fatt 1955 The electrical properties of the motoneurone. Ibid., *130:* 291–325.

Coombs, J. S., D. R. Curtis and J. C. Eccles 1956 Time course of motoneuronal responses. Nature, *178:* 1049–1050.

——— 1957a The interpretation of spike potentials of motoneurones. J. Physiol., *139:* 198–231.

——— 1957b The generation of impulses in motoneurones. Ibid., *139:* 232–249.

De Castro, F. 1932 Cytology and Cellular Pathology of the Nervous System. Hoeber, New York.

del Castillo, J., and B. Katz 1954 The membrane change produced by the neuromuscular transmitter. J. Physiol., *125:* 546–565.

Eccles, J. C. 1955 The central action of antidromic impulses in motor nerve fibers. Pflüg. Arch. Ges. Physiol., *260:* 385–415.

Eccles, R. M. 1955 Intracellular potentials recorded from a mammalian sympathetic ganglion. J. Physiol., *130:* 572–584.

Fatt, P., and B. Katz 1951 An analysis of the end-plate potential recorded with an intracellular electrode. J. Physiol., *115:* 320–369.

Fatt, P. 1957 Sequence of events in synaptic activation of a motoneurone. J. Neurophysiol., *20:* 61–80.

Frank, K., and M. G. F. Fuortes 1955 Prespike potentials in elements of spinal cord. Am. J. Physiol., *183:* 616–617.

Fuortes, M. G. F., K. Frank and M. D. Becker 1957 Steps in the production of motoneuron spikes. J. Gen. Physiol., *40:* 735–752.

Huber, B. C. 1899 A contribution on the minute anatomy of the sympathetic ganglia of the different classes of vertebrates. J. Morphol., *17:* 27–90.

Ito, M. 1957 The electrical activity of spinal ganglion cells investigated with intracellular microelectrodes. Jap. J. Physiol., *7:* 297–323.

Koketsu, K., and S. Nishi 1957 Action potentials of single intrafusal muscle fibers of frogs. J. Physiol., *137:* 193–209.

Koketsu, K., J. A. Cerf and S. Nishi 1959 Effect of quaternary ammonium ions on electrical activity of spinal ganglion cells in frogs. J. Neurophysiol., *22:* 177–194.

Nishi, S., and K. Koketsu 1959 Membrane characteristics of sympathetic ganglion cells and synaptic transmission in sodium-free hydrazinium solution. Fed. Proc., *18:* 114.

The Effects of Temperature on Some Mechanochemical Properties of Actomyosin Fibers

I. DYNAMIC PROPERTIES[1,2]

BERNARD D. TUNIK
Department of Zoology, Columbia University, New York, N. Y.[3]

The nature of the tension-bearing forces of resting and active muscle and its models has been considered pertinent to theories describing the mechanochemical events underlying contraction (Aubert, '56; Buchtal, '51; Feng, '32; Hill, '51, '52; Hill et al., '50; Meyer and Picken, '37).

These forces may arise from an increase of potential energy or a decrease of entropy with increasing length. The nature of these forces has been deduced from the sign of the temperature change caused by a stretch applied to whole muscle (Hill, '52, '53). However, there are present in muscle complicating passive structural elements, in series and in parallel with the contractile elements. As a result, the sign of the temperature change observed may not be characteristic of the tension-bearing forces of the contractile elements.

These complicating structures are absent in a model of muscle, the actomyosin fiber. Nevertheless, as in muscle, the response of these fibers to deformation is complex, consisting of rapid and retarded components (Hayashi and Rosenbluth, '53, '54; Joseph, '52). It has been found by these authors that ATP affects the retarded response to deformation, but not the rapid response. A mechanical model has been proposed (Hayashi and Rosenbluth, '53) that describes the fiber behavior in terms of a rapidly responding passive element connected in series with a slowly responding contractile element.

These components of the response of the fiber to deformation may be due to rapid and retarded processes within a homogeneous macromolecular structure, as is the case for any high polymer (Alfrey, '48). If so, the nature of the tension-bearing forces of this model, as deduced from the sign of the net tension change accompanying a causative temperature change (Botts and Morales, '51), may be pertinent to theories describing the mechanochemical events underlying contraction. However, the rapid and retarded components of the response of the fiber to deformation may be due to separate rapid and retarded structural elements, connected in series, in a heterogeneous macromolecular structure. If so, the nature of the tension-bearing forces of the retarded, contractile element alone would be pertinent to such theories, not that of the whole fiber.

The dynamic responses of the tension of actomyosin fibers to a quick stretch, in both low salt and ATP-$MgCl_2$, are examined in this portion of the investigation. Differences in the effects of temperature on the rapid and retarded components of these responses are interpreted as supporting the hypothesis that separate passive and contractile structural elements exist.

EQUIPMENT

Tensions were measured by a quartz cantilever (12, fig. 1) previously used (Hayashi et al., '58). Slowly changing tensions could be read to ± 0.12 mg with the least sensitive lever employed. Transient tensions, i.e., the peak tension resulting from a quick stretch and the minimum tension resulting from a quick release, could

[1] Submitted in partial fulfillment of the requirements for the degree of Doctor of Philosophy in the Faculty of Pure Science, Columbia University, 1959.

[2] This investigation was supported by Predoctoral Fellowships to the author from the National Institutes of Health, U.S.A., and in part by grants to Dr. Teru Hayashi from the Muscular Dystrophy Association of America, Inc.

[3] Present address: Department of Anatomy, School of Medicine, University of Pennsylvania, Philadelphia, Pa.

be determined to ±5%. The departure from isotonicity of isometric contractions was 0.2% or less.

Length changes, produced in the fiber by vertical motion of a screw (5) having 20 threads per inch, were measured by a linear scale (2) and cylindrical vernier (4) to $\pm 2.5 \times 10^{-3}$ mm ($\pm 10^{-4}$ in.). By means of a knurled knob (1) the screw could be rotated by hand through one complete revolution, or less, at the rate of circa 0.2 sec./rev. A stop (3), that could be clamped to the vernier, made it possible to simultaneously observe the lever and subject the fiber to a quick stretch or release of any predetermined size less than 1.3 mm (0.05 in.). In this way the peak tension developed by a stretch or the minimum tension resulting from a release could be easily observed. The motion of the screw, opposed by a strong spring (10), was transferred to the lower end of the fiber (18) via a base (8), dovetail (7), and carriage (9) to which the reaction vessel (16) was fastened. The lower end of the fiber was fixed to the reaction vessel by a hook embedded in a paraffined lead weight (19). Applied stretches were reduced no more than 10% by displacement of the lever at the suspension (20). No corrections have been made for this reduction.

Temperature control was obtained with a water bath supplied from reservoirs held at 20 ± 0.05°C and −1.5 ± 0.05°C. The bath temperature could be changed the full range in 30 sec. The temperature

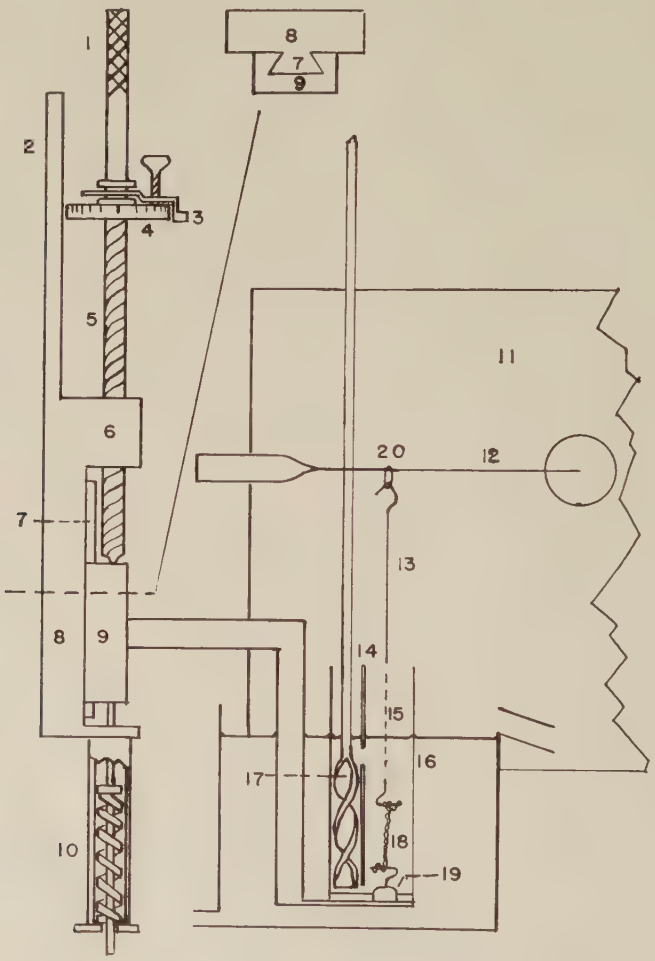

Fig. 1 Apparatus. For details see text.

of the reaction vessel contents, measured to ±0.1°C by a copper-constantan thermocouple, was kept uniform by means of an archimedean screw stirrer (17) which completely mixed the vessel contents in 10 sec. A plastic partition (14) with openings at the top and bottom reduced disturbance of the fiber without interfering with circulation.

MATERIALS AND METHODS

1. *Reagents and solutions*

Single distilled water passed once through 50 cm of Amberlite MB-3 ion-exchange resin was used throughout. Chemicals were commercial reagent grade except where noted.

Neutralized ATP. The crystalline disodium salt (Sigma Chemical Co.) was dissolved in water, adjusted to pH 7.6 with KOH and diluted to a final concentration of 6.4×10^{-2} M ATP.

Stock $MgCl_2$ solution. The calculated amounts of HCl and $MgCO_3$ were adjusted to pH 7.0 and diluted to 10^{-1} M.

Trough substrate. This was a solution of 0.05 M KCl in 1/10 strength Veronal buffer, pH 7.0.

Low salt. This consisted of 0.05 M KCl in 1/10 strength Veronal buffer, pH 7.6.

ATP-$MgCl_2$. This was a solution of 3×10^{-3} M neutralized ATP and 10^{-3} M $MgCl_2$ in low salt.

2. *Actomyosin*

This was prepared from rabbit back and leg muscles by a modification of the procedure of A. Szent-Györgyi (see Hayashi, '52).

3. *Fibers*

Preparation. A diluted actomyosin solution was surface-spread by the method of Hayashi (Hayashi and Rosenbluth, '52) at room temperature on the trough substrate in a 100 ×10 cm trough for 6 minutes. The surface film was then completely compressed between lucite barriers. These were moved from both ends of the trough toward the center, 30 cm during the first minute of compression, 13 cm during the second minute and 7 cm during the last. The dilution of the stock actomyosin solution was adjusted so that striae, which form in the surface film parallel to the barriers, were first visible when the barriers were circa 10 cm apart; and so that the collapse of the film caused its lateral edges to retract from the barriers when these were circa 5 cm apart. These standardized procedures resulted in films, and therefore fibers, of approximately equal protein content.

Mounting. This was accomplished by affixing the ends of a uniform portion of the fiber, still in the trough, to the suspension hook and weighted hook. Hooks and slack fiber were quickly removed from the trough and immersed in a measured amount of low salt in the reaction vessel. During the transfer, evaporation of water from the fiber was reduced by keeping the fiber in contact with the paraffined surface of the weight. The reaction vessel was raised so that the fiber remained slack when the suspension was hooked onto the lever.

Equilibrium length. This was defined and determined under each condition of temperature and chemical environment as follows: The ends of the mounted slack fiber were separated a standard amount by lowering the bottom hook 0.6350 cm every 30 sec. The position of the lever was noted just before each succeeding standard separation. When the change of the lever position produced by a standard separation finally increased markedly, the fiber was released 0.3175 cm. The free length between the hooks, never less than 10 mm, was taken as equilibrium length L_e. It was measured with a cathetometer to ±1%. The equilibrium position of the lever at this length was considered as indicating zero tension.

Changes of the reaction mixture. The change from low salt to ATP-$MgCl_2$ was accomplished by adding 0.16 cm^3 stock $MgCl_2$, 0.09 cm^3 Veronal buffer, pH 7.6 and 0.75 cm^3 neutralized ATP, in that order, to 15 cm^3 low salt in the reaction vessel.

Cycling. This was a standard treatment in which each fiber was subjected to a length determination followed by a fixed number of stretch-holds and release-holds (fig. 2). Each stretch, the same size as the first, was followed by a 6-minute hold. After at least 6 of these standard stretch-holds, the fiber was released to its original

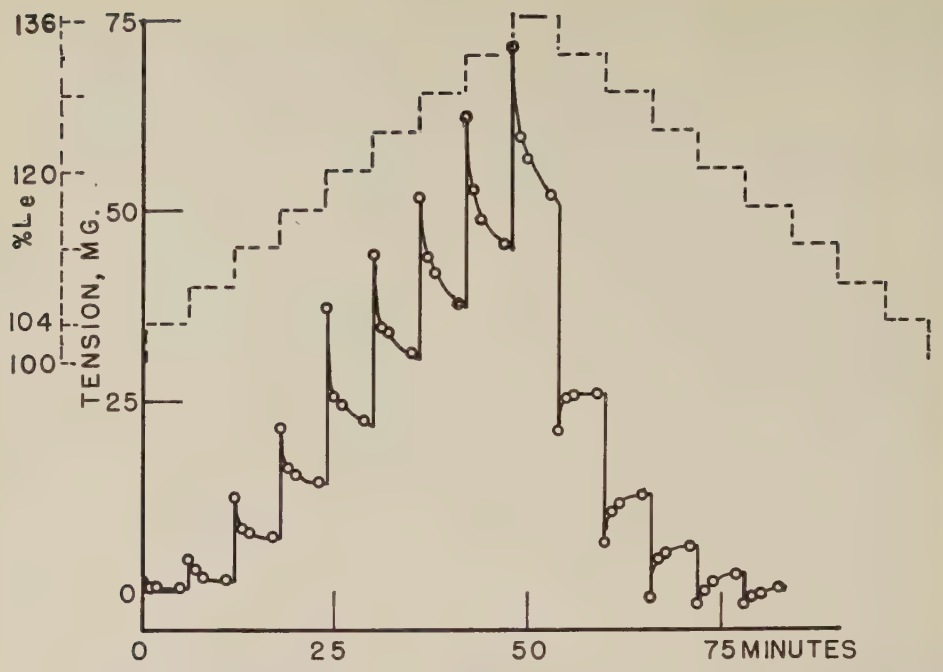

Fig. 2 The time relationships of a cycle. Conditioned fiber in low salt. Ordinates: tension, —○—; relative length, – – – –. Abscissa: time. Each quick stretch was followed by a 6-minute hold accompanied by a decay. Releases were continued to 100% L_e even though the tension had reached zero at 116% L_e.

equilibrium length by an equal number of standard release-holds. Each quick release was the same size as the preceding quick stretches, and each hold also lasted 6 minutes. The new, longer equilibrium length was then determined. It served as the initial equilibrium length for the next series of standard stretch-holds and release-holds, which was started immediately. In this series the stretches and releases were the same size, in terms of per cent initial equilibrium length, as those of the first series. The number of stretch-holds and release-holds were also the same in the second series as the first. Each series of standard stretch-holds and release-holds is referred to as a cycle.

EXPERIMENTS AND RESULTS

Both rapid and retarded responses to deformation are revealed by a stretch-hold. These are: a rapid increase of tension during the stretch; and a slow decay during the hold (Joseph, '52; fig. 2). These responses were obtained over an extended range of lengths and tensions by the cycling process described in the Materials and Methods section.

A. Native fibers

Freshly formed fibers, otherwise untreated, will be termed native fibers. These were cycled a number of times in low salt at 20°C.

The tension at each length after a 5-minute decay was the result of both the rapid and retarded responses (fig. 2). For this reason, the general response to the stretch-hold portion of each cycle may be represented, in a plot relating length and tension (fig. 3), by the slope of a line through the 5-minute tension points of each decay. The general response slopes of the succeeding cycles were more alike than those of the first and second cycles, and were steeper than the general response slope of the first cycle (fig. 3). However, the general response slope in a given cycle was found to decrease towards that of the preceding cycle if the peak tension of the preceding cycle was exceeded (cf. cycles 1 and 2, fig. 3).

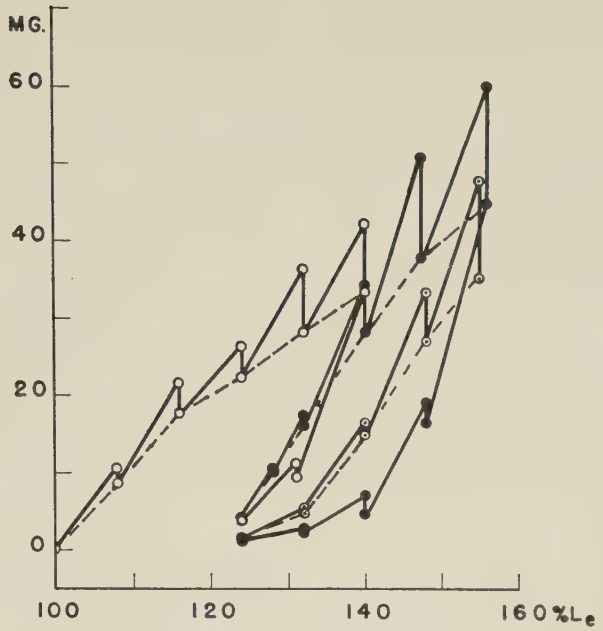

Fig. 3 Three cycles at 20°C. Native fiber in low salt. Ordinate: tension. Abscissa: relative length. First cycle, ○; second cycle, ●; third cycle, ⊙. Each decay is represented by a vertical line. The general response is summarized by the dashed line connecting the 5-minute tension at each length. Note the change of slope of this line between the last two points of the stretch-hold portion of the second cycle. For details see text. The steep initial portion of the first cycle is atypical; usually, the slope of the general response in the stretch-hold portion of a cycle increases with length, as in the second and third cycles.

The first cycle thus conditioned the fiber so that the changes in the general response, resulting from subsequent cycles, were appreciably reduced. This reduction was also true for changes in the set (i.e., change of equilibrium length) (fig. 3), and for changes in the rapid and retarded responses (figs. 5 and 8. For details see B. below). For these reasons, in all further experiments native fibers were subjected to a preliminary cycle in low salt at 20°C. Fibers treated in this way will be referred to as conditioned fibers. To eliminate the change of the general response slope discussed above, the peak tensions of the subsequent cycles were kept below that of the conditioning cycle. This was accomplished by subjecting the fiber to fewer and smaller standard stretches in the subsequent cycles than in the conditioning cycle.

B. Conditioned fibers in low salt

In a control experiment designed to determine the effects of cycling alone on the rapid and retarded responses, conditioned fibers were cycled 5 times at 20°C.

To determine the effect of temperature on these responses, each of several conditioned fibers was cycled first at 20°C, then at 0°C and again at 20°C; other conditioned fibers were cycled first at 0°C, then at 20°C and again at 0°C. Each temperature sequence served both as an additional control of the effect of cycling and as a test of the reversibility of any temperature effect that might occur.

1. *The retarded response.* As noted before, this is a slow decay of tension. The tension during each decay, S_t, depends on both the time, t, elapsed from the onset of the decay and the peak tension, S_p, at $t = 0$. The decays obtained in a series of standard stretch-holds were progressively larger and occurred at increasing rates (fig. 2). However, these tension vs. time curves differed from each other by only constant factors. That is, when the tensions during each decay were normalized as per cent of S_p, the resulting normalized tension vs.

time curves followed the same time-course, within the error of determination of S_p (fig. 4); i.e.,

$$100\,(S_t/S_p) = f(t) \qquad (1)$$

It is evident from figure 4 that the loss of normalized tension during a 5-minute decay, $100\,(S_p - S_5)/S_p$ (where S_5 is the 5-minute tension) may be used as a convenient[4] measure of the normalized decay rate. As a corollary of (1), a plot of the loss of actual tension during each 5-minute decay, $(S_p - S_5)$, vs. S_p yields a straight line which must pass through the origin. The slope of the least squares line through the $(S_p - S_5)$, S_p points, forced through the origin, is thus a weighted average of the losses of normalized tension over a wide range of peak tensions. The numerical values of this slope will be referred to as the mean decay rate, or MDR.

The results seem contradictory (table 1,a). In some cases the MDR was greater at 20°C than at 0°C; in others the opposite was true; and in some cases the MDR decreased with cycling independently of the temperature change. The data derived from the control experiment described above show that cycling alone decreased the MDR (fig. 5).

2. *The rapid response.* As previously described, this is the increase of tension accompanying each quick stretch. The increase of quick stretch tension, ΔS_q, was recorded as the difference between S_5 of the preceding decay and the peak tension, S_p, resulting from each stretch.

For a series of quick stretches, $\Delta\%\,L_e$, of standard size in terms of per cent equilibrium length, ΔS_q increases with the fiber length (fig. 2). The stiffness of the rapid response can be expressed as the ratio $\Delta S_q/\Delta\%\,L_e$. The value of this ratio for each

[4] Neither the tension vs. time curves nor the normalized curves could be fitted by the sum of as many as three exponential terms in t over the initial 5 minutes of decay.

TABLE 1

Mean decay rate[1]

a. Conditioned fibers in low salt

Cycle no.	Fiber no.							
	II 6	II 14	III 24	III 69	III 72	III 79	III 82	III 77
1[2]	0.286[3]	0.257	0.608	0.622	0.531	0.572	0.624	0.607
2	0.150	0.224	0.511	0.564	*0.466*	*0.573*	*0.505*	*0.469*
3	*0.184*	*0.206*	*0.493*	*0.460*	0.389	0.506	0.462	0.469
4	*0.170*	0.244	0.528	0.400	*0.378*	—	*0.446*	*0.476*
5	0.155	—	—	—	—	—	—	—
6	0.166	—	—	—	—	—	—	—

b. Shortened fibers in ATP-$MgCl_2$. The $L_{es}20$—$L_{es}0$ comparison

Cycle no.	Fiber no.					
	II 132	III 9	III 13	III 92	III 95	III 101
1[2]	0.500	—	0.578	0.687	0.639	0.614
2	0.681	0.689	0.738	0.791	0.810	0.784
3	*0.475*	*0.575*	*0.637*	*0.698*	*0.706*	*0.614*
4	0.565	0.678	0.733	0.786	0.795	0.779

c. Unshortened fibers in ATP-$MgCl_2$ at 0°C compared to shortened fibers in ATP-$MgCl_2$ at 20°C. The $L_{eu}0$—$L_{es}20$ comparison

Cycle no.	Fiber no.			
	III 17	III 21	III 75	III 84
1[2]	0.639	0.591	0.531	0.478
2	*0.661*	*0.530*	*0.423*	0.532
3	0.728	0.729	0.519	0.680

[1] Defined in text.
[2] The first cycle is the conditioning cycle in low salt.
[3] Cycle at 20°C. Italic figures refer to cycles at 0°C.

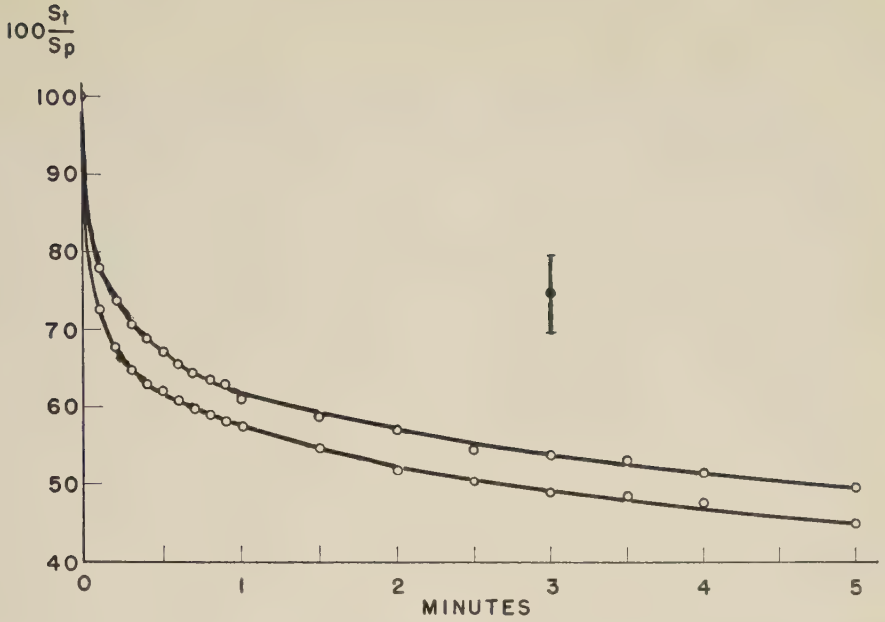

Fig. 4 Decay curve. Conditioned fiber in low salt. Ordinate: tension, S_t, normalized with respect to S_p, the peak tension at the onset of the decay. Abscissa: time. The curves are extremes of 6 consecutive decay curves in the stretch-hold portion of a single cycle. The bar represents the error of determination of S_p, as $\% S_p$.

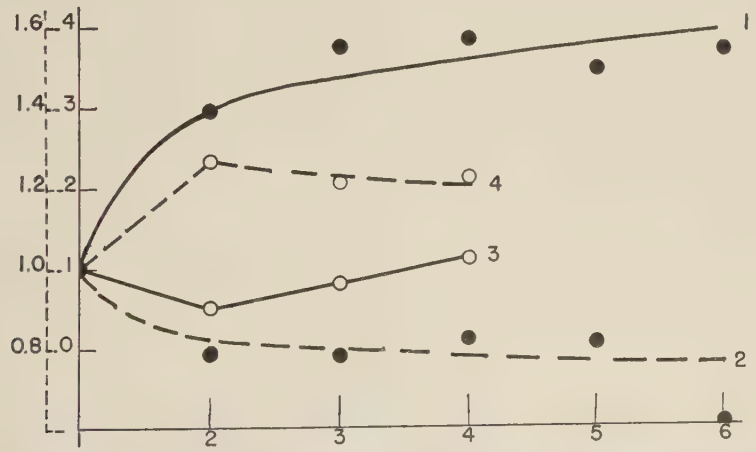

Fig. 5 The effects of cycling at constant temperature. Ordinate: ratio of the general response slope ——, or of the MDR – – – –, of any cycle, to that of the first, conditioning cycle. Abscissa: cycle number; the first cycle is the conditioning cycle. Conditioned fibers in low salt, ●; fibers shortened in ATP-$MgCl_2$, ○. Note change of scale for the MDR.

of the quick stretches of a cycle was plotted (fig. 6) vs. the average tension[5] during each stretch, $(S_5 + \Delta S_q/2)$ (where S_5 is the 5-minute tension of the preceding decay). No effect of temperature on the rapid response stiffness is apparent. This is in accord with results obtained in a previous study of these fibers (Hayashi and Rosenbluth, '54).

[5] Tension, dependent on time and length during each cycle, was chosen in preference to length, which was an independent variable.

An approximation of the length vs. tension curve[6] of the rapid response was derived from the stiffness of the rapid response. For each stretch the ratio $\Delta\% L_e/\Delta S_q$ is an approximation of the slope dL/dS_q of such a curve at the tension $(S_s + S_q)/2$; that is

$$\Delta\% L_e/\Delta S_q = dL/dS_q = p'(S_q)$$

Thus, when the curve obtained by plotting $\Delta\% L_e/\Delta S_q$ vs. $(S_s + \Delta S_q/2)$ was integrated graphically with respect to tension, an approximation (fig. 7, e.g.) of the curve $L = p(S_q)$ was obtained. The derived areas were numerically equal to differences of $\% L_e$. These, and the related differences of S_q, were located with respect to the origin by the values of ΔS_q and $\Delta\% L_e$ of the initial stretch.

This treatment of the data revealed a temperature effect not immediately evident from inspection of either the rapid response stiffness itself, or the slopes of the derived curves (cf. fig. 6 and Hayashi and Rosenbluth, '54 to fig. 7). The obvious effect of temperature is a change of the quick stretch tension at a given length, $(S_q)_L$. This tension was either greater at 20°C than at 0°C for either temperature sequence (figs. 7a, 7b) or differed very little from cycle to cycle (fig. 7c). The data of the control experiment (see B.), when treated as described above, showed that cycling alone increased $(S_q)_L$ (fig. 8).

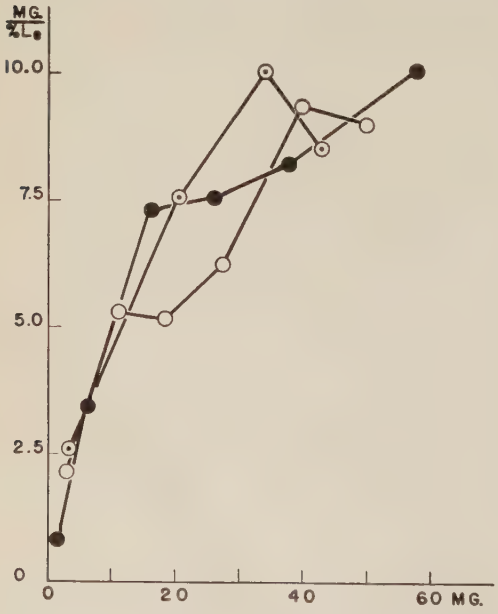

Fig. 6 The rapid response stiffness. Conditioned fiber in low salt. Ordinate: rapid response stiffness. Abscissa: average tension during the stretch. First cycle, 20°C, ○; second cycle, 0°C, ●; third cycle, 20°C, ⊙.

C. Conditioned fibers in ATP-$MgCl_2$

In contrast to conditioned fibers in low salt, which have a unique equilibrium length reversibly altered by temperature changes (Tunik, '60), conditioned fibers in ATP-$MgCl_2$ have two possible equilibrium lengths which depend on the treatment of the fiber. These are:

1. The shortened equilibrium length, L_{e_s}, reversible altered by changes of temperature (Tunik, '60). This was obtained at 20°C by releasing a conditioned fiber to 30% of its equilibrium length in low salt. When the reaction mixture was converted to ATP-$MgCl_2$, the fiber contracted freely to L_{e_s}, which was determined by the procedure described in the Materials and Methods section.

2. The unshortened equilibrium length, L_{e_u}. This was obtained by treating the fiber as described in 1. above, but at 0°C. No detectable shortening occurred. When the temperature was raised to 20°C the fiber shortened irreversibly to L_{e_s}; that is, return to L_{e_u} at 0°C was possible only via an applied stretch (Tunik, '60).

C(a). Conditioned fibers shortened in ATP-$MgCl_2$

In a control experiment these fibers were cycled several times in ATP-$MgCl_2$ at 20°C. This tested the effects of ATP-$MgCl_2$ and shortening on the conditioned state, and the effects of cycling alone on the various responses. The MDR of these fibers changed as slowly with cycling as did the MDR of conditioned fibers in low salt (fig. 5; cf. curves 2 and 4). This was also true for the general response slope (fig. 5; cf. curves 1 and 3). Thus the result of conditioning, which is a reduction of the effect of cycling on the responses of the fiber, was not reversed by treatment with ATP-$MgCl_2$ and shortening.

[6] If decay curves differ by a constant factor only, the variables time and length are separable and a length vs. tension curve may be obtained (Guth, '47).

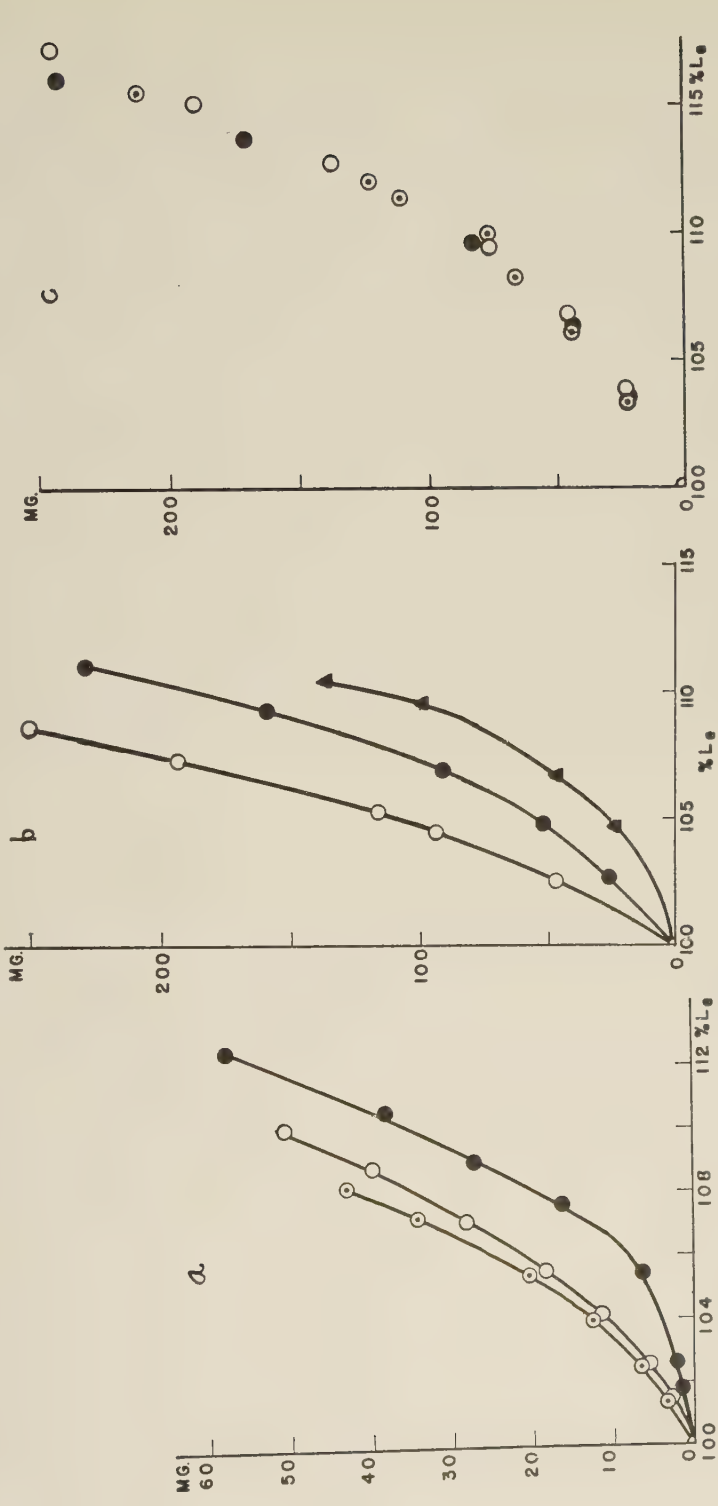

Fig. 7 Derived length vs. tension curve for the rapid response. Conditioned fiber in low salt. Ordinate: quick stretch tension, S_q. Abscissa: per cent original equilibrium length, $\%L_e$. a, First cycle, 20°C, ○; second cycle, 0°C, ●; third cycle, 20°C, ⊙. b, First cycle, 0°C, ●; second cycle, 20°C, ○; third cycle, 0°C, ▲. c, Symbols as in a. The curves have been ommitted to avoid confusion.

To determine the effects of temperature on the rapid and retarded responses, each of several conditioned fibers, shortened in ATP-$MgCl_2$, were cycled in this solution, starting from L_{e_s}, first at 20°C, then at 0°C, and again at 20°C.

1. *The retarded response.* The MDR was greater at 20°C than at 0°C (table 1,b). Data derived from the control experiment described above shows that cycling alone decreased the MDR (fig. 5).

2. *The rapid response.* The quick stretch tension at any given length, $(S_q)_L$, was either greater at 20°C than at 0°C (fig. 9a), or increased with cycling independently of the temperature change (fig. 9b). Data derived from the control experiment showed that cycling alone increased $(S_q)_L$.

C(b). Conditioned fibers not shortened in ATP-$MgCl_2$

The equilibrium length, L_{e_u}, of a conditioned fiber in ATP-$MgCl_2$ was determined at 0°C. The fiber was then cycled at this temperature. The effects of temperature on the characteristics of the rapid and retarded responses of the fiber in the unshortened state could not be determined, since the fiber shortened freely to L_{e_s} when the temperature was raised to 20°C. The characteristics of these responses of the fiber in the shortened state were nevertheless determined by cycling the fiber, after shortening, at 20°C. The stretches of this second cycle, at 20°C, were made equal to those of the first cycle, at 0°C, in terms of the respective equilibrium lengths.

1. *The retarded response.* The MDR of the shortened fiber, at 20°C, was greater than that of the unshortened fiber, at 0°C (table 1,c).

2. *The rapid response.* The quick stretches were expressed as per cent equilibrium length for each state of the fiber. Accordingly, $(S_q)_L$ was plotted vs. % L_{e_s} for the length vs. tension curve of the shortened fiber, at 20°C, and vs. % L_{e_u} for the curve of the unshortened fiber, at 0°C. In some cases $(S_q)_L$ was greater at 20°C than at 0°C, increasing with cycling (fig. 10a). In others, in contrast to results so far described $(S_q)_L$ was smaller at 20°C than at 0°C, decreasing with cycling (fig. 10b).

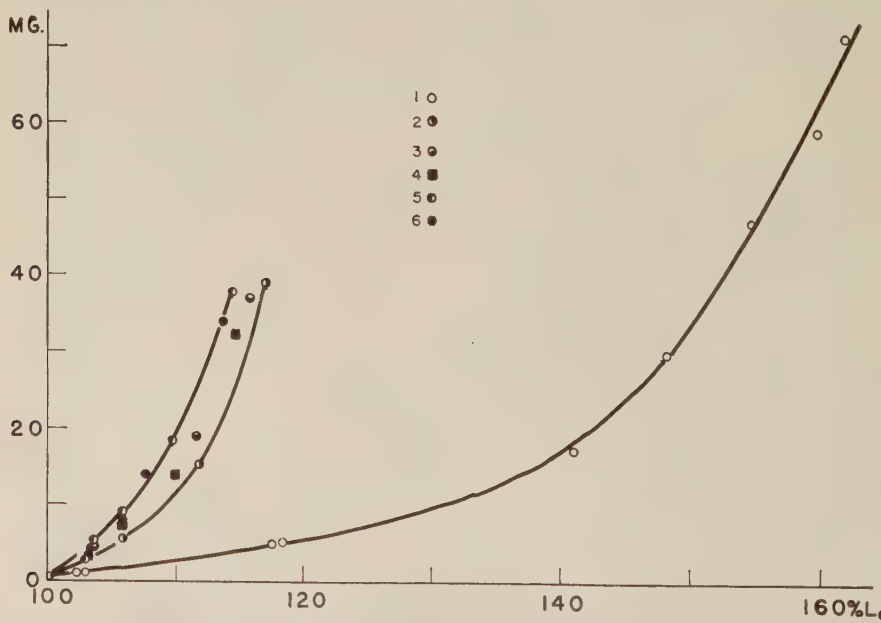

Fig. 8 Derived length vs. tension curve for the rapid response. The effect of cycling at constant temperature. Conditioned fiber in low salt. Ordinate: quick stretch tension, S_q. Abscissa: per cent equilibrium length at the start of each cycle, % L_e. Numbers adjacent symbols refer to the cycle; cycle 1 is the conditioning cycle. Curves for cycles 3, 4 and 5 have been ommitted for clarity.

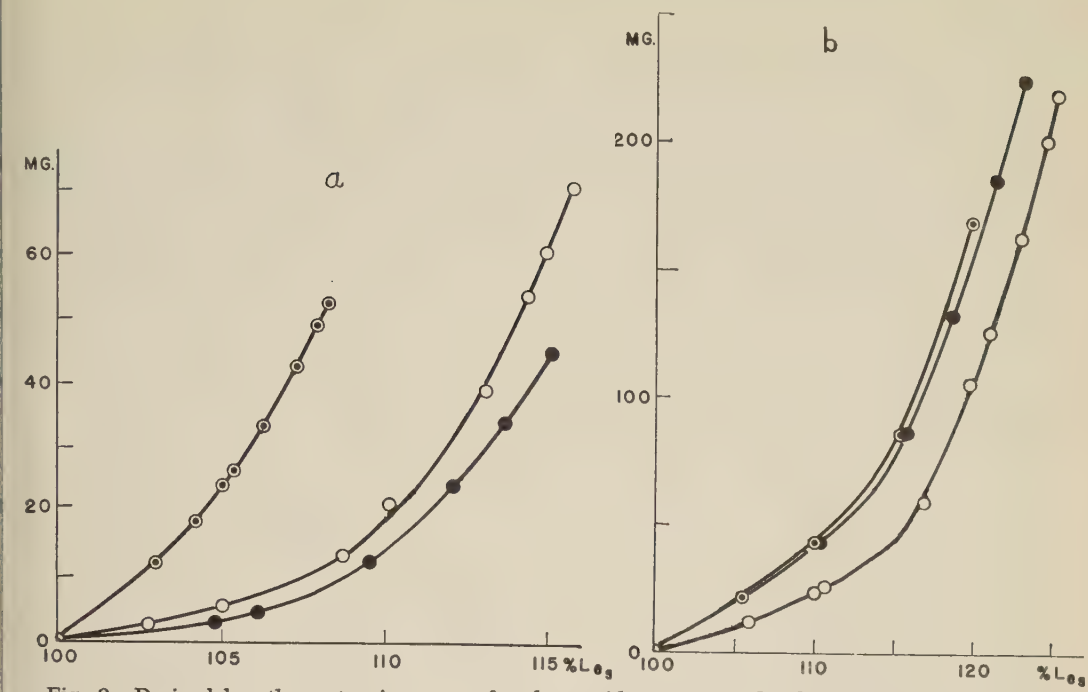

Fig. 9 Derived length vs. tension curve for the rapid response. Conditioned fiber shortened in ATP-$MgCl_2$. Ordinate: quick stretch tension, S_q. Abscissa: per cent shortened equilibrium length, % L_{eq}. Symbols as in figure 7a.

DISCUSSION

I

The effects of temperature alone on the rapid and retarded responses may be deduced by correlating the control experiments, in which cycling alone affected these responses, with those experiments in which both cycling and temperature changes affected these responses. The control experiments show that repeated cycling at constant temperature decreased the MDR (fig. 5) and increased $(S_q)_L$ (fig. 8) at a decreasing rate. When the temperature was changed from cycle to cycle, any effect of temperature on these responses would have been modified by the effects of cycling.

For three successive cycles at constant temperature it follows from figure 5 that the MDR of the second cycle should be intermediate between that of the first and third cycles, and closer to that of the third cycle. As the temperature was changed from cycle to cycle, these relations were obtained in fibers III 72 and III 82 (table 1,a). This data suggests either that there was no effect of temperature on the MDR or that, if a temperature effect existed, it was smaller than the effect of cycling. In fiber II 6 (table 1,a) the MDR did not decrease regularly with cycling, but was greater in the second and third cycles, at 0°C, than in either the first or 4th cycles, at 20°C. This data clearly indicates that the MDR was greater at 0°C than at 20°C. The data of fibers II 14 and III 24 (table 1, a) lead to the opposite conclusion; that the MDR was greater at 20°C than at 0°C. When the data of only two cycles was available, and the MDR decreases with cycling, as in fiber III 77 (table 1,a), the temperature effect cannot be directly determined from the data.

From correlations similar to the above, some qualitative conclusions about the effects of temperature follow. These are:

1. The MDR of a conditioned fiber shortened in ATP-$MgCl_2$ was greater at 20°C than at 0°C. The MDR of a conditioned fiber in the shortened state in ATP-$MgCl_2$ was greater at 20°C than the MDR

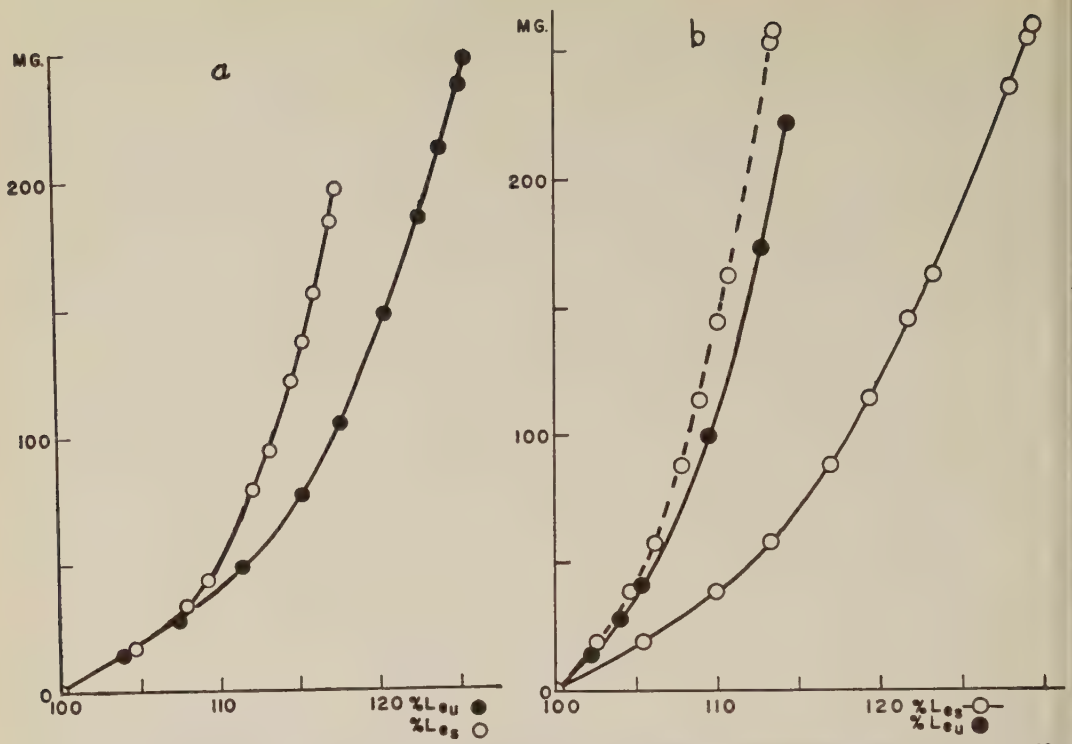

Fig. 10 Derived length vs. tension curve for the rapid response. Conditioned fiber in ATP-$MgCl_2$. The unshortened state at 0°C, first cycle, ●, compared to the shortened state at 20°C, second cycle, ○. a, Abscissa: per cent shortened equilibrium length at 20°C, % L_{es}, and per cent unshortened equilibrium length at 0°C, % L_{eu}. Ordinate: quick stretch tension, S_q. b, Ordinate and abscissa as in a. Dashed curve is the derived curve for the shortened state at 20°C computed on the basis of the unshortened equilibrium length, % L_{eu}.

TABLE 2
Temperature and cycling coefficients[1]

Coefficient	Mean decay rate	$(S_q)_L$[2]
a. Conditioned fibers in low salt		
a	+0.0137	+0.338
b	−0.0310	+0.127
b. Shortened fibers in ATP-$MgCl_2$		
a	+0.176	+0.271
b	−0.00234	+0.247
c. Unshortened fibers in ATP-$MgCl_2$ at 0°C compared to shortened fibers in ATP-$MgCl_2$ at 20°C		
a	(+0.247)[3]	(−0.983)[3,4] (+0.464)[3,5]

[1] Defined in the text.

[2] Means computed from individual values of a taken at integer values of $(S_q)_L$; see table 3 and text.

[3] Computed by assuming b has the same value as in table 2(b).

[4] Integer values of $(S_q)_L$ taken from curves based on L_{es} at 20°C and L_{eu} at 0°C.

[5] Integer values of $(S_q)_L$ taken from curves based on L_{eu} only.

of this fiber in the unshortened state in ATP-$MgCl_2$ at 0°C.

2. Where the effect of temperature could be directly determined, the $(S_q)_L$ of a conditioned fiber in low salt, and of a conditioned fiber shortened in ATP-$MgCl_2$, was greater at 20°C than at 0°C. The MDR of a shortened fiber in ATP-$MgCl_2$ at 20°C was greater than the MDR of this fiber in the unshortened state in ATP-$MgCl_2$ at 0°C.

II

The temperature effects discussed above can be separated from the concurrent effects of cycling and expressed quantitatively as follows:

Let y represent either the MDR or $(S_q)_L$. If y were not affected by cycling, a temperature coefficient, a, could be defined by the relation

$$y_{20^\circ} = y_{0^\circ} + a(y_{0^\circ}) \qquad (2)$$

At constant temperature, the effects of cycling on y can be expressed in terms of a cycling coefficient, b, defined by the relation

$$y_{n+1} = y_n + b(y_n) \quad (3)$$

where n signifies the nth cycle. In the actual experiments both temperature and cycling effects occurred together; this may be expressed by combining[7] (2) and (3) to give

$$y_{n+1,\,20^\circ} = y_{n,\,0^\circ} + a(y_{n,\,0^\circ}) + b(y_{n,\,0^\circ}) \quad (4)$$

$$y_{n+1,\,0^\circ} = y_{n,\,20^\circ} - a(y_{n,\,20^\circ}) + b(y_{n,\,20^\circ}) \quad (5)$$

from which

$$R_1 \equiv y_{n+1,\,20^\circ}/y_{n,\,0^\circ} = 1 + a + b \quad (6)$$

$$R_2 \equiv y_{n+1,\,0^\circ}/y_{n,\,20^\circ} = 1 - a + b \quad (7)$$

whence

$$a = (R_1 - R_2)/2 \quad (8)$$

$$b = (R_1 + R_2 - 2)/2 \quad (9)$$

For the MDR, the coefficients a and b were evaluated from the weighted mean values of the individual ratios R_{1i} and R_{2i} computed for each fiber. For $(S_q)_L$ the individual ratios were taken at integer values of $\%\,L_e$, and temperature coefficients were computed for each value of $\%\,L_e$ (table 3).

III

From these temperature coefficients and a proposed (Alfrey, '48) macromolecular basis for the behavior of homogeneous, oriented, three-dimensionally cross-bonded high polymers, a heterogeneous mechanochemical structure of the actomyosin fiber is deduceable. The validity of this deduction rests on the validity of these concepts, which are continually changing (see Flory, '56a, '56b) and on the validity of treating the actomyosin fiber as such a polymer. For these reasons the final conclusions arrived at are presented with strong reservations.

A. The following summarizes the proposed (Alfrey, '48) macromolecular basis for high polymer behavior. The polymer molecules in a fiber of the designated polymer type are divided by the cross-bonds into flexible chain-like segments. The distance between the ends of each segment is varied by thermokinetic forces. For each distance the segment assumes a different curled configuration. All configurations are assumed to be at the same potential energy level. When the fiber is at equilibrium length, each segment has an equilibrium configuration possessing maximum configurational entropy. When the fiber is stretched, the distance between the ends of

[7] It is assumed that b is constant over the small range of three cycles, and independent of a; and that a is constant over the small range of absolute temperature studied, and independent of b.

TABLE 3

Temperature coefficients of $(S_q)_L$ at integer values of $\%\,L_e$

a. Conditioned fiber in low salt		b. Shortened fiber in ATP-$MgCl_2$		c. Unshortened fiber in ATP-$MgCl_2$ compared to shortened fiber in ATP-$MgCl_2$		
$\%\,L_e$	a	$\%\,L_{es}$	a	$\%\,L_{eu}$ or $\%\,L_{es}$	a^1	$a^{1,2}$
101	+0.405	101	+0.182	101	−1.025	−0.227
102	+0.380	102	+0.267	102	−1.020	+0.095
103	+0.380	103	+0.291	103	−1.029	+0.220
104	+0.398	104	+0.282	104	−1.006	+0.307
105	+0.392	105	+0.346	105	−1.002	+0.430
106	+0.400	106	+0.289	106	−0.927	+0.564
107	+0.353	107	+0.328	107	−0.988	+0.617
108	+0.269	108	+0.245	108	−0.978	+0.671
109	+0.216	109	+0.234	109	−0.971	+0.721
110	+0.266	110	+0.277	110	−0.965	+1.243
111	+0.306	111	+0.265	111	−0.952	—
112	+0.322	112	+0.250	112	−0.937	—
mean	+0.338		+0.271		−0.983	+0.464

[1] Each coefficient computed from values of R_1 (see text) and an assumed value of b = +0.247, the value for shortened fibers in ATP-$MgCl_2$.

[2] Coefficients computed from curves based on $\%\,L_{es}$ only (see Discussion) and values of R_1 and b as in footnote above.

each segment increases as the segments uncurl to configurations of lower entropy. Also, entire molecules may be shifted past each other as cross-bonds are broken and reformed. When the fiber is released, each segment recurls under the influence of thermokinetic forces to its original equilibrium length of maximum entropy. The fiber itself, however, may not quite return to its original equilibrium length, due to the shifting of molecules; this process thus results in an increase of equilibrium length, or set.

Variation of the rate of the uncurling process is the basis for the rapid and retarded aspects of the response of the fiber to a quick stretch. The rate varies from extremely rapid for some structural elements to extremely slow for others. The molecular shifting also proceeds at a slow rate. The structural elements (i.e., segments, parts of segments, and cross-bonded combinations of segments) may be divided into two groups, based on the rate of stretch. The rapid elements are those whose components attain equilibrium configurations at a rate at least as rapid as that of the stretch. The retarded elements are those whose components attain equilibrium configurations more slowly. The abrupt rise of tension characteristic of the rapid response results from uncurling of the rapid elements to configurations of lower entropy, and from distortion of bond angles and distances. The slow decay of tension characteristic of the retarded response commences when the stretch is completed. This decay results from later stages of both the uncurling process of the retarded elements, and the molecular shifting process. The earlier stages of these processes, occurring during the stretch, reduce the effect of the stretch on the rapid elements.

B. The effect of temperature on the rapid response of the fiber to a quick stretch has been expressed as a temperature coefficient (defined in II) of the tension at any given length, $(S_q)_L$. That $(S_q)_L$ (derived in Experiments and Results, Section B. 2.) is an equilibrium tension is evident from the following: (a) The rapid elements by definition (see III, A) have attained equilibrium configurations at all times during a stretch. As a result, tensions exerted by these elements are equilibrium tensions. (b) These elements may be considered to be connected in series with the retarded elements, by virtue of the postulated cross-bonded structure of the fiber.[8] Consequently the fiber tension and the total tension exerted by the rapidly responding elements are equal. Thus a change of fiber tension, ΔS_q, is a change of equilibrium tension of these elements, and $(S_q)_L$, derived from $\Delta S_q/\Delta\% L_e$, is likewise such an equilibrium tension.

The concepts outlined in III, A lead via thermodynamic and statistical considerations to the following equation[9] relating equilibrium tension to relative elongation (Flory, '44):

$$S/A = (RT\rho/M_c)(a - 1/a^2) \qquad (10)$$

at constant length this may be written as:

$$(S)_L = (RTm/M_c)K \qquad (11)$$

From the above discussion it is evident that (11) is applicable to $(S_q)_L$. If thermokinetic forces alone affect $(S_q)_L$, i.e., M_c and m in (11) are independent of temperature, then the temperature coefficient of $(S_q)_L$ should be 0.073. Since it is circa 4 times larger (tables 2,a and 2,b), m and/or M_c must be temperature-dependent. Because there is no extra protein available in the reaction mixture, m remains constant. The larger value of the temperature coefficient thus results from the temperature dependence of M_c.[10] Evidently, M_c decreases as the temperature increases, i.e.,

---

[8] Wherever rapid elements are cross-bonded in parallel to retarded elements, the resulting compound structure behaves like a retarded element.

[9] Symbols for (10) and (11) are: S, equilibrium tension; A, area of average fiber coss-section; R, gas constant; T, absolute temperature; ρ, fiber density; M_c, average molceular weight of a segment, inversely proportional to the extent of cross-bonding; a, relative extension; m, mass of polymeric material; K, temperature independent constant.

[10] The occurrence during a stretch of the processes underlying the retarded response does not alter, but strengthens, this conclusion. As a result of this occurrence, the amount by which the rapidly responding elements are elongated by a stretch is reduced. This reduction is greater at higher temperatures, since the rate of the retarded response increases with temperature (see discussion, III, C). Consequently, if the rapidly responding elements were extended the full amount of, e.g., the first stretch, the ratio of the tension obtained at 20°C to that obtained at 0°C would be higher than that observed.

cross-bonding increases with temperature. This increase is nearly the same for fibers both in low salt (table 2,a) and shortened in ATP-$MgCl_2$ (table 2,b).

C. The effect of temperature on the retarded response of the fiber has been expressed as the temperature coefficient of the MDR (mean decay rate, defined in Experiments and Results, Section B. 1.). This effect may be considered as due to the temperature dependence of the rates of the uncurling and molecular shifting processes. These are essentially flow processes, according to the theory outlined in III, A. The flow units are small groups of chain atoms in the segments of the polymer molecules. It has been proposed (Eyring, '41) that the primary event in flow is the random jump of a flow unit, under the influence of thermokinetic forces, from one potential energy well to another over a potential energy barrier. Stress causes flow, i.e., the uncurling and molecular shifting processes, by biasing the direction of these jumps (Eyring, '41). The rate of the uncurling and molecular shifting processes, and therefore of the tension decay which they underlie, accordingly increases with the stress and the thermokinetic force, i.e., temperature; and decreases as the potential energy barrier increases.

This barrier to the jump of a flow unit is probably at least as high in the fiber as it is in water and many organic liquids, since the net effect of the intermolecular forces is greater in the fiber than in these liquids (e.g., the fiber sustains tension). From this estimate of the relative sizes of these barriers, it may be predicted, by applying the above concepts, and those presented in III, A, that the increase of the decay rate of the fiber tension with temperature should be at least of the same order of magnitude as the increase of the flow rate of these liquids with temperature.

For fibers in low salt, however, the temperature coefficient of the mean decay rate, MDR, (table 2,a) is at least one order of magnitude lower than that of the flow rate of liquids.[11] Apparently, increasing temperature produced changes in these fibers that compensate for the predicted increase of rate. The increase of cross-bonding with temperature (see III, B) produces changes that could be the source of this compensation. These are: (a) an increase of the height of the potential energy barrier; (b) at a given fiber tension, a decrease of the stress that biases the jumps of the flow units. Both of these changes tend to reduce the decay rate and thus oppose the increase of this rate resulting from the increase of thermokinetic force with temperature.

For shortened fibers in ATP-$MgCl_2$, the temperature coefficient of the MDR is circa 10 times larger than for fibers in low salt. It has been shown in III, B, however, that cross-bonding increases nearly as much in ATP-$MgCl_2$ as in low salt. Consequently the changes in the height of the potential energy barrier, and in the size of the biasing stress, would also be nearly the same for fibers in these two solutions. These changes may, as they did in fibers in low salt, oppose the increase of the decay rate in shortened fibers in ATP-$MgCl_2$. If so, then, to account for the higher temperature coefficient of the MDR in these fibers, the effect on the decay rate of increased thermokinetic force, as the temperature rises, must be greater for these fibers than it is for fibers in low salt. This greater effect could result from: (a) a reduction of the potential energy barrier as the temperature rises, and/or (b) a higher barrier in ATP-$MgCl_2$ than in low salt.[12] Alternative (a) is not compatible with the increase of this barrier with temperature resulting from increased cross-bonding. Alternative (b) must also be rejected for, if it were so, then at a given energy level of temperature and tension, the decay rate should be smaller in ATP-$MgCl_2$ than in low salt. The reverse is the case. At 0°C the average value of the MDR, corrected for the effects of cycling, is 0.616 for shortened fibers in ATP-$MgCl_2$, 0.391 for

[11] The temperature coefficient of the flow rate of liquids was computed from viscosity values for the liquids at 0°C and 20°C (Hodgman, '51), assuming Newtonian viscosity.

[12] Or (c) the effects of temperature on the mechanochemical events of contraction, which are probably reversed in the decay process (see Hayashi and Rosenbluth, '53). However, since the decay process involves movement of a flow unit over a potential energy barrier, the effects of ATP-$MgCl_2$ on this process results basically from the effects of ATP-$MgCl_2$ on the potential energy barrier, i.e., alternative (b).

fibers in low salt. The relative magnitude of these values is in qualitative agreement with results obtained in other isometric experiments (Joseph, '52) in which the effects of ATP on the retarded responses of the actomyosin fiber were studied; and with the results obtained in isotonic experiments on the glycerinated psoas (Bozler, '52, '56).

From this analysis it may be concluded that increased cross-bonding does not compensate for the increased effects of the thermokinetic force in shortened fibers in ATP-$MgCl_2$, i.e., it does not affect the decay rate. It may be further concluded that treating the conditioned fiber in low salt with ATP-$MgCl_2$ decreases cross-bonding. This latter conclusion parallels the interpretation of experiments on actomyosin solutions (Gergely, '56; Weber, '56) that ATP decreases the aggregation of actomyosin.

IV

The conclusions of the preceding discussion may now be adduced to support the hypothesis that the rapid and retarded components are not simply two aspects of a single physico-chemical structure. It has been concluded in III from the effect of temperature on the rapid response that cross-bonding increases in conditioned fibers both in low salt and in ATP-$MgCl_2$. It has been concluded further that increased cross-bonding does not affect the decay rate in ATP-$MgCl_2$, but does in low salt. If the fiber has a homogeneous macromolecular structure in ATP-$MgCl_2$, increased cross-bonding in this structure should affect both the rapid and the retarded aspects of the mechanical response. A homogeneous structure is thus not compatible with the conclusions of III. Fibers in ATP-$MgCl_2$ must therefore consist of separate rapid and retarded structural elements; cross-bonding increases with temperature in only the rapid element.

There are two alternatives for fibers in low salt: (a) They could consist of a single structural element in which cross-bonding increases with temperature. This would be converted to separate rapid and retarded series elements by ATP-$MgCl_2$. After the conversion, thermally induced cross-bonding would occur in the rapid element only. The extent of cross-bonding of the retarded element would be reduced to a level lower than that which exists in the conditioned fiber in low salt. (b) They could consist of separate series elements. There would be no effect of ATP-$MgCl_2$ on the thermally induced cross-bonding of the rapid element. However, the cross-bonding of the retarded element would be effected as described in alternative (a). Alternative (b) seems the more probable because of evidence presented and discussed elsewhere (Tunik, '60).

V

Analysis of the data from another viewpoint further supports the conclusion that separate elements exist in ATP-$MgCl_2$. It has been shown (Hayashi and Rosenbluth, '53) that the rapid and retarded aspects of the response of the actomyosin fiber are imitated by a mechanical model consisting of rapidly responding elastic springs in series with slowly responding contractile links. If the links and springs have structural counterparts in the fiber, then, after isotonic contraction, the relative size of the rapid element would be increased. Consequently, when tensions of the rapid element are compared at the same relative extension of this element, anomalous temperature effects might be obtained if these relative extensions are expressed in terms of varying fiber lengths. For example, in the comparison of $(S_q)_L$ of a condtioned fiber in ATP-$MgCl_2$ in the unshortened state at 0°C to $(S_q)_L$ of this fiber in the shortened state at 20°C, the quick stretches were expressed respectively as $\Delta\%\ L_{eu}$ and $\Delta\%\ L_{es}$. The results were, in fact, anomalous: $(S_q)_L$ decreased with cycling and increasing temperature (fig. 11b, solid curves), and had a negative temperature coefficient (table 2,c). This contrasts to the results obtained when $(S_q)_L$ of a conditioned fiber in the shortened state in ATP-$MgCl_2$ was compared at 0°C and 20°C (fig. 10 and table 2,b); and to the results obtained for the fiber in low salt (fig. 8 and table 2,a). If the quick stretches are expressed uniformly as $\Delta\%\ L_{eu}$, however, the results agree in every case (fig. 11b, dashed curve and table 2,c). This circumstance further supports the conclusion that separate rapidly and slow-

ly responding structural elements exist in conditioned fibers in ATP-$MgCl_2$. Since ATP affects the retarded, but not the rapid aspect of the mechanical response of the actomyosin fiber, as has been shown here and elsewhere (Hayashi and Rosenbluth, '53, '54; Joseph, '52), it may be concluded that the retarded structural element is the contractile element.

VI

To the extent that the conclusions presented here are valid, the nature of the tension-bearing forces of the actomyosin fiber as a whole, deduced from the sign of the net tension change accompanying a causative temperature change, is not pertinent to elucidation of the mechanochemical events underlying contraction. Rather, the nature of the tension-bearing forces of the slowly responding contractile element only should be considered for this purpose.

SUMMARY

1. The rapid and retarded responses to a quick stretch and hold of a mechanically conditioned actomyosin fiber were obtained over an extended range of length and tension by a cycle consisting of a series of standard stretch-holds and release-holds.

2. The tension decays during the holds of each cycle were superimposable if the tensions were normalized with respect to the peak tension at the onset of each decay. The MDR is defined as the mean of the normalized tension lost during each of the decays of a cycle. It serves as a convenient measure of the decay rate over a wide range of peak tensions.

3. A length-tension curve for the rapid response was derived graphically for each cycle from the amount of each quick stretch and its accompanying abrupt rise of tension. The tension at any given length in this curve is designated $(S_q)_L$.

4. Fibers were cycled alternatively at 20°C and 0°C. The effects of temperature on the rapid and retarded responses were separated from those of cycling by defining cycling and temperature coefficients. These were computed from the data.

5. The positive temperature coefficient of the MDR obtained from cycles in low salt (0.05 M KCl, 1/10 Veronal, pH 7.6) is one-tenth that obtained from cycles in ATP-$MgCl_2$ (3×10^{-3} M ATP, 10^{-3} M $MgCl_2$, in low salt). In length-tension curves derived from cycles in low salt, the positive temperature coefficient of $(S_q)_L$ is nearly the same as it is in curves derived from cycles in ATP-$MgCl_2$.

6. The data is analyzed within the framework of certain theories proposing a molecular basis for the mechanical behavior of high polymers. The analysis leads to some conclusions about the macromolecular structure of the actomyosin fiber.

LITERATURE CITED

Alfrey, T., Jr. 1948 Mechanical Behavior of High Polymers. Interscience, New York and London, pp. 93 ff; pp. 103 ff.

Aubert, X. 1956 Structure et physiologie du muscle strié I. Le mecanisme contractile in vivo: aspects mecaniques et thermiques. J. de Physiol., *48:* 105–154.

Botts, J., and M. F. Morales 1951 The elastic mechanism and hydrogen bonding in actomyosin threads. J. Cell. and Comp. Physiol., *37:* 27–55.

Bozler, E. 1956 The effects of polyphosphates and magnesium on the mechanical properties of extracted muscle fibers. J. Gen. Physiol., *39:* 789–800.

Buchtal, F., and E. Kaiser 1951 Rheology of the cross striated muscle fiber. Det. Kgl. Danske Vidensk. Selskab, Biol. Medd., *21* no. 7.

Eyring, H. 1941 Theory of Rate Processes. Ed. by Glasstone, Laidler and Eyring. McGraw-Hill, New York, pp. 447 ff.

Feng, T. P. 1932 The thermo-elastic properties of muscle. J. Physiol., *74:* 455–470.

Flory, P. J. 1944 The network structure and the elastic properties of vulcanized rubber. Chem. Rev., *35:* 51–75.

——— 1956a Role of crystallization in polymers and proteins. Science, *124:* 53–60.

——— 1956b Theory of elastic mechanisms in fibrous proteins. J. Am. Chem. Soc., *78:* 5222–5235.

Gergely, J. 1956 The interaction between actomyosin and adenosinetriphosphate. Light scattering studies. J. Biol. Chem., *220:* 917–926.

Guth, E. 1947 Muscular contraction and rubberlike elasticity. Ann. N. Y. Acad. Sci., *47:* 715–766.

Hayashi, T. 1952 Contractile properties of compressed monolayers of actomyosin. J. Gen. Physiol., *36:* 139–152.

Hayashi, T., and R. Rosenbluth 1952 Contraction-elongation cycle of loaded surface-spread actomyosin fibers. J. Cell. and Comp. Physiol., *40:* 495–506.

——— 1953 Mechanochemical properties of fibers of surface-spread actomyosin. Proc. Nat. Acad. Sci., *39:* 1285–1290.

——— 1954 Mechanical properties of organized components of surface-spread actomyosin fibers. J. Cell. and Comp. Physiol., *44:* 337.

Hayashi, T., R. Rosenbluth, P. Satir and M. Vozick 1958 Actin participation in actomyosin contraction. Biochim. et Biophys. Acta, *28:* 1–8.

Hill, A. V. 1951 Thermodynamics of muscle. Nature, *167:* 377–380.

——— 1953 "Instantaneous" elasticity of active muscle. Proc. R. Soc. London, Series B, *141:* 161–178.

Hill, A. V., and others 1950 A discussion on muscular contraction and relaxation: their physical and chemical basis. Proc. R. Soc. London, Series *B, 137:* 40–87.

Hill, A. V., and others 1952 Discussion on thermodynamics of elasticity in biological tissues. Ibid., *139:* 464–527.

Hodgman, C. D. 1951 Handbook of Chemistry and Physics, 33d ed. Ed. by Hodgman. Chemical Rubber Co., Cleveland, pp. 831 ff.

Joseph, R. 1954 Mechanical and contractile properties of surface-spread actomyosin fibers. Ph.D. thesis, Columbia University, New York.

Meyer, K. H., and L. E. R. Picken 1937 The thermoelastic properties of muscle and their molecular interpretation. Proc. R. Soc. London, Series B, *124:* 29–56.

Tunik, B. D. 1960 The effects of temperature on some mechanochemical properties of actomyosin fibers. II: Static properties. J. Cell. and Comp. Physiol., *55:* 49–60.

Weber, A. 1956 The ultracentrifugal separation of L-myosin and actin in an actomyosin solution under the influence of ATP. Biochim. et Biophys. Acta, *19:* 345–351.

The Effects of Temperature on Some Mechanochemical Properties of Actomyosin Fibers

II. STATIC PROPERTIES[1,2]

BERNARD D. TUNIK
Department of Zoology, Columbia University, New York, N. Y.[3]

From the effects of temperature on the equilibrium tension of actomyosin fibers in low salt, conclusions have been drawn concerning the nature of the tension-bearing forces of the system (Botts and Morales, '51). The experiments of these authors are extended in the present investigation in light of evidence that is compatible with the hypothesis that separate rapid passive and retarded contractile elements exist in these fibers in low salt, and that supports the hypothesis that these elements exist in these fibers in ATP-$MgCl_2$ (Tunik, '60).

If separate rapid and retarded elements exist, the effect of temperature on two static properties of these elements, equilibrium tension and equilibrium length, should be biphasic. That is, the change of each of these properties, produced by a temperature change, should have rapid and retarded components. The nature of the tension-bearing forces of the retarded, contractile element could then be deduced from the sign of the retarded change of tension with temperature, by applying classical thermodynamics.

EQUIPMENT

Tensions were produced and measured with equipment described previously (Tunik, '60). *Length changes* were investigated in subfibers held horizontally between two hooks (9, fig. 1) at the ends of glass rods. A glass guide plate (2) and a guide tube (5) were fastened to the standing rod (6). A moving rod (7) travelled within the guide tube. Fit was improved with rubber sleeves (4). Whenever the position of the moving rod was changed, the rod was pressed by rotation (1) against the guide plate to prevent any changes in the alignment of the hooks. Measurements were made between wire reference points (3) fastened to the rods. *Temperature* was controlled and measured as described previously (Tunik, '60). In experiments on length changes, to reduce disturbance of the fiber, vessel contents were not stirred except during addition of reagents.

MATERIALS AND METHODS

The reagents and solutions used, the method of preparation of actomyosin and of fibers, and the mounting of fibers, were as previously described (Tunik, '59).

Subfibers

Preparation. This was the same as that for fibers, except that compression proceeded very slowly in the final stages to prevent formation of bubbles which otherwise appear (Hayashi, '52). When the barriers were circa 0.5 cm apart, the partially compressed fiber was separated from them and split lengthwise in the trough into subfibers 50–100 μ in diameter.

Mounting. This was accomplished by affixing the ends of a uniform subfiber at least 14 mm long to the glass hooks of the apparatus while hooks and subfiber were in the trough. Apparatus and slack fiber were lifted from the trough, and fiber and

[1] Submitted in partial fulfillment of the requirements for the degree of Doctor of Philosophy, in the Faculty of Pure Science, Columbia University.

[2] This investigation was supported by Predoctoral Fellowships to the author from the National Institutes of Health, U. S. A., and in part by grants to Dr. Teru Hayashi from the Muscular Dystrophy Association of America, Inc.

[3] Present address: Department of Anatomy, School of Medicine, University of Pennsylvania, Philadelphia, Pa.

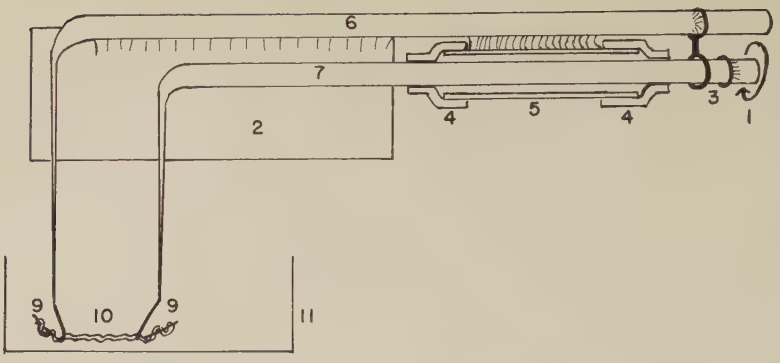

Fig. 1 Apparatus. For details see text.

hooks immersed quickly in 10 cm³ of low salt in the reaction vessel (11, fig. 1).

Equilibrium length. This was defined under each condition of temperature and chemical environment by slowly separating the moving hook from the standing hook until a further slight increase of the distance between the hooks produced no further visible straightening of the fiber. The distance between reference points was measured, and the fiber released. The process was repeated several times. Before the fiber was mounted, several zero readings, to ±0.2 mm, were taken of the distance between the reference points when the glass hooks were in contact with each other. The method resulted in determinations of equilibrium length reproducible to ±1.4% of the mean length determined.

Contractions

Isometric contractions. These were produced in fibers at equilibrium length by changing the reaction mixture from low salt to ATP-$MgCl_2$ in the manner previously described (Tunik, '60). Tensions were measured with the apparatus and in the manner previously described (Tunik, '60).

Unloaded isotonic contractions. These were produced by changing the reaction mixture from low salt to ATP-$MgCl_2$. Five cm³ of low salt was withdrawn from the reaction vessel and mixed with 0.11 cm³ stock $MgCl_2$, 0.06 cm³ Veronal buffer pH 7.6, and 0.5 cm³ neutralized ATP. This mixture was then added to the low salt remaining in the reaction vessel. Before this addition, the subfiber was released to 30% of its equilibrium length in low salt. This release insured slackness of the fiber at the time of the first length determination during the contraction. Length was measured at two minute intervals by a single operation as described for measurement of equilibrium length. During the time the fiber was held straight between the hooks, contraction was actually isometric. This condition lasted only 15 sec. however; then the fiber was released again. Measurements were continued for 15 min. or until no further change of length occurred, whichever was longer.

EXPERIMENTS AND RESULTS

A. Length changes

1. *Native*[4] *subfibers shortened in ATP-$MgCl_2$.* The equilibrium length, L_e, of a fiber was determined in low salt at 20°C. Then the fiber was released to less than 30% of this length so that when it was equilibrated in ATP-$MgCl_2$ for 15 minutes it remained slack, even though it was contracting isotonically. The shortened equilibrium length, L_{es}, was then determined by taking up the slack as previously described. While the fiber was held straight between the hooks at this length the temperature was lowered to 0°C. An appreciable amount of slack developed.

To measure the amount of this elongation, and in order to eliminate the fiber weight as a factor, a subfiber, contracted in ATP-$MgCl_2$ at 20°C as described above, was released to well below L_{es}. Most of its length was supported by the bottom of the

[4] These had received no treatment other than the process of formation.

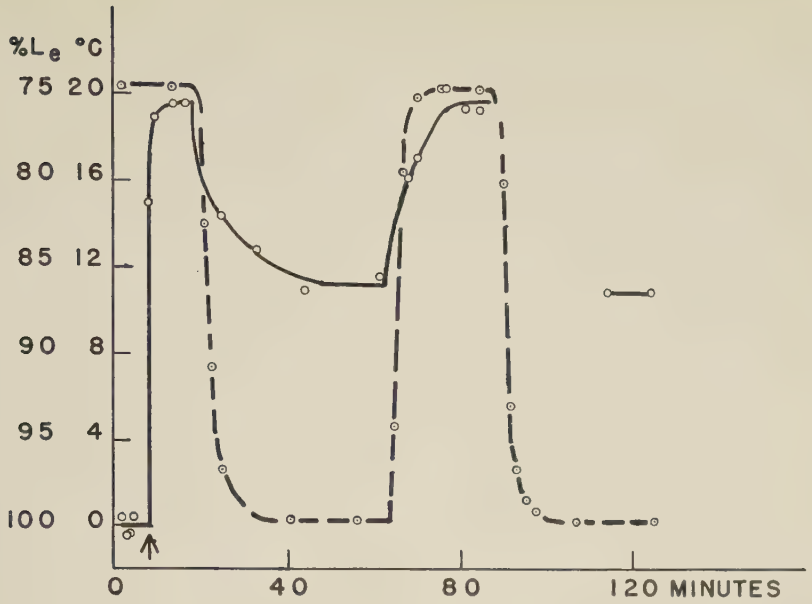

Fig. 2 Shortened native fiber in ATP-$MgCl_2$. Change of length with temperature; effects of frequency of length measurements. Ordinate: per cent equilibrium length —○—; temperature – –○– –. Abscissa: time. Reaction mixture changed to ATP-$MgCl_2$ at the arrow.

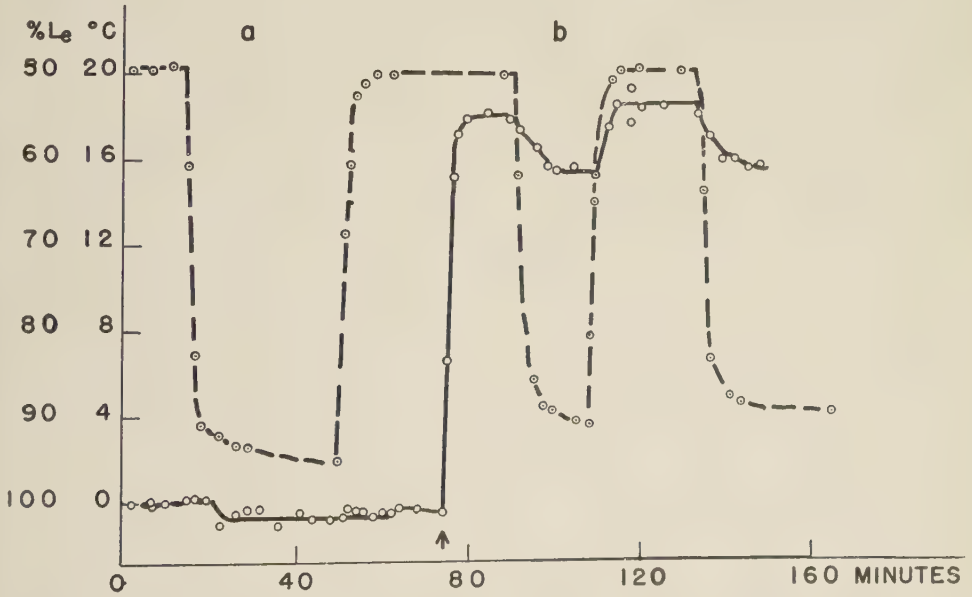

Fig. 3 Change of length with temperature. Ordinate: per cent equilibrium length —○—; temperature – –○– –. Abscissa: time. Reaction mixture changed to ATP-$MgCl_2$ at the arrow. a, Native fiber in low salt. b, Native fiber shortened in ATP-$MgCl_2$. The completely shortened fiber was released until slack and supported on the bottom of the reaction vessel between each determination of length.

vessel. The temperature was reduced and the equilibrium length determined. An increase of equilibrium length was observed which was reversed by a subsequent increase of temperature to 20°C (fig. 3).

The length measurement itself might have stretched the fiber, producing the observed elongation. To test this, the equilibrium length of a shortened fiber was first measured at 20°C. Length determinations were then carried out while the reaction mixture was being cooled. They were repeated several times after the temperature had reached equilibrium (fig. 2). After warming the reaction mixture to 20°C the equilibrium length of the fiber was again determined. The temperature was again lowered, but measurement of the equilibrium length was made only after the same time had elapsed as was previously required for the fiber to reach equilibrium length at 0°C. The results (fig. 2) show that stretching was not the source of the elongation.

2. *Native subfibers in low salt.* No reversible temperature induced elongation could be detected (fig. 3). However, it was possible that minute shape changes might nevertheless be occurring. If so, they would produce either a change of length at constant tension, or a change of tension at constant length. Since no change of length was detectable, the more sensitive method of observing changes of tension at fixed length was applied.

B. Changes of static tension

1. *Native fibers at equilibrium length in low salt.* The tension changed reversibly and inversely with the temperature; i.e., the temperature coefficient of tension was negative. The rate of the tension change was less than that of the causative temperature change (fig. 4a).

2. *Native fibers above equilibrium length in low salt.* These fibers were treated as follows. The fiber was stretched to the desired length and the resulting tension was allowed to decay until the decay rate fell to 1 mg/min. or less. The temperature was then lowered and held at the lower level until all ensuing tension changes, due to the temperature change, had reached equilibrium. Then the temperature was raised again.

At small extensions, the temperature coefficient of tension was negative (fig. 4b). The rate of the reversible change of tension with temperature was slower than that of the causative temperature change. At somewhat larger extensions, a small, positive, rapid component of the tension change appeared (figs. 4b and 4c). At still greater lengths the temperature coefficient of tension became completely positive (fig. 4d). This reversal of the sign of the temperature coefficient of tension from negative to positive was itself reversible (fig. 6). It took place at circa 135% L_e (fig. 5). This reversal of sign did not invariably occur, however. When it did not take place, the temperature coefficient of tension remained negative at lengths much greater than 135% L_e (fig. 5).

In order to determine whether or not the sign reversal described above was the result of either the temperature change or the duration of the experiment, two control experiments were performed. In one, fibers held at L_e were subjected to repeated temperature changes. In the other, fibers held at L_e were aged 1,440 hours at 4°C. Neither treatment altered the properties of the fiber, to the extent that the temperature coefficient of tension remained negative at lengths less than ca. 135% L_e.

3. *Native fibers at equilibrium length in ATP-$MgCl_2$.* The active isometric tension developed by changing the reaction mixture from low salt to ATP-$MgCl_2$ at 20°C fell with the temperature (fig. 7). When the temperature was raised, the tension increased at least as rapidly as the temperature (fig. 7). This has been shown to be the case for the glycerinated psoas model (Varga, '50). The tension of the actomyosin fibers reached its maximum value in an average of 2.3 min. before the temperature had reached equilibrium. A contraction produced by changing the reaction mixture to ATP-$MgCl_2$ at 20°C required an average of 8.2 min. longer to reach equilibrium (a, fig. 7) than a temperature-induced contraction required to attain maximum tension (b, fig. 7). The effects of an ATP-$MgCl_2$ induced contraction at 20°C were not prerequisite for the rapidity of the temperature-induced contraction in ATP-$MgCl_2$ (cf. figs. 7 and 8).

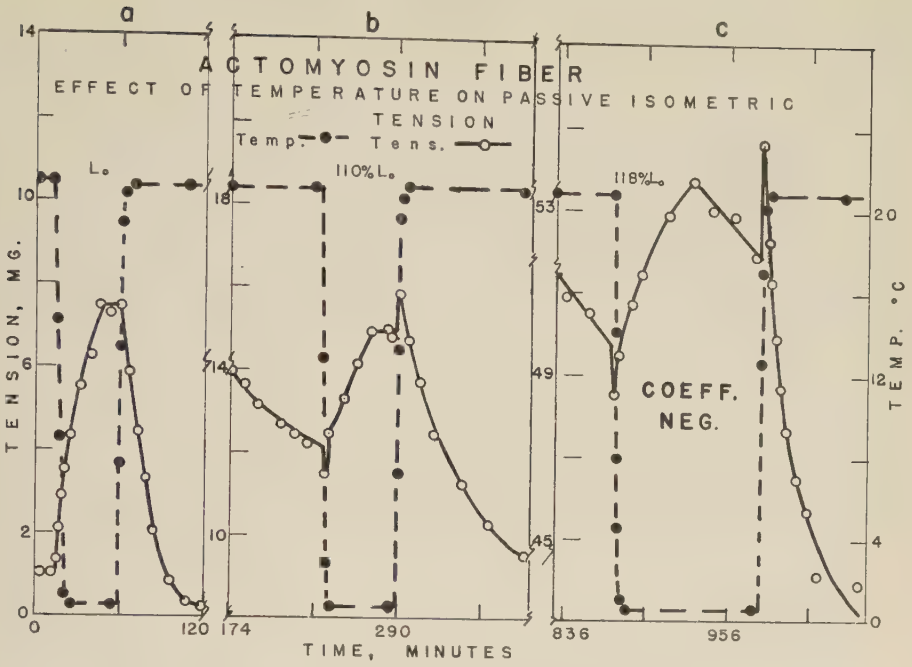

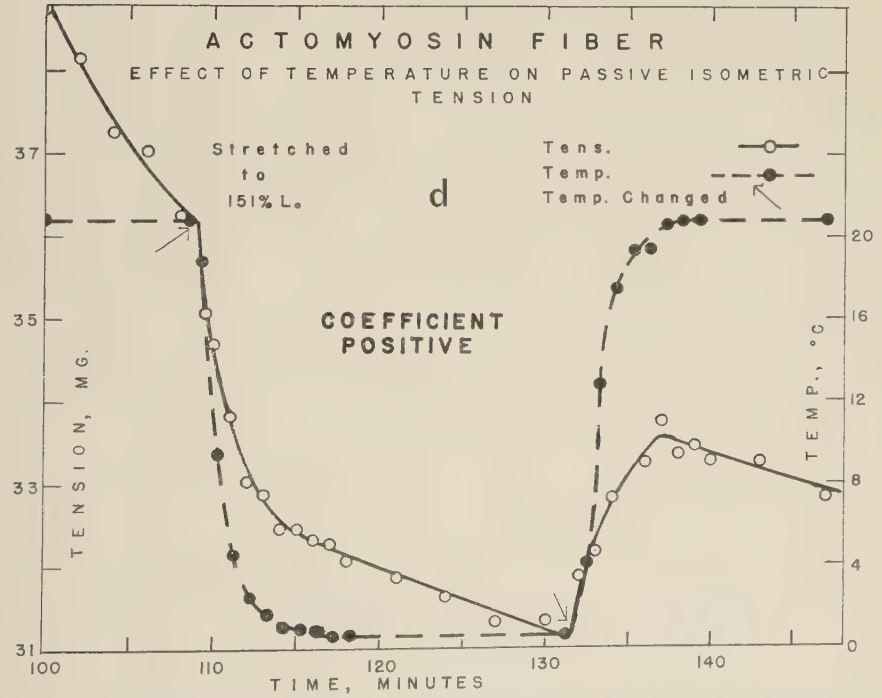

Fig. 4 Native fiber in low salt; change of tension with temperature. Ordinate: tension in mg. Abscissa: time. a, At equilibrium length, L_e. b, At 110% L_e. c, At 118% L_e. d, At 151% L_e. Temperature, ●. Tension, ○.

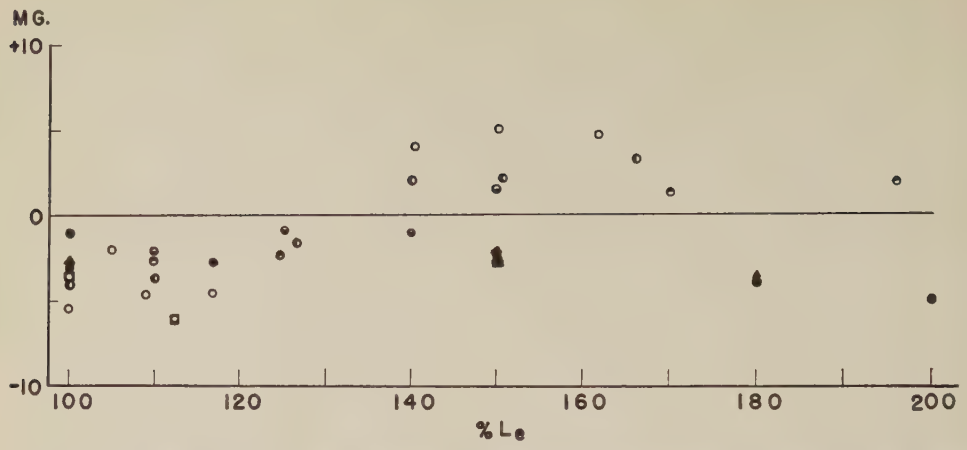

Fig. 5 Change of sign of the net tension change with temperature. Ordinate: net change of tension per 20°C temperature change. Positive values indicate tension and temperature changed in the same sense. Abscissa: fiber length. Each symbol represents fibers made from a different batch of actomyosin.

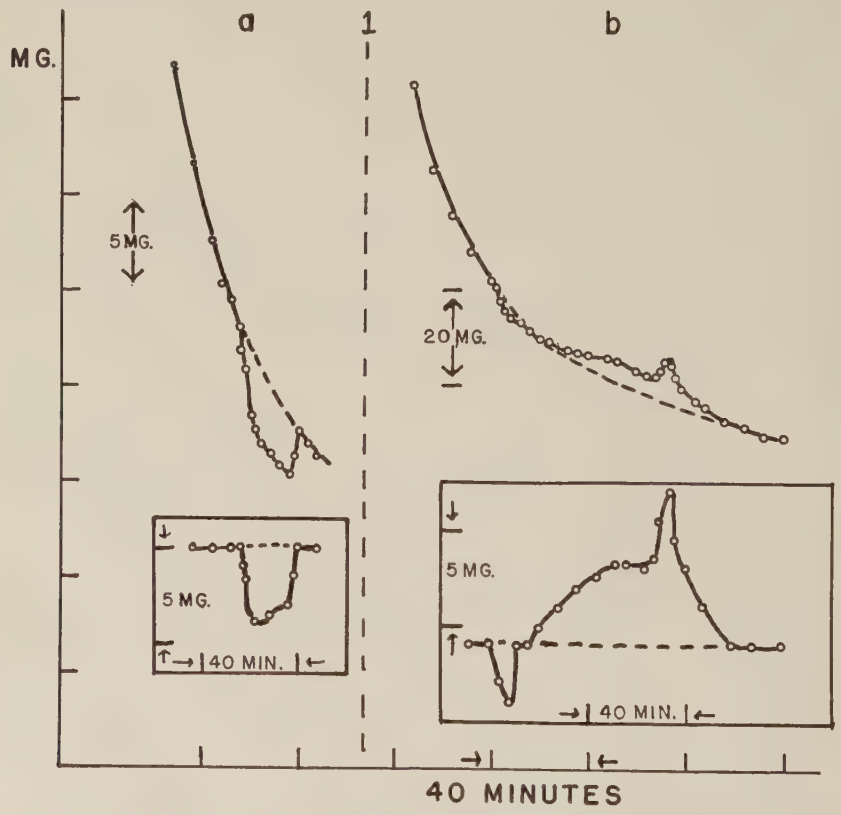

Fig. 6 Native fiber in low salt. Reversibility of the reversal of sign of the change of tension with temperature. Ordinate: tension. Abscissa; time. a, Fiber stretched to 140% L_e. At 1, 135 min. after the stretch, the fiber was released completely, equilibrated 135 min., and stretched to 118% L_e. b, Fiber at 118% L_e. Insets: difference between the observed tension and tensions calculated from the decays using a single exponential term in t.

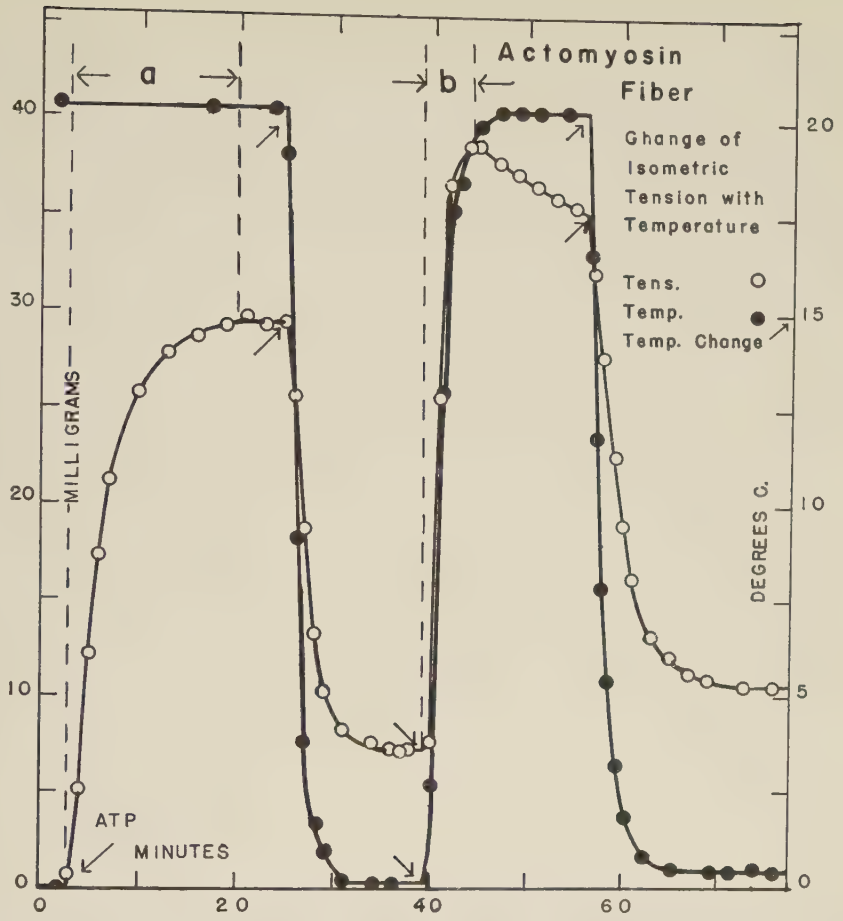

Fig. 7 Native fiber at equilibrium length. Effect of temperature on tension developed in ATP-$MgCl_2$. Ordinate: tension —○—; temperature —⊙—. Abscissa: time. Reaction mixture changed to ATP-$MgCl_2$, ↙. Temperature changed, ↗ ↘.

The tension at 0°C was, for 20 fibers, an average of 29.4% of the tension developed by changing the reaction mixture to ATP-$MgCl_2$ at 20°C.

DISCUSSION

I

The temperature-induced elongation observed in shortened fibers in ATP-$MgCl_2$ may be due merely to the fact that the fiber is subjected to small stretches in the procedure for determining its length, resulting in an extension at 0°C which is reversed by recontraction at 20°C. If so, the measured length at 0°C should increase as each measurement is taken; should never reach an equilibrium; and should depend on whether one or several measurements are taken. The length in fact did reach an equilibrium (fig. 2) at 0°C as measurements were taken. This equilibrium was the same as that obtained when measurements were taken only after enough time had elapsed for the fiber to reach equilibrium at 0°C again.

Another possibility exists. Passive elements could be compressed when the fiber contracts at 20°C and then expand when the contractile force is reduced at 0°C, extending the fiber. To function as proposed, these passive elements must be in parallel with the contracting portions of the fiber. It follows that the amount of compression and therefore of reextension should be cor-

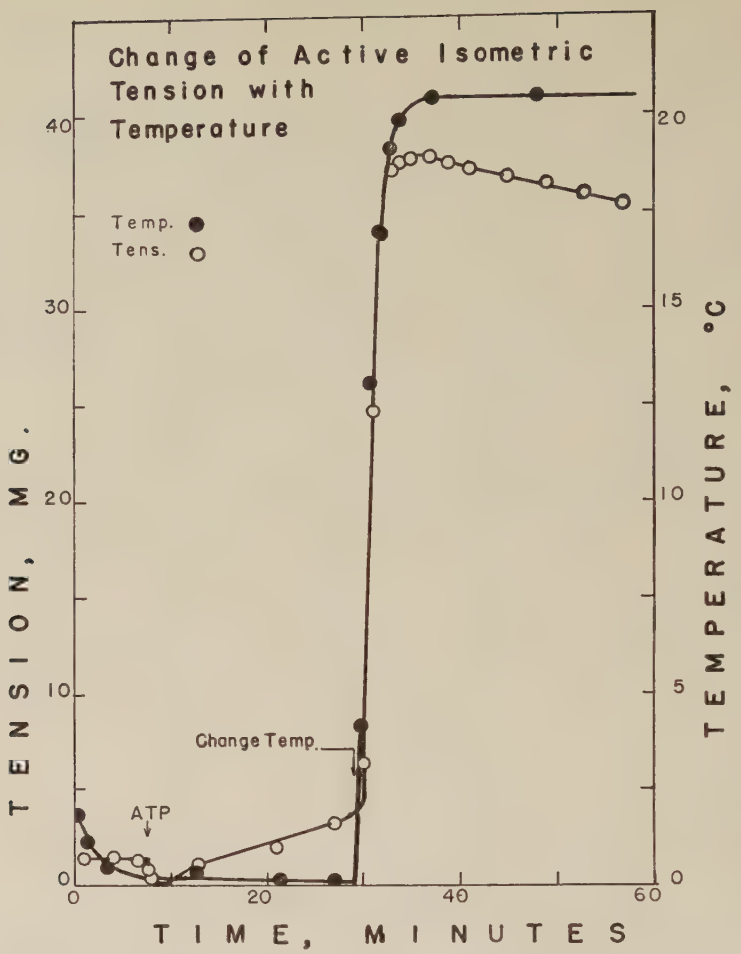

Fig. 8 Native fiber at equilibrium length. Effect of temperature on tension developed in ATP-$MgCl_2$. Symbols as in figure 7.

related with the contracted length[5] at 20°C. The coefficient of correlation, r, between the contracted length, 59% L_e, and the elongation, 10% L_e (means for 57 fibers) was 0.0016, with confidence limits $-0.28 \leq r \leq +0.28$, at the 90% confidence level. Thus there is extremely little if any correlation between the contraction and the elongation.

From the above discussion it may be concluded that the elognation is not due to passive parallel elements, nor to strechning, but is an active elongation of the series elements being considered in this investigation. To avoid the implication in the word "active" that chemical energy is involved, the term autoelongation will be used.

The monophasic character of this length change (figs. 2 and 3) may be due to the fact that the vessel contents were not stirred, resulting in a slow temperature change. If the length change were actually biphasic, as is the tension change, the response of the component changing as rapidly as the temperature would have been retarded by the slowness of the temperature change. The rapid component would have thus become indistinguishable from the retarded component. Even though rapid and retarded components of the length change were not observed, the re-

[5] As a result of uncontrolled variables, the contracted length varied from 38% L_e to 86% L_e.

sults may be used to test some theories of contraction.

The fiber in the uncontracted state has been described (Pryor, '50) as a body in which entropic contracting forces are opposed by cross-bonds. When these bonds are broken by a chemical energy source acting as a plasticizer (e.g., ATP), the unopposed entropic forces are free to develop tension. According to high-polymer theory as previously discussed (Tunik, '60), reduction of cross-bonding would also increase the decay rate. If the tension were produced by the proposed mechanism, the temperature dependence of the decay rate and of the tension should be the same. From the data presented here, a temperature coefficient of tension, as defined previously (Tunik, '60) may be computed. Its value, 2.4, is cicra 10 times that of the temperature coefficient of the mean decay rate (Tunik, '60). The tension developed by the actomyosin fiber in ATP-$MgCl_2$ thus does not seem to result from increased plasticity as such. This conclusion is in accord with the occurrence in the glycerinated psoas model of plasticization without contraction (Portzehl, '52) and of contraction without stiffness changes (Bozler, '56); and with the observations that whole muscle is stiffer during the active state than during the resting state (Buchtal, '51; Hill, '50, '51). Furthermore, as is shown in II below, in low salt the tension of the retarded, contractile element is not due to entropy but entirely to potential energy. Thus this proposed mechanism is not in accord with the facts.

The fiber has also been described as a system in which elastic shortening forces of the magnitude of the isometric tension are balanced in the uncontracted state by the electrostatic repulsion of positive charges (Morales and Botts, '52; Morales et al., '55). Contraction supposedly occurs when ATP binds to the molecule and neutralizes these repulsive charges. Applying this concept, the 70% reduction of the isometric tension developed at 20°C that occurs when the temperature is lowered to 0°C occurs because the proposed process of charge neutralization has been partially reversed; cicra 70% of the charges have been reconstituted. If this were true, then in a fiber which has been contracted isotonically circa 40% of its original length at 20°C, lowering the temperature to 0°C should produce an autoelongation equal to circa 70% of the contraction, i.e., a 28% autoelongation. An autoelongation of this size does not occur; it is only 10%. Also, one would expect a correlation between contraction and autoelongation. No such correlation was detected. Thus this proposed mechanism is not in accord with the facts.

II

If the reversal of the sign of the temperature coefficient of static tension of the native fiber in low salt were a basic property of the contractile material itself, it should occur invariably. Since it does not, this reversal is probably not due to a tension-produced conversion of the contractile material from a system in which tension is due to potential energy[6] to one in which tension is due at least in part to entropy,[6] as has been proposed (Meyer and Picken, '37) to explain a similar sign reversal in whole muscle (Meyer and Picken, '37; Feng, '32). Rather, the sign reversal, the difference in the rates of the negative and positive responses of tension to a temperature change, and the existence at intermediate lengths of both of these responses, are all probably due to the existence of two distinct elements in the fiber in low salt, a structure previously proposed (Tunik,

[6] A negative change of tension with temperature, equivalent to a positive change of length with temperature, is characteristic of a system in which the tension is due solely to potential energy. A positive change of tension with temperature is characteristic of a system in which the tension is due at least in part to entropy (Botts and Morales, '51). Since these relations are based on an equation derived from thermodynamic considerations (Elliott and Lippman, '45), they apply rigorously only if the tensions are equilibrium tensions. If the system is not at equilibrium, the relations may nevertheless apply if the tension changes resulting from the decay are small with respect to the temperature-induced change of tension during the time required for completion of this change (Guth, '47). Even under conditions where the change of tension due to the decay process is relatively large (figs. 4b and 4c), the change of tension with temperature is still qualitatively similar to the change of tension with temperature at equilibrium length, i.e., equilibrium tension. The change of tension with temperature can therefore be considered to be superimposed on the process of tension decay whenever the latter occurs (see fig. 6).

'60). The sign reversal in this view could then be due to changes in the relative contribution of the change of tension of each element to the total change of tension observed. Those instances in which the sign reversal of the temperature coefficient of tension does not occur, could result from complete dominance of the tension change by the contribution of the retarded element.

The temperature coefficient of the quick stretch tension[7] of the fiber in low salt and in ATP-$MgCl_2$ (Tunik, '60), and of the rapid aspect of the change of static tension with temperature in low salt, are all positive. From this, and thermodynamic considerations[6] it may be concluded that the tension of the rapid, passive element is due at least in part to entropy, in both low salt and ATP-$MgCl_2$.

Since the retarded response alone is affected by ATP-$MgCl_2$ (Hayashi and Rosenbluth, '53, '54; Joseph, '52; Tunik, '60), it has been concluded that the retarded element of the fiber in low salt is the contractile element (Tunik, '60). As a consequence of this, and the negative temperature coefficient of tension of the retarded response reported here, it may be concluded that the tension of the contractile element is due solely to potential energy when the fiber is in low salt.

Interpretation of the nature of the tension-bearing forces of the contractile element in ATP-$MgCl_2$ by classical thermodynamics may not be valid because of the possibility that a temperature-sensitive steady state transfer of energy occurs under these conditions. Application of the principles of steady state thermodynamics may be required. A further study of the temperature induced changes of length and tension of the fiber in ATP-$MgCl_2$ is being undertaken along these lines.

SUMMARY

1. A 10% monophasic autoelongation occurs when native actomyosin fibers in ATP-$MgCl_2$, fully contracted at 20°C, are cooled to 0°C. No length change of the native fiber in low salt is detectable.

2. These fibers, held at their equilibrium length, L_e, in low salt at 20°C, develop tension when cooled to 0°C. This tension change thus has a negative temperature coefficient. The change is reversible and is slower than the causative temperature change.

3. The passive tension developed by stretching these fibers to moderate lengths also has a negative temperature coefficient and changes reversibly more slowly than the temperature.

4. The sign of the temperature coefficient occasionally becomes positive above ca. 135% L_e. This sign reversal, when it occurs, is itself reversible. When the coefficient is positive, the reversible change of tension occurs as rapidly as the causative temperature change.

5. At intermediate lengths the change of tension with temperature is sometimes biphasic, with both a rapid component having a positive temperature coefficient and a retarded component having a negative temperature coefficient.

6. Active isometric tension is developed more slowly by adding ATP-$MgCl_2$ to native fibers at 20°C than by quickly warming fibers in ATP-$MgCl_2$ from 0°C to 20°C. The tension rises as rapidly as the temperature. It falls on cooling to 0°C to 70.5% of the tension developed by adding ATP-$MgCl_2$ at 20°C.

7. Conclusions based on these and previously reported results are presented which describe the nature of the tension-bearing forces of the component structural elements of the actomyosin fiber.

ACKNOWLEDGMENTS

The loving encouragement and understanding endurance of my wife were instrumental to the progress and completion of this investigation.

To Dr. Teru Hayashi go my sincere thanks for his judicious advice, patience, and exhaustive appraisal of the manuscript.

It is with pleasure that I acknowledge the inestimable value of informal discussions with my colleagues.

---

[6] See footnote 6, page 9.

[7] It has been shown (Tunik, '60) that the quick stretch tension may be considered an equilibrium tension. The need for equilibrium is discussed in footnote 6.

LITERATURE CITED

Botts, J., and M. F. Morales 1951 The elastic mechanism and hydrogen bonding in actomyosin threads. J. Cell. and Comp. Physiol., *37:* 27–55.

Bozler, E. 1956 The effects of polyphosphates and magnesium on the mechanical properties of extracted muscle fibers. J. Gen. Physiol., *39:* 789–800.

Buchtal, F., and E. Kaiser 1951 Rheology of the cross striated muscle fiber. Det. Kgl. Danske Vidensk. Selskab, Biol. Med., *21* no. 7.

Elliott, D. R., and S. A. Lippmann 1945 The thermodynamics of rubber at small extensions. J. Appl. Phys., *16:* 50–54.

Feng, T. P. 1932 The thermo-elastic properties of muscle. J. Physiol., *74:* 455–470.

Guth, E. 1947 Muscular contraction and rubberlike elasticity. Ann. N. Y. Acad. Sci., *47:* 715–766.

Hayashi, T. 1952 Contractile properties of compressed monolayers of actomyosin. J. Gen. Physiol., *36:* 139–152.

Hayashi, T., and R. Rosenbluth 1952 Contraction-elongation cycle of loaded surface-spread actomyosin fibers. J. Cell. and Comp. Physiol., *40:* 495–506.

——— 1953 Mechanochemical properties of fibers of surface-spread actomyosin. Proc. Nat. Acad. Sci., *39:* 1285–1290.

Hill, A. V. 1950 The development of the active state of muscle during the latent period. Proc. R. Soc. London, Series B, *137:* 320–329.

——— 1951 The earliest manifestation of the mechanical response of striated muscle. Ibid., *138:* 339–348.

Meyer, K. H., and L. E. R. Picken 1937 The thermoelastic properties of muscle and their molecular interpretation. Ibid., *124:* 29–56.

Morales, M. F., and J. Botts 1952 A model for the elementary process in muscle action. Arch. Biochem., *37:* 283–299.

Morales, M. F., J. Botts, J. J. Blum and T. Hill 1955 Elementary processes in muscle action: an examination of current concepts. Physiol. Rev., *35:* 475–505.

Portzehl, H. 1952 Der arbeitszyklus geordneter aktomyosinsysteme. Z. Naturforsch., *7b:* 1–10.

Pryor, M. G. M. 1950 Mechanical properties of fibers and muscle. Progress in Biophysics, *1:* 216–268.

Tunik, B. D. 1960 The effects of temperature on some mechanochemical properties of actomyosin fibers. I: Dynamic properties. J. Cell. and Comp. Physiol., *55:* 31–48.

Varga, L. 1950 Observations on the glycerol-extracted *musculus psoas* of the rabbit. Enzymologia, *15:* 196–216.

The Haptoglobins, Hemoglobins and Serum Proteins of the Alaskan Fur Seal, Ground Squirrel and Marmot

B. S. BLUMBERG,[1] A. C. ALLISON[2] AND BARBARA GARRY[1]
National Institutes of Arthritis and Metabolic Diseases, National Institutes of Health, Bethesda, Maryland, and National Institute for Medical Research, London, N.W. 7

There has been an increasing interest in the study of systems of genetically controlled polymorphic proteins in humans and other animals. During the course of field investigations in Alaska on the distribution of genetically determined biochemical traits in humans, an opportunity arose to collect blood specimens from some Arctic animals. The present paper is a report of observations of starch gel and paper electrophoresis studies on the hemoglobin and serum of these animals and a contribution to the comparative biochemistry of proteins which in some species have been shown to be genetically determined.

Two or more hemoglobin types, distinguishable by electrophoresis, chromatography and other techniques have been identified in several species. In some cases, there is a polymorphism, one or two major hemoglobin components being produced under the control of allelomorphic genes in different members of a single species. The presence of sickle-cell and other abnormal hemoglobin types in man and different hemoglobin types in cattle (Cabannes and Serain, '55; Bangham and Blumberg, '51) and sheep (Evans et al., '56) exemplify this situation. Variations in monkeys (Jacob and Tappen, '58) probably fall into the same category, although no genetical investigations have been made. In man a major (A_1) and two minor (A_2 and A_3) hemoglobin components are found in all normal subjects, and there is evidence that the formation of the A_1 and A_2 components is under independent genetical control (Ceppellini, Kunkel and Dunn, in preparation). In other cases, two or more main hemoglobin components are present in all members of a species or strain, and presumably their synthesis is again under independent genetic control. This is true of the horse (Cabannes and Serain, '55), mouse (Ranney and Glucksohn-Waelsch, '55), chickens (Johnson and Dunlap, '55; Saha, Datta and Ghosh, '57), various birds (Datta, Ghosh and Guha, '58) and various reptiles including turtles (Ramirez and Dessauer, '57).

The haptoglobins are a family of serum proteins which bind hemoglobin and have been studied extensively in humans by Jayle and his associates (Jayle, Boussier and Tonnelat, '56). By means of starch gel electrophoresis human sera can be typed in three groups, the determining difference being the pattern of haptoglobins (Smithies, '55). In type 1-1 there is a single haptoglobin band migrating near the β-globulins. In type 2-2 there are three or more fine bands in the region between α and β-globulins. Type 2-1 contains 4 or more bands, one corresponding to the haptoglobin of type 1 and the others similar to, but not identical with, three bands of type 2-2. By family studies, Smithies and Walker ('55) and Galatius-Jensen ('57) have shown that these patterns are genetically determined by a pair of autosomal allelic genes designated Hp^1 and Hp^2 with full expression in the heterozygote. Others have shown that their incidence varies in different populations (e.g. Allison, Blumberg and ap Rees, '58). We are not aware of any published reports of intraspecies

[1] National Institutes of Arthritis and Metabolic Diseases, National Institutes of Health, Bethesda, Maryland.

[2] National Institute for Medical Research, London, N.W. 7.

variations of haptoglobin type in animals other than man.

Differences between the patterns obtained by zone electrophoresis of serum proteins of different species have been described by Woods, Paulsen, Engle, and Pert ('58). Intraspecies differences have been found on starch gel electrophoresis of β-globulins in man (Smithies, '57), and cows, sheep, and goats (Ashton and McDougall, '58; Smithies and Hickman, '58).

METHODS

Bloods from the fur seal (*Callorhinus ursinus*) were collected on St. Paul's Island in the Pribilof group, Alaska, during the 1958 killing season through the courtesy of Mr. Ford Wilkie, Chief, Marine Mammal Research, Bureau of Commerical Fisheries of the Fish and Wildlife Service, Seattle, Washington. The samples were from males approximately three years old. The ground squirrels (*Citellus parryii* barrowensis) and marmots (*Marmota caligata* broweri) were collected through the courtesy of Ensigns L. Nash and E. J. Hancock and Commander A. E. Fisher, U.S.N.R. at the Arctic Research Laboratory, Barrow, Alaska. After the animals were killed, the blood was withdrawn from the heart or great vessels, placed in suitable containers, and the red blood cells separated from the sera by centrifugation. In some cases clotting was prevented by the use of oxalate as an anticoagulant, but these specimens showed no differences from the clotted ones. The sera were kept frozen and the red blood cells at 4°C until the tests could be performed in Bethesda.

The Guernsey cow hemoglobin used in the comparative studies had two components on paper and gel electrophoresis. This has been designated cow hemoglobin type AB by Bangham ('57). It was collected through the courtesy of Dr. J. F. Sykes, Agricultural Research Center, Beltsville, Maryland.

A hemoglobin solution was obtained from red cells washed with normal saline by freezing a suspension of the cells in distilled water, thawing and centrifuging for 30 minutes at 10,000 rpm. Specimens were run on paper and gel electrophoresis as oxyhemoglobin and cyanmethemolobin after treatment with sodium ferricyanide or nitrite and sodium cyanide; no obvious differences between the results using these hemoglobin derivatives were noted.

Paper electrophoresis was done with the Spinco model R apparatus (Beckman/Spinco Division, Palo Alto, California) using Whatman no. 3 filter paper. Barbiturate buffer pH 8.6, ionic strength 0.075 was used for the serum protein experiments and barbiturate buffer pH 8.6, ionic strength 0.05 for the hemoglobin determinations. Hemoglobins, serum proteins, and serum haptoglobins were studied by starch gel electrophoresis using the conditions for serum proteins described by Smithies ('55). Trays of 40 mm and 80 mm width were used and up to 8 sera could be compared side by side. Haptoglobins were identified by adding homologous hemoglobin to the sera before electrophoresis and identifying the hemoglobin-binding protein bands by staining with benzidine and hydrogen peroxide as described elsewhere (Allison and ap Rees, '58; Allison and Blumberg, '58). Hemoglobin concentration was determined by the method of Drabkin ('59). Protein staining was done with amido black 10B (Hartman-Ledden Co., Philadelphia) dissolved to saturation in a solution containing methyl alcohol and distilled water in equal proportions and 10 per cent glacial acetic acid. Differentiation was carried out with the alcohol, water, acetic acid mixture alone. Paper strips were stained with Bromphenol Blue (Spinco dye B-1). For the comparative studies, the sera and hemoglobin solutions were dialyzed in the same container against 0.9 per cent sodium chloride solution for 24 hours with three changes each of 1000 ml of dialysate. There was no difference in migration between the dialyzed and undialyzed specimens.

The hemoglobins of 27 seals, 8 ground squirrels and 4 marmots and the sera of 36 seals, 8 ground squirrels, and 4 marmots were studied. Each of the hemoglobins and serum proteins studied were repeated 4 or 5 times on the same specimen with consistent results. Freezing and thawing of specimens up to 10 times did not have a significant effect on the identification of the patterns.

RESULTS

Hemoglobins. The migration of the hemoglobins was studied by means of paper and starch gel electrophoresis. The relative migrations observed were the same by both techniques although more detail could be seen by the starch gel method. The starch gel results are shown in figure 1 compared to the major band of normal human adult hemoglobin A and to cow hemoglobin AB. Seal hemoglobin has two major components, the faster designated A and the slower B, and a slower diffuse minor component which can be detected by benzidine or amido black staining. All of these peaks migrate more slowly than human hemoglobin and either peak of cow hemoglobin type AB. Ground squirrel hemoglobin has a single component (although the band is broad) which migrates slightly faster than seal hemoglobin B and slightly slower than human hemoglobin A. Marmot hemoglobin migrates with about the same mobility as ground squirrel hemoglobin. In some runs it was a single peak and in others it was resolved into two components. No intraspecies differences were seen, from which limited data it appears that there may be no hemoglobin polymorphism in these animals.

Serum proteins; paper electrophoresis. The patterns observed after paper electrophoresis all show interspecies differences (fig. 2). While the names of the protein bands, both for paper and starch gel, are assigned according to their apparent correspondence to the human bands, this does not imply that they are the same proteins. The fur seal alpha$_2$ globulin band was broad and could be resolved into two components. The albumin traveled somewhat faster than that of humans. The ground squirrel had two peaks in the β-globulin region with most of the staining in the slow-moving component, and most of the alpha globulin traveled in the alpha$_1$ position. Two patterns were seen in the marmot. All but one showed a single beta peak with approximately the same mobility as human beta. The alpha$_1$ and albumin bands traveled faster than the corresponding human one. One animal was quite different from these and had two beta peaks with most of the staining in the slower-moving bands. It had no alpha$_1$ globulin. This was the same animal which had the type 2 haptoglobin pattern (see below). No intraspecies differences were apparent in the gamma globulins in any of the species.

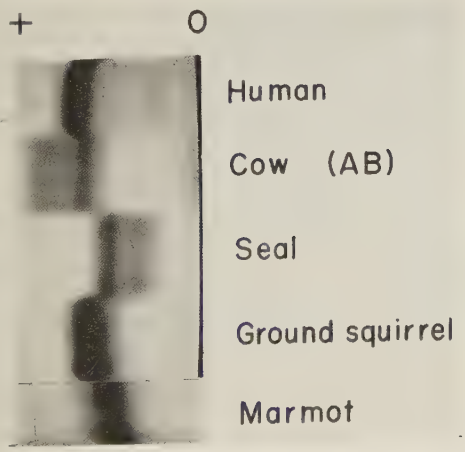

Fig. 1 Starch gel electrophoresis of hemoglobins after staining with amido black. 0, origin; the positive pole is indicated.

Serum proteins; starch gel electrophoresis. The gel slab was split in two, one half stained with amido black to reveal the serum proteins and the other with benzidine to indicate the position of the haptoglobins. The amido black staining will be described first using the nomenclature of Smithies ('55). In figure 3 two different seal sera are compared to a type 2-1 human sera. All the specimens contained homologous hemoglobin. The slow alpha$_2$ migrates with approximately the same velocity in both species. The alpha-beta bands are generally not seen in seal sera with the exception of one animal where a band corresponding approximately to the second human alpha-beta band was seen (fig. 3, seal 5170). However, this does not bind hemoglobin as it does in humans. An intense staining band which appears to correspond to the human β-globulin contains the hemoglobin-binding haptoglobin (see below) as it does in the human types 1-1 and 2-1. Adjacent to and faster than the beta globulin band is another band, which in some sera contains haptoglobin and binds hemoglobin and in others does not (see below). Another band which corresponds approximately to the human

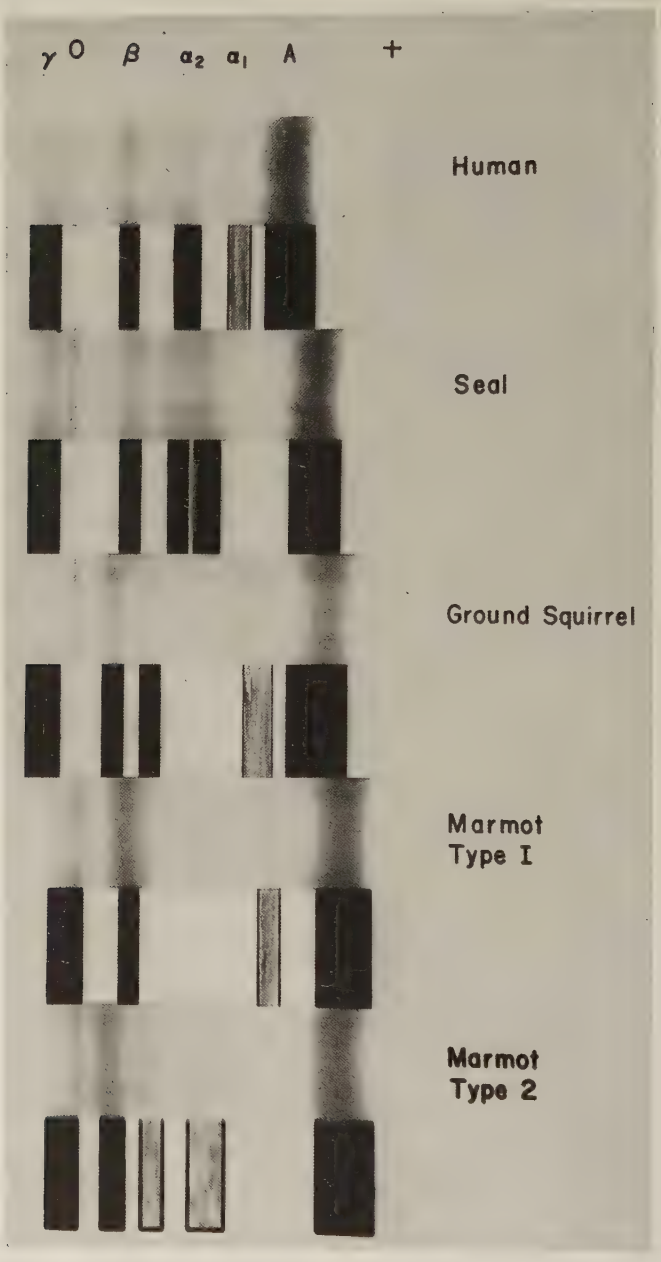

Fig. 2 Paper electrophoresis of human, seal, ground squirrel, and marmot sera. See text for details of techniques and description of patterns. In the marmot studies, types 1 and 2 refer to the nomenclature used in figure 7 and the text. A, albumin; α_1, alpha$_1$ globulin; α_2, alpha$_2$ globulin; β, beta globulin; O, origin; γ, gamma globulin. The positive pole is indicated.

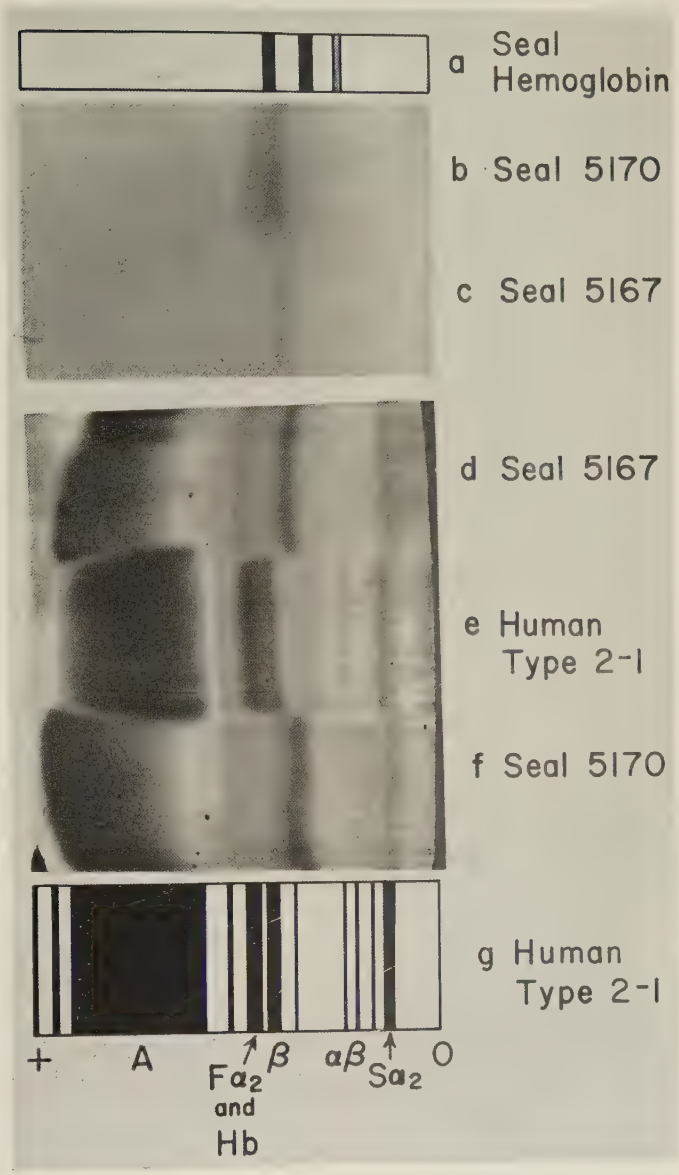

Fig. 3 Starch gel electrophoresis studies of seal sera compared to a human serum and seal hemoglobin. a, A diagram of the starch gel electrophoresis of seal hemoglobin (see fig. 1) showing the relative position of the hemoglobin bands; b, c, benzidine staining of the hemoglobin-binding bands showing the type 1 (c) and type 2 (b) haptoglobin patterns; d, e, f, g, amido black staining of two seal sera compared to a human serum. The bands of the human serum are diagramed in g to facilitate identification. A, albumin; $F\alpha_2$, Hb, fast alpha$_2$ globulin and excess hemoglobin; β, beta globulin; $S\alpha_2$ slow alpha$_2$ globulin; 0 origin. The positive pole is indicated.

fast alpha 2 will be discussed below. Some sera had one and others two postalbumin bands (fig. 4). Albumin traveled slightly faster than human albumin and no prealbumins were seen.

Haptoglobins. Benzidine staining showed two major haptoglobin patterns in the seal (fig. 3). In one, seal 5167, (type 1), a single band corresponding to the human type 1-1 haptoglobin or the fastest moving haptoglobin band of the human type 2-1 is seen. The second type (seal 5170) (type 2) has two bands, one the same as type 1 and the second traveling slightly faster. This corresponds to the band immediately in front of the beta band on amido black staining. In addition to these two types, there was one serum with a haptoglobin band traveling slightly slower than the haptoglobin band of type 1. As noted above, seal hemoglobin has two main peaks on paper and gel electrophoresis with a minor peak visible on starch gel electrophoresis (fig. 1), and the position of these bands relative to the haptoglobins are shown in figure 3. It is clear that all the hemoglobin bands bind to the single haptoglobin of type 1 and to the two haptoglobins of type 2. If seal hemoglobin in excess of approximately 150 mg/100 ml of sera is added to the sera, then a benzidine staining band corresponding to free hemoglobin can be seen traveling slower than the haptoglobin bands.

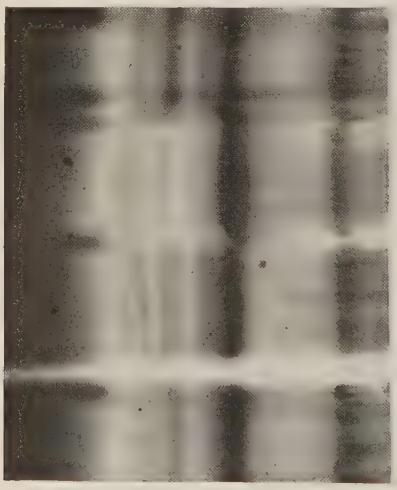

Fig. 4 Starch gel electrophoresis and amido black staining. Varieties of seal serum protein patterns; a, d, have one postalbumin band; b, c, have two postalbumins; a and c are haptoglobin type 2 and have a double beta band. In b, there is a band moving slower than the major beta band; d is a type 1 haptoglobin and has a single peak in the beta region.

As increasing amounts of seal hemoglobin are added to a type 2 haptoglobin sera, the fastest-moving band decreases in mobility and when approximately 150 mg/100 ml is added, only one intensely staining band is seen in the position of the slowest moving haptoglobin band. As the second haptoglobin band slows to join the slower one, the thickness of the fast alpha$_2$ band decreases and when more than 150 mg/100 ml of hemoglobin have been added it remains as a thin line (fig. 5). Apparently, as hemoglobin is added to the serum, a protein traveling in the slow portion of the fast alpha$_2$ band is removed and forms a haptoglobin-hemoglobin complex which eventually moves with the mobility of the slower haptoglobin peak. If further hemoglobin is now added, a benzidine-staining smear is seen in the region of migration of the free seal hemoglobin. Of a total of 36 sera tested, 20 were of haptoglobin type 1 and 15 of haptoglobin type 2. (In addition, there was one type 1 which had a faintly-staining haptoglobin band moving slower than the major band.) Since some of the sera were hemolyzed and the addition of excess hemoglobin can "convert" a type 2 to an apparent type 1, an excess of type 1's may have been recorded. Seal haptoglobin binds normal adult human hemoglobin in about the same concentrations as it binds seal hemoglobin, and the resultant hemoglobin-haptoglobin complex travels with the same mobility as the seal hemoglobin-haptoglobin complex. When added to a type 2 hemoglobin serum, human hemoglobin has the same effect as seal hemoglobin in "converting" a type 2 to a type 1. Cow hemoglobin of type AB (two peaks) also combines with seal haptoglobin. It has the same conversion effect as human and seal hemoglobin just described. Only a single haptoglobin peak is seen when sufficient cow hemoglobin has been added to a type 2 seal serum as was the case for the multiple peaked seal hemoglobin, and the cow hemoglobin-seal haptoglobin complex travels with the same mobility as the seal hemoglobin-haptoglobin complex. Bands corresponding to the two

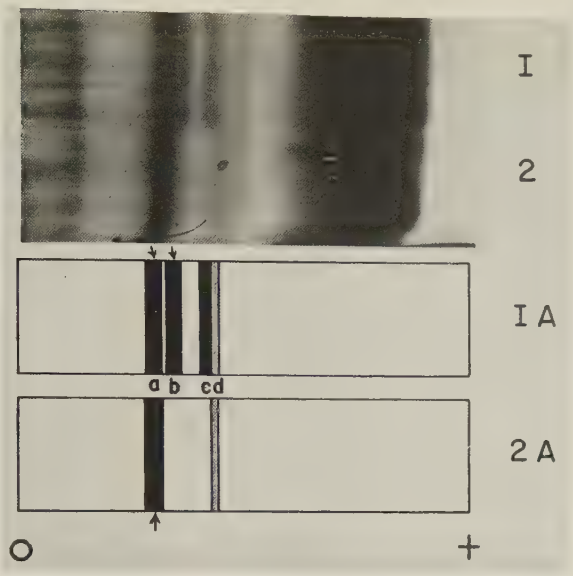

Fig. 5 The effect of adding increasing amounts of seal hemoglobin solution to a haptoglobin type 2 seal serum.

The upper two strips (1,2) are photographs of the amido black stained gel half, and the two lower strips (1A, 2A) are diagrams showing the position of the proteins discussed in the text. The small arrows indicate the position of the hemoglobin binding protein bands. In strip I and 1A the serum contains seal hemoglobin at a concentration of 80 mg/100 ml. Two distinct hemoglobin containing bands can be seen (a and b) and are indicated by the arrows in strip 1A. The band corresponding to human fast alpha$_2$ (cd) is broad and heavily staining but binds no seal hemoglobin. As further hemoglobin is added, the fast alpha$_2$ band becomes thinner until after the addition of approximately 150 mg/100 ml of hemoglobin only the fastest moving portion (d) remains (strip 2 and 2A). Simultaneously, the slower moving haptoglobin band (a) becomes more intense staining and broader at the expense of the faster moving band cd. After approximately 150 mg/100 ml of seal blood is added, only one haptoglobin band (a) remains (strip 2). O, origin. The positive pole is indicated.

separate cow hemoglobin peaks are never seen unless an excess of cow hemoglobin is added.

Ground squirrel. The appearance of the starch gel after amido black staining is shown in figure 6. The slow alpha$_2$ globulin migrates slightly slower than that of humans, and there are two bands bracketing the position of the human beta globulin band. These bands carry the haptoglobin (fig. 7). The fast alpha$_2$ band has approximately the same mobility as the human fast alpha$_2$ and one (or more) postalbumin bands are seen. The albumin migrates further than human albumin and pre-albumins were never seen. The haptoglobins were similar to those of the seal but traveled somewhat slower. Of 6 sera studied, all showed two bands similar to the seal haptoglobin type 2.

Marmot. After amido black staining, two patterns were seen (fig. 6). Of 5 animals studied, 4 showed a pattern designated type 1. The slowest moving band was slower than that of human slow alpha$_2$. The next band is an intensely staining one in the approximate position of the human beta band. This contains the haptoglobins (fig. 7). There is another band in the approximate position of human fast alpha$_2$, several postalbumins and an albumin which travels faster than human albumin. No prealbumin was seen. The second pattern (type 2) was seen in one of the 5 sera studied and is shown in figure 6. Here the haptoglobins are contained in two bands, one which just barely leaves the origin and a second which travels slower than the paired haptoglobin bands of type 1 (fig. 7).

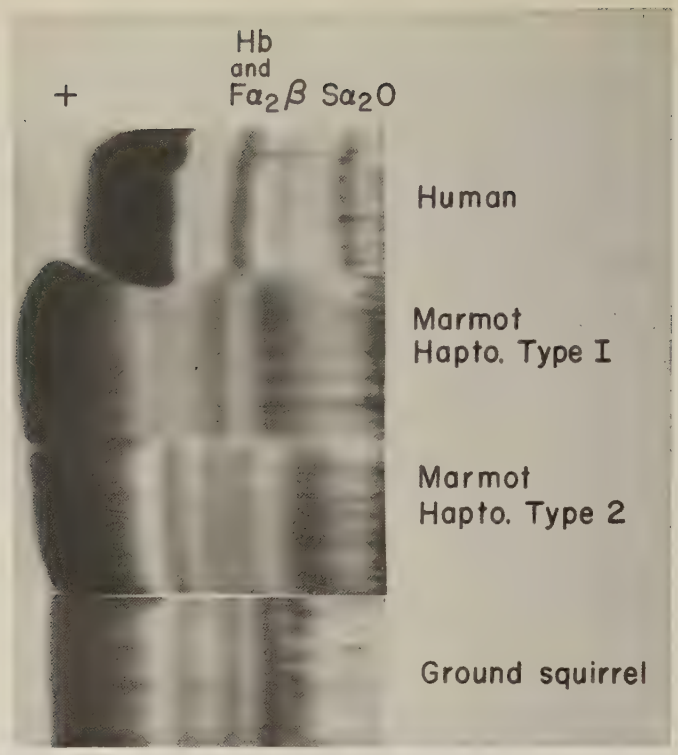

Fig. 6 Starch gel electrophoresis with amido black staining. See text for description. The symbols have the same meaning as in figure 3.

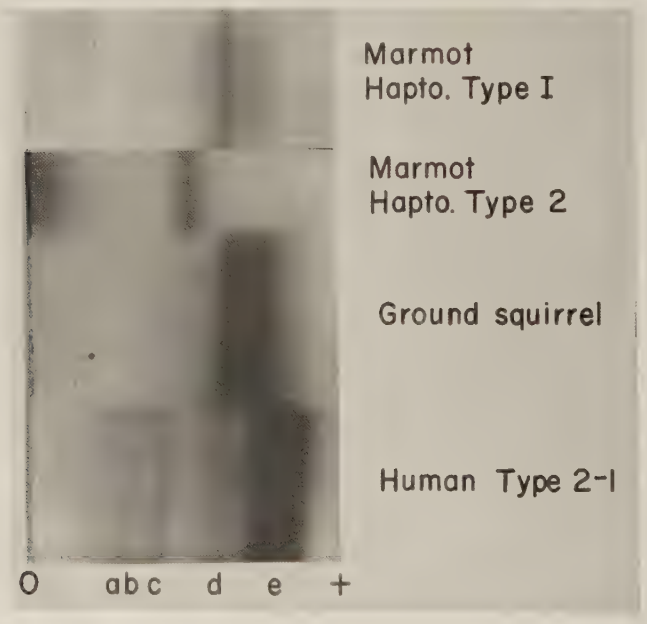

Fig. 7 Starch gel electrophoresis with benzidine staining. A comparison of the marmot haptoglobin type 1, marmot haptoglobin type 2, ground squirrel, and human type 2-1. 0, origin; a, b, c, d, are the human haptoglobin bands; e, excess human hemoglobin. The origin and positive pole are indicated.

DISCUSSION

Hemoglobins from all the seals showed the same pattern of two major components and one minor component. The situation resembles that in horses and birds and, as outlined in the introduction, is probably due to the presence of independent genes controlling the synthesis of at least the two major components. The finding that the relative mobilities of the hemoglobin components in paper and in starch gels is the same suggests that the major components differ in charge rather than size or shape. It is remarkable that when seal hemoglobin is bound by haptoglobin in the type 1 seal sera only a single band is seen; i.e., the differences in mobility between the major hemoglobin components disappears. This is also the case when the cow hemoglobin, with two components (type AB), is added to seal haptoglobin. The seal haptoglobin complexes with human and cow hemoglobin travels with the same mobility as the seal hemoglobin-haptoglobin complex, although the mobility of the three hemoglobins is different (fig. 1). This suggests that the charged groups responsible for the mobility differences in the hemoglobin components are masked by the combination with haptoglobins. This is different from the situation in man in which the complexes of haptoglobin with sickle-cell hemoglobin and hemoglobin C have different electrophoretic mobilities from the complex with hemoglobin A (Allison, unpublished). The second haptoglobin band appears to come from the fast $alpha_2$ band, (fig. 5) as is the case for type 1-1 human haptoglobin (see Smithies, '55, fig. 6). The seal haptoglobin can bind approximately the same amount of seal hemoglobin as the human haptoglobin binds human hemoglobin. Because of the unusual breeding habits of the fur seal, it is difficult to show whether the two haptoglobin types are genetically determined as seems likely.

With the exception of the marmot type 2, the haptoglobins are most similar to the human type 1-1. The sera of 150 monkeys (*Macaca mulatta*), 4 chimpanzees (*Pan satyrus*), 15 baboons (*Papio papio*), 6 rabbits and 20 Guernsey cows have been studied by one of us by means of starch gel electrophoresis (24). In none have haptoglobins similar to the three bands of human type 2-2 been seen. Most of these have haptoglobins similar to human type 1-1. It is suggested that the type 2-1 and 2-2 phenotypes (and the Hp^2 allele) might be unique to humans, a matter of evolutionary interest.

Intraspecies differences in β-globulins have been found in seals as in man (Smithies, '57), monkeys (Blumberg, '59), and other animals (Ashton and McDougall, '58; Smithies and Hickman, '58). This implies that β-globulin polymorphisms are present in a wide variety of species. The human polymorphism concerns the iron-binding protein transferrin; which of the β-globulins of the animals of the present study is affected has not been determined and may vary from species to species.

The marmot showed two distinct haptoglobin patterns. Type 1 is very similar to the human type 1-1 while marmot type 2 is quite unlike any other haptoglobin so far studied. Its slowest moving haptoglobin component probably consists of large molecules which migrate through the starch gel only very slowly. There are also intraspecies specific differences in the β-globulins of the marmots (fig. 6).

Blumberg and Robbins ('59), using starch gel electrophoresis, have shown that humans bind radioactive thyroxine in 4 separate bands in and near the albumin. One of these bands corresponds to the fastest-moving of the two human prealbumins, i.e., bands traveling faster than albumin (Smithies, '55). Monkeys have a polymorphism for the prealbumin band and for the thyroxine binding to it. Baboons and chimpanzees also have the prealbumin but the seals, marmots, and ground squirrels have no prealbumin and also no band corresponding to the fast moving thyroxine binding band of humans. The specific distribution of this trait is currently under study. Smithies has described a polymorphism in the postalbumin bands in humans (Smithies, '59). The variations in postalbumin seen in the seal (fig. 4) may correspond to this.

Genetically determined traits provide useful material for the study of evolutionary changes. They may be of taxonomic

value, and they may yield information about the adaptation of animals to different climatic and other conditions, including the severe cold to which the Alaskan animals are exposed. Studies of other species, including laboratory animals, are currently being undertaken and may provide material for the experimental investigation of selective forces acting on these polymorphic systems.

SUMMARY

1. Starch gel electrophoresis of hemoglobin was studied in 27 seals, 8 ground squirrels and 4 marmots. There are two major and one minor component in fur seals, two components in marmots, and one in ground squirrels.

2. All of these species have haptoglobins. Two phenotypes have been observed in seals, one showing a single band and the other two bands of approximately the same mobility as haptoglobins in human subjects of haptoglobin group 1-1. The ground squirrels and most marmots have a similar haptoglobin pattern except in one of the marmots in which a component apparently having a high molecular weight was observed.

3. These findings may have taxonomic and evolutionary significance.

ACKNOWLEDGMENTS

Our studies in Alaska were facilitated by many individuals and agencies to whom we are indebted. In particular, Mr. Joseph Flakne of the Arctic Institute of North America and Col. H. F. Currie and Mr. Channing Murray of the Arctic Aeromedical Laboratory, Ladd Field, Fairbanks, Alaska. The participation of one of us (A.C.A.) in the field work in Alaska was made possible by a grant from the Wenner-Gren Foundation for Anthropological Research.

LITERATURE CITED

Allison, A. C., and W. ap Rees 1957 The binding of haemoglobin by plasma proteins (haptoglobins). Brit. Med. J., *2:* 1137–1143.

Allison, A. C., and B. S. Blumberg 1958 The genetically determined serum haptoglobins in rheumatoid arthritis. Arthritis and Rheumatism, *1:* 239–243.

Allison, A. C., B. S. Blumberg and W. ap Rees 1958 Haptoglobin types in British, Spanish Basque and Nigerian populations. Nature, *181:* 824–825.

Ashton, G. C., and E. I. McDougall 1958 Beta-globulin polymorphism in cattle, sheep and goats. Ibid., *182:* 945–946.

Bangham, A. D. 1957 Distribution of electrophoretically different haemoglobins among cattle breeds of Great Britain. Ibid., *179:* 467–468.

Bangham, A. D., and B. S. Blumberg 1958 Distribution of electrophoretically different haemoglobins among some cattle breeds of Europe and Africa. Ibid., *181:* 1551–1552.

Bangham, A. D., and H. Lehmann 1958 "Multiple" haemoglobins in the horse. Ibid., *181:* 267–268.

Blumberg, B. S. 1960 Biochemical polymorphisms in animals. Haptoglobins and transferrins. Proc. Soc. Exp. Biol. Med., in press.

Blumberg, B. S., A. C. Allison and B. Garry 1959 The haptoglobins and hemoglobins of Alaskan Eskimos and Indians. Ann. Hum. Genet., *23:* 349.

Blumberg, B. S., and J. Robbins 1959 Polymorphisms in thyroxine-binding serum proteins of man and other mammals. J. Clin. Invest., *38:* 988–989.

Cabannes, R., and C. Serain 1955 Étude électrophorétique des hemoglobines des mammiferes domestiques d'Algérie. C. R. Soc. Biol., Paris, *149:* 1193–1197.

——— 1955 Hétérogénéité de l'hemoglobine des Bovides. Identification électrophorétique de deux hemoglobines bovines. Ibid., *149:* 7–10.

Ceppellini, R., H. G. Kunkel and L. C. Dunn in preparation.

Datta, R., J. Ghosh and B. C. Guha 1958 Electrophoretic behaviour of avian haemoglobins. Nature, *181:* 1204–1205.

Evans, J. V., J. W. B. King, B. L. Cohen, H. Harris and F. L. Warren 1956 Genetics of haemoglobin and blood potassium differences in sheep. Ibid., *178:* 849.

Galatius-Jensen, F. 1957 Further investigations of the genetic mechanism of the haptoglobins. Acta Genet., *7:* 549–564.

Jacob, G. F., and N. C. Tappen 1958 Haemoglobins in monkeys. Nature, *181:* 197–198.

Jayle, M. F., G. Boussier and J. Tonnelat 1956 Isolement a partir du serum humain de la combinaison hemoglobine-haptoglobine a l'etat homogène. Bull. Soc. Chim. Biol., *38:* 343–349.

Johnson, V. L., and J. S. Dunlap 1955 Electrophoretic separation of hemoglobins from the chicken. Science, *122:* 1186.

Ramirez, J. R., and H. C. Dessauer 1957 Isolation and characterization of two hemoglobins found in the turtle, Pseudemys scripta elegans. Proc. Soc. Exp. Biol. Med., *96:* 690–694.

Ranney, H. M., and S. Gluecksohn-Waelsch 1955 Filter paper electrophoresis of mouse haemoglobin: Preliminary note. Ann. Hum. Genet., *19:* 269–272.

Saha, A., R. Datta and J. Ghosh 1957 Paper electrophoresis of avian and mammalian hemoglobins. Science, *125:* 447–448.

Smithies, O. 1955 Zone electrophoresis in starch gels: group variations in the serum proteins of normal human adults. Biochem. J., *61:* 629–641.

——— 1957 Variations in human serum β-globulins. Nature, *180:* 1482.
——— 1959 An improved procedure for starch-gel electrophoresis: Further variations in the serum proteins of normal individuals. Biochem. J., *71:* 585–587.
Smithies, O., and C. G. Hickman 1958 Inherited variations in the serum proteins of cattle. Genetics, *43:* 374–385.
Smithies, O., and N. F. Walker 1955 Genetic control of some serum proteins in normal humans. Nature, *176:* 1265–1266.
van der Helm, H. J., and T. H. J. Huisman 1958 The two hemoglobin components of the chicken. Science, *127:* 762.
Woods, K. R., E. C. Paulsen, R. L. Engle, Jr. and J. H. Pert 1958 Starch gel electrophoresis of some invertebrate sera. Ibid., *127:* 519–520.

The Stimulation of Frog Skeletal Muscle by Light and Dye[1]

WILLIAM I. ROSENBLUM
Department of Pharmacology, New York University College of Medicine

Frog skeletal muscle which is exposed to visible light after staining with a fluorescent dye, twitches and develops a sustained contracture (Lippay, '29, '30a, '30b). Lippay believed that the twitches are due to the stimulation of nerve endings in the muscle, while contracture is due to stimulation of the contractile mechanism within the muscle fibers. Later workers disagreed with Lippay's interpretation and reviewers of photodynamic sensitization decided that the Lippay's evidence is inconclusive (Blum, '41; Clare, '56). The question has now been re-investigated and the evidence strongly supports the idea of Lippay that there are two sites at which light stimulates a stained muscle.

Lippay ('30b) favored the two-site interpretation for the following reasons. Stained muscle depolarized with KCl gives a contracture but does not twitch when exposed to light. Curare prevents twitching but does not effect the contracture. This experiment was ambiguous, however, because Lippay noted that curare also precipitated the dye, hence the results could be explained on the basis of a lowered dye concentration. But in another experiment it was found that chronically denervated muscle also fails to twitch when stained and exposed to light, though it undergoes a contracture. These results, then, support a theory which states that the sites responsible for the twitch responses differ from the sites responsible for the contracture.

However, Lippay's ('32) subsequent work served to confuse the issue. Turning to isometric recording, he found that light caused stained muscle to give "brief tension changes," even in the presence of trimetheylammonium, a curare like agent. However, Lippay notes that the records obtained in this series of experiments with isometric recording differ in shape from those obtained in his previous experiments with isotonic recording and this discrepancy makes difficult any interpretations in terms of his earlier theory.

Other workers, nevertheless, dismiss the earlier experiments in favor of the latter (Blum, '41) and conclude that the neuromuscular junction is not involved in the action of light on stained muscle. The results of Lillie et al. ('35) are taken to support this point of view; they found that light increased the stimulatory effect of Cl, Br, NO_3 on stained muscle. These authors felt that the effects of light and dye ". . . depends primarily on photoxdative reactions occurring at the surface of the muscle cells." They felt that sodium salts of these anions dispersed the membrane colloids and that light and dye ". . . produce a further change of the same kind, sufficient to initiate the process of stimulation." Apparently, these authors assumed that if ions acted upon the muscle membrane anything which alters the effects of these ions must act at the same site.

Kosman ('38) showed that response of frog skeletal muscle to electrical and potassium stimulation was increased if the muscle was stained and exposed to light. He also states ". . . . the primary effect of light is upon the membrane colloids."

Finally, Kosman and Lillie ('35) found that muscle protein increased its uptake of oxygen if stained and illuminated. This was true even if the protein was boiled. Still assuming that ". . . the photochemical reaction . . . produces a state of increased sensitivity in the muscle cells" they conclude that " . . . it is the membrane proteins" which are involved in the photo-

[1] This investigation was supported by a research grant B-1870 from the Institute of Neurological Diseases and Blindness, U. S. Public Health Service, and by grant 1-01-731 from the National Science Foundation.

chemical reactions. All of the arguments summarized in the last three paragraphs are notably indirect and for this reason scarcely compelling. With this background the present work was undertaken.

METHODS AND MATERIALS

Muscles. The muscles used were either gastrocnemii or sartorii from *Rana pipiens* supplied by the New York Scientific Supply Company during the months of June, July and August.

Solutions. The Ringer's consisted of 117 mM NaCl, 3 mM KCl, 2.7 mM $CaCl_2$, and 3 mM $NaHCO_3$. The dye used was rose bengal (1:25,000), the muscles were stained 1.5 to 2 hours. Acetylcholine (ACh) was used as the bromide.

Neuromuscular block. Neuromuscular block was produced by placing muscles in Succinyl choline bromide (50 μg/ml) or in a Ringer's in which 20 mM of the NaCl was replaced with $MgCl_2$. The effectiveness of the block was tested by stimulating the nerve with supramaximal stimuli from an inductorium. When the muscle no longer responded to stimulation through the nerve, the muscle was stimulated directly to test its viability. The effects of these agents on the myoneural junction could be reversed by returning the muscles to ordinary Ringer's.

Illumination. The source of light was a tungsten lamp, either a clear 300 w bulb or a 300 w projection lamp. The set-up was as described by Lippay ('30b). The light beam was passed through a three-liter round bottom flask filled with water. This filtered the heat and focussed the light. The ordinary 300 w light source was placed 18 inches from the muscle, and the projection lamp was placed 24 inches from the muscle. In most experiments the muscle was suspended in air in a glass chamber with a water saturated atmosphere; in a few experiments the chamber was filled with mineral oil.

Temperature. The first attempts to excite the muscle at room temperature failed, but the twitch was elicitable approximately 80% of the time in a cold room at 4°C. Later the response was obtained at room temperature (22–24°) about 70% of the time. The reasons for the early failures are unknown.

Recording. The response of the muscle was recorded isotonically on a smoked drum, whenever experiments were done in the cold room. When experiments were performed at room temperature, the muscle's response was recorded isometrically via a phonograph crystal, cathode follower and one beam of a Dumont dual beam oscillograph. Electrical recordings from the sciatic nerve in nerve-muscle preparations were made with platinum electrodes through a preamplifier leading to the other beam of the oscillograph. The nerve was laid upon the electrodes and kept moist with mineral oil. A ground electrode was thrust into the muscle. In recording directly from the muscle, all electrodes were placed in the muscle. The shortening of glycerated fibers was recorded with a Grass polygraph.

RESULTS

First, Lippay's experiments on the effect of light on stained muscles which were depolarized with isotonic potassium solu-

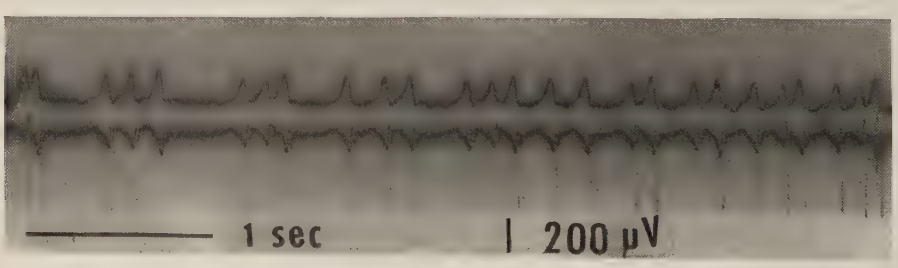

Fig. 1 Recording of action potentials from the gastrocnemius of *Rana pipiens*. Each action potential immediately precedes a twitch of the muscle. The muscle has been stained in a 1:25,000 concentration of rose bengal. The recording is made while the muscle is exposed to light. The upper line records the twitches. Lower line records potential changes. Read figure from right to left.

tions were repeated. In agreement with his results the potassium solution abolished the twitch without interfering with the contracture. Therefore, the polarization of the muscle membrane seems prerequisite for the appearance of the twitches.

This result suggests that electrical events in the membrane may precede the twitch and this idea was tested by recording from the stained muscle during illumination. Such recordings (fig. 1) show that the twitch response coincides with action potentials in the muscle. Unstained muscle exposed to light, and dyed but unirradiated muscle show neither response. It is clear that there are two distinct responses in a stained and illuminated muscle. One of these is a contracture which can occur in a muscle with a depolarized membrane and the other is a twitch depending on electrical excitation of the muscle membrane. The question now remains as to whether the membrane is directly or indirectly excited.

Origin of twitches. To answer this question muscles were treated with magnesium or succinyl choline to block neuromuscular transmission (Bovet et al., '51; del Castillo and Engbaek, '54). Mg was used because it was not expected to complex with or precipitate the dye. Neither it nor succinyl choline were, in fact, observed to precipitate the dye. Ten consecutive experiments were performed; 4 with Mg and 6 with succinyl choline. In every case the twitch was blocked while contracture remained (fig. 2). It we take a value of 30% for the normal percentage of trials on which a twitch may *not* be expected to occur then we see that these results could occur by chance only 0.3^4 and 0.3^6 times for Mg and succinyl choline respectively. Hence, results with each are significant beyond the 1% level of confidence. Fur-

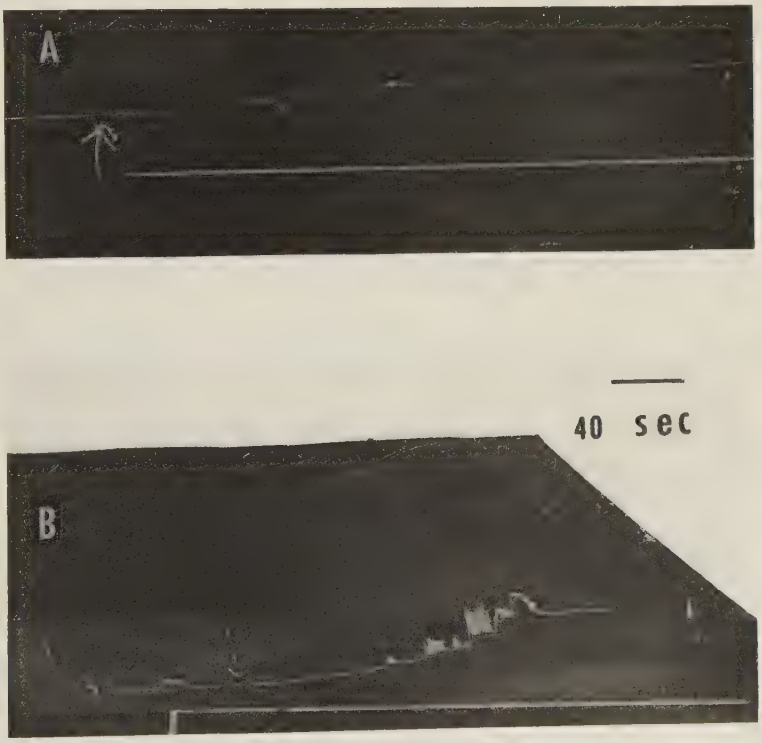

Fig. 2 Upper line of each section of the figure represents change in muscle length. Lower line in each case is a base line. Arrow indicates onset of illumination. A, Record obtained with NMJ blocked by magnesium. B, Record obtained with a gastrocnemius not treated with any blocking agent. Both muscles stained with rose bengal.

ther, a stained muscle, first blocked with succinyl choline and then washed until the block was removed, gave a twitch when illuminated.

The pharmacological evidence clearly shows that the muscle is activated through the neuromuscular junction to produce the twitch. Presumably then, the light excites the nerve endings or the nerve itself. To test this hypothesis directly, recordings were made from the sciatic nerve of stained nerve-muscle preparations during the illumination. Figure 3 shows that each twitch is preceded by an action potential in the nerve. The sequence of the positive and negative phases of the recorded action potentials showed that these impulses are traveling along the nerve from the region of nerve endings in the muscle toward the periphery of the nerve. The impulses could not have arisen by stimulation of the nerve peripheral to the electrodes. The electrodes were very close to the muscle, which makes it highly unlikely that the muscle was fired by excitation of an area of free nerve between electrodes and muscle. It seems most likely that the record represents backfiring from excited nerve endings in the muscle. Consequently, the electrical and pharmacological evidence, in agreement with Lippay's ('29) original conclusion, supports the idea that the nerve endings in the dyed muscle are excited by light and that it is this neural excitation which causes the stained and illuminated muscle to twitch.

Interaction with anion stimulation. Lillie et al. ('35) showed that light and dye increased the effects of anions on skeletal muscle. These authors felt that light stimulated the stained muscle membrane directly and thus its effect was able to accentuate the effect of ions known to act on the membrane. However, no precautions (e.g., curare) were taken to eliminate the possible effects of nerve stimulation. Since it has been shown that light and dye stimulate the nerve endings in the muscle, we must consider whether it was this neural activity rather than some effect of light and dye directly on the muscle membrane which caused the observed increase in the

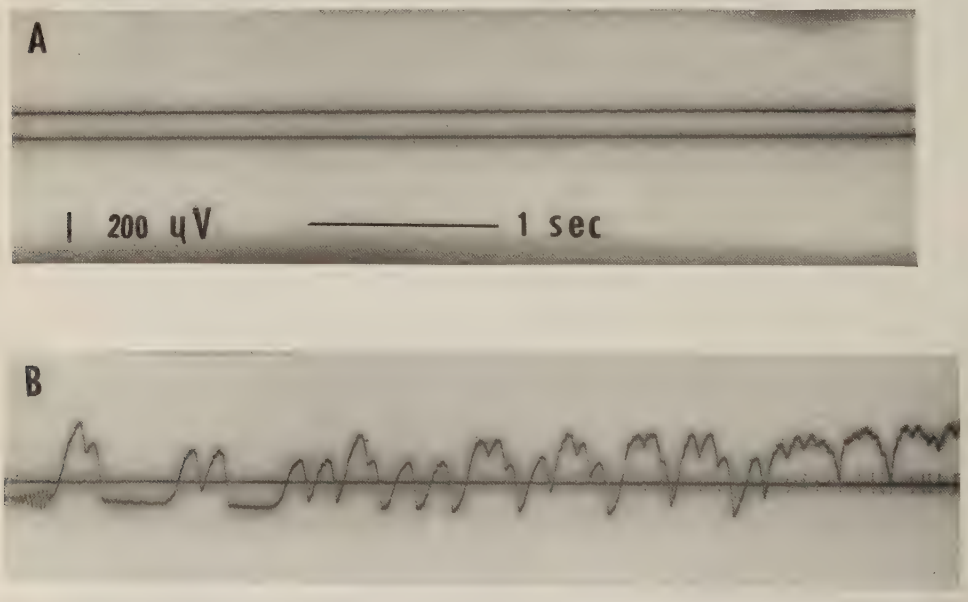

Fig. 3 Recording from the sciatic nerve of a sciatic-gastrocnemius preparation. The upward deflections of the upper line represent the muscle twitches while the lower line records the potential changes in the nerve. Read figure from right to left. Part A of the figure was recorded with the light off; part B with the light on. In both cases the muscle has been stained with rose bengal. For evidence that the firing in the nerve originates in the region of the nerve endings, see text. The downward slant of the upper line in part B is an artifact of recording.

response to anions. A sartorius was placed in Ringer's and a subthreshold dose of ACh applied. Then the muscle was washed in Ringer's and placed in isotonic (M/8) $NaNO_3$, which caused the muscle to twitch. When the heretofore subthreshold dose of ACh was given immediately after the nitrate effect had subsided, a very large response was obtained, which greatly exceeded the response to nitrate alone (fig. 4). The results indicate that the response of a muscle to anions may be effected by ACh; the work of other authors (Chao, '35) has shown that the response to anions may be effected by direct stimulation of the muscle membrane. In Lillie's experiment both types of interaction would have been possible and thus his work cannot be used to decide where light acts on a stained muscle.

Contracture in glycerated fibers. The twitch response to light depends upon stimulation of the nerve endings in the muscle. But the contracture occurs even when neuromuscular transmision is blocked and when the membrane is made electrically inexcitable. Therefore, the light and dye must be acting on a different site in bringing about contracture. It seemed possible that the contractile mechanism of the muscle was activated directly by dye and light. One test of this idea would be to glycerate muscle fibers and to obtain contraction simply by staining and irradiating them. The assumptions here are that we have the contractile mechanism in relatively "pure" form and that the ATP, which is removed in glycerating, would not be necessary since the energy utilized in contraction would come either directly from light energy absorbed by the dye or from some substance synthesized in the muscle with the aid of this captured energy.

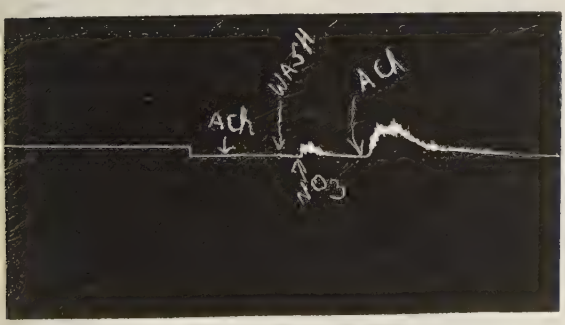

Fig. 4 Record shows how a subthreshold dose of ACh in the presence of isotonic $NaNO_3$ brings about a response in the muscle greater than that to $NaNO_3$ alone.

Fibers were glycerated according to the method of Szent-Gyorgyi ('49). They were stained with rose bengal both in the usual 1:25,000 concentration and also in a 1:1000 concentration. They failed to shorten when exposed to light. The fibers were then stained with 10^{-2} M acridine orange, a fluorescent dye which competes with ATP for the same site in the glycerated fiber (Szent-Gyorgyi, '57). Contraction failed to occur upon exposure to light. It must be concluded that some factor or factors necessary for contracture under the influence of light and dye are removed in the glycerating process. We known that light and dye do not damage the fibers, because after 6 minutes of exposure to light, fibers stained with rose bengal still contract in response to 0.25% solution of ATP.

DISCUSSION

The results of the experiments are clear. Twitching of a stained and illuminated muscle is due to the stimulation of nerve endings in the muscle. Evidence for this comes from two sets of experiments. The first experiments demonstrated inhibition of the twitch by agents which block myoneural transmission. The second group of experiments demonstrated that twitches are preceded by an action potential in the nerve and suggest that the action potentials start at the nerve endings.

A second response of stained and illuminated muscle is irreversible contracture. This response occurs even when the membrane is depolarized by potassium salts; hence, it does not depend upon electrical events in the nerve endings or muscle membrane. The glycerated muscle fibers do not show contracture after being stained and illuminated. It may be that the ATP removed by glycerating is necessary for the contracture induced by light and dye, and that the contracture is brought about in the intact fiber through stimulation of a site bringing about utilization of the energy stored in ATP.

The evidence of Kosman ('38) suggests that light and dye also acts on the mem-

brane of the muscle fibers. He showed that a light focussed on the non-innervated end of a stained muscle increases the response of the muscle to K or to electrical stimulation. It can be concluded that in a stained muscle light acts on the nerve endings, on the membrane of the muscle fibers, and at some step involving the contractile machinery of the fibers. It may be that more than three sites in a stained muscle can be effected by light and that work thus far has elucidated only three targets because our tests allow us to observe the results of stimulation of only the most sensitive sites in the muscle.

In the experiments of Lillie, Hinrichs and Kosman ('35), it was shown that light can increase the response of a stained muscle to isotonic solutions of the sodium salts of negative ions. But in these experiments, either the nerve endings or the muscle membrane could have been effected by the light. Earlier in the present paper it was shown that stimulation of the nerve endings could result via the release of ACh in an increase in the muscle's response to negative ions; hence, the experiments of Lillie et al. do not allow us to say whether it was the action of light on the membrane per se or on the nerve endings which was responsible for the results reported in their paper.

The question also arises as to the importance of experiments involving sensitization of muscle or nerve to light in leading to a better understanding of naturally occurring photochemical processes. Chalazonitis ('57), for example, has utilized data gathered from experiments involving sensitized *sepia* neuron to support a theory of excitation in which the chief hypothesis is that the acceleration of respiratory enzyme activity is crucial to the excitatory process. Arvanitaki and Chalazonitis ('58) have sought to explain with this theory the excitation by light of the naturally pigmented neurones of *Aplysia*. Before speculating further along these lines, it is necessary to point out that there is, as yet, no evidence that stimulation of dyed nerve by light is truly reversible. Lippay ('29, '30) presents figures indicating that the muscle continues to twitch after the light is turned off. Similarly, I was unable to stop the twitches by turning off the light. Even if the light was turned off after the first twitch, the muscle as often as not continued to twitch for a variable length of time. Nor was it possible to predict how soon, if at all, the muscle will twitch when the light is again turned on. Thus in its grosser characteristics there is no analogy between the stimulation of nerve by an electric current and by light and dye.

The most popular postulate about the mechanism by which light and dye act, involves a series of reactions beginning with the excitation of the dye and ending with oxidation of some excited substrate (Clare, '56). It remains to be seen whether some substance produced in this chain caused reversible stimulation or merely destruction. The destruction of each group of endings would result in the successive firing of different groups of muscle fibers. Until this problem is resolved, it would seem better to avoid the use of "reversible" in referring to the photostimulation of stained skeletal muscle, or isolated nerve preparation.

It may be significant that Kolm and Pick ('20) *were* successful in reversibly increasing the tonsus of stained frog intestine with light, the tonus falling when the light was turned off and rising when the photostimulation was repeated. Furthermore, they were able to show that the effect of light was reversed by atropine and by adrenaline. Blocking the parasympatheic ganglia with a large dose of nicotine did not prevent the response; hence, they conclude that light and dye were acting on the postganglionic, parasympathetic endings in the intestine. Thus, the mechanism of action of light and dye on both smooth and striated muscle of the frog would seem to involve the stimulation of nerve endings releasing acetylcholine.

SUMMARY

1. When skeletal muscle of the frog is stained with rose bengal and the muscle is then illuminated, twitches occur due to stimulation of the nerve endings in the muscle. The evidence for this conclusion is that neuromuscular block by magnesium or succinyl choline prevents the twitches and that a nerve impulse originating in the region of the nerve endings precedes each twitch.

2. Subthreshold doses of ACh were shown to augment the effects of anion stimulation on skeletal muscle. Since illumination of stained muscle stimulates the nerve endings in that muscle ACh will be released. Other workers have shown that anions interact with an electric impulse effecting only the non-innervated portion of the muscle membrane. Therefore, results showing that the effects of light and dye augment the response of non-curarized muscle to anions may be due either to stimulation of the nerve endings by light and dye or to the stimulation of the muscle membrane per se, by these agents.

3. Muscles stained with rose bengal and then illuminated give a twitch response only 75% of the time. But the muscles invariably develop a contracture. The contracture occurs even in muscles which are rendered electrically inexcitable by depolarization of the muscle membrane with potassium. Contracture will not occur in glycerated muscle fibers, however, when such fibers are stained and illuminated.

4. Evidence that light and dye have effects directly upon the muscle membrane and the muscle fiber proper, is discussed, as is the possible relationship between photostimulation of nerve endings in the stained muscle and naturally occurring photo-processes.

The author would like to express his sincere thanks to Dr. William Van der Kloot for his advice during all stages of this work.

LITERATURE CITED

Arvanitaki, A., and N. Chalazonitis 1958 Activation par la lumiere des neurones pigmentes. Arch. des Sciences Physiologiques, *12* (H2): 73–106.

Blum, H. F. 1941 Photodynamic Action and Diseases Caused by Light. Reinhold, New York, p. 108.

Bovet and others 1951 Recherches sur les poisons curarisants de synthese III[e] partie-succinyl choline et derives aliphatiques. Arch. int Pharmacodyn. *88:* 1–50.

Chalazonitis, N. 1957 Effets de la lumiere sur l'evolution des potentials cellulaires et sur quelques vitesse's d'oxydoreduction dous les neurones, BOSC Freres, Lyon, France.

Chao, I. 1935 Action of electrolytes on the electrical stimulation of skeletal muscle. J. Cell. and Comp. Physiol., *6:* 1–19.

Clare, N. T. 1956 In: Radiation Biology III, ed. Hollaender. National Research Council, McGraw-Hill, New York. pp. 693–723.

del Castillo and Engbaek 1954 Action of magnesium on neuromuscular transmission. J. Physiol., *124:* 370–384.

Karreman, M., and Szent-Gyorgyi 1957 Competitive binding of ATP and acridine orange by muscle. Proc. Nat. Acad. Sci., U.S.A., *43:* 373–379.

Kolm, R., and E. P. Pick 1920 Über Beeinflussung der Automatischen Tatigkeit des Uberlebenden Kalt und Warmbluterdarmes durch Fluoreszenzstrahlen, Arch. Exp. Path. Pharmakol., *86:* 1–20.

Kosman, A. J. 1938 The influence of photodynamic sensitization on electrical and chemical stimulation of muscle and cutaneous nerve endings in the frog. J. Cell. and Comp. Physiol., *11:* 279–289.

Kosman, A., and R. S. Lillie 1935 Photodynamically induced oxygen comsumption in muscle and nerve. Ibid., *6:* 505–515.

Lillie, R. S., Hinrichs and A. Kosman 1935 Influence of neutral salts on photodynamic stimulation of muscle. Ibid., *6:* 486–503.

Lippay, F. 1929 Über Wirkungen des Lichtes auf den quergestreiften Muskel. I Mitteilung. Pfluger's Arch. Ges. Physiol., *222:* 616–639.

——— 1930a Über Wirkungen des Lichtes auf den quergestreiften Muskel. II Mitteilung. Ibid., *224:* 587–599.

Lippay, F., and L. Wechsler 1930b Über Wirkungen des Lichtes auf den quergestreiften Muskel. III Mitteilung; Ibid., *224:* 600–607.

——— 1932 Über Wirkungen des Lichtes auf den quergestreiften Muskel. V Mitteilung; Ibid., *229:* 173–179.

Spealman, C. R., and H. F. Blum 1933 Studies of photodynamic action V. J. Cell. and Comp. Physiol., *3:* 387–404.

Szent-Gyorgyi, A. 1949 Free energy relations and contraction of actomyosin. Biol. Bull., *96:* 140–161.

Glucose Metabolism in Carp[1]

W. DUANE BROWN[2]
Department of Food Science and Technology, University of California, Davis, California

The composition and certain aspects of the physiology of fish have been studied to a considerable extent. Recently there have also appeared some reports dealing with fat metabolism in fish (Brown and Tappel, '59; Kelly et al., '58a, b). Generally, however, there have been but few specific studies of intermediary metabolism in fish (Gumbmann et al., '58; Tarr, '58) and any reports of the pathways of metabolism of glucose in these organisms are lacking.

This paper presents results from studies intended to demonstrate the manner in which glucose is oxidized *in vivo* in teleosts, specifically whether the classical Embden-Meyerhof scheme or the pentose cycle is of primary importance. They indicate that the pentose cycle does not make a major contribution to glucose metabolism in carp; the conclusion that the Embden-Meyerhof pathway is responsible for essentially all glucose oxidation in this organism is in agreement with all the results presented.

EXPERIMENTAL PROCEDURE

Treatment of animals. Live carp, approximately 8 inches in length, were obtained from a local minnow supply house and maintained in the laboratory in 15-gallon tanks containing aerated tap water at room temperature. For an experiment, an individual carp was removed from the tank and placed in a smaller vessel for a period of approximately 24 hours prior to the start of the experiment; the animals were not fed during this time. The metabolism chamber used consisted of a large mouth culture flask of about 2800 ml capacity. The flask was fitted with a rubber stopper through which were placed an inlet tube, an outlet tube, electrodes for pH determination, a thermometer, and the tip of a burette containing 1 M HCl. The outlet tube was connected through a Y joint to two suction flasks each containing 34 ml of 1 N NaOH; these flasks served to trap the respired CO_2. They were kept under slight vacuum to insure rapid air flow through the system. The inlet tube had a fritted glass tip and introduced air that had been rid of CO_2 by passage through alkali trapping solutions. For an experiment the flask was nearly filled with about 2500 ml of distilled water that had previously been acidified to pH 4–5 with HCl and boiled. The stopper was inserted and CO_2-free air was passed through the system for at least an hour. The fish was then injected intraperitoneally with a solution of radioactive glucose (5 μc, C-1 or C-6 labeled) in isotonic saline and quickly placed in the chamber, which was then resealed.

The respired CO_2 was swept out into the trapping solutions which were changed at periodic time intervals. During the course of the experiment the pH was kept at 5.0 or below by the occasional addition of dilute HCl. This was done to insure the rapid release of CO_2 from the chamber. Preliminary tests indicated that such a procedure was satisfactory. The temperature of the water was 24–25°C and did not vary more than 1°C at any time during any of the experiments. Other preliminary studies showed that the fish could be easily maintained under these conditions, provided that distilled water was used and the pH kept at 5.0 or slightly below with HCl. Acidified tap water could not be used since the fish were obviously adversely affected, apparently due to the large amounts

[1] This research was supported in part by funds made available through the Saltonstall-Kennedy Act and administered by means of a collaborative agreement between the U. S. Fish and Wildlife Service and the University of California.

[2] Present address: Institute of Marine Resources, Marine Food Technology Laboratory, University of California, Berkeley, Calif.

of acid required to maintain the proper pH; the use of buffers was similarly unsatisfactory. At the conclusion of an experiment the fish was removed from the chamber, killed by pithing, and the liver removed, packaged and quick-frozen in an acetone-dry ice mixture.

MATERIALS AND METHODS

D-glucose-1-C^{14} (G-1-C^{14}), activity 1.5 mc/mM, was obtained from Isotopes Specialties Company, Inc. and D-glucose-6-C^{14} (G-6-C^{14}) activity 2.0 mc/mM was obtained from Nuclear-Chicago, Inc. The activities were checked by wet combustion and subsequent radioassay of portions of the materials.

The CO_2 was recovered from the trapping solutions by the addition of 5 ml of 12% $BaCl_2$ which contained a small amount of NH_4Cl. The precipitated $BaCO_3$ was collected in planchet size by means of a filtering apparatus, washed repeatedly with CO_2-free water and ethanol, dried, and counted in a gas-flow counter at infinite thickness. Normally the trapping solutions were split into at least two portions prior to $BaCO_3$ precipitation in order to get duplicate samples for radioassay.

The livers were thawed, homogenized (1:5 wt./vol.) in an alcohol-ether (3:1) solution, and the homogenates refluxed at 60°C for one hour. The material was centrifuged and the precipitate washed with alcohol-ether. The washed material was saved for amino acid isolation. The alcohol-ether solution was evaporated almost to dryness and extracted with petroleum ether. This fraction (total lipids) was put on a planchet for radioassay, dried to constant weight and counted. All operations with this and other lipid fractions, except for the actual counting procedure, were conducted in a nitrogen atmosphere. After being counted, the total lipids were extracted from the planchet with petroleum ether, dried and extracted with acetone. The acetone fraction (triglycerides) was placed on a planchet and counted. That portion not soluble in acetone (phospholipids) was taken up in petroleum ether, put onto a planchet and counted. The triglyceride fraction was then dissolved in alcohol and saponified with alcoholic KOH under nitrogen. Following acidification and removal of KCl from the saponified mixture the fatty acids were extracted in ether and counted. The remainder of the mixture was taken nearly to dryness, the glycerol extracted with absolute ethanol and the ethanol extract counted. Since the quantities of these various lipid fractions were not sufficient for radioassay at infinite thickness, self-absorption curves were run and the appropriate corrections made.

The protein fraction of each liver was acid-hydrolyzed, the hydrolyzate treated with activated charcoal, and the amino acids alanine and glutamic acid isolated by salt precipitation techniques (Kruse et al., '57) following addition of carrier. Alanine was isolated as the phenyl-azobenzene-*p*-sulfonic acid salt and glutamic acid as the hydrochloride. The isolated salts were counted at infinite thickness in the gas-flow counter. The glutamic acid-HCl was converted to glutamic acid and again counted.

Assays for glucose-6-phosphate dehydrogenase and 6-phosphogluconate dehydrogenase were done on isotonic sucrose homogenates of fish liver by the conventional determination of triphosphopyridine nucleotide reduction (Kornberg et al., '55).

RESULTS AND DISCUSSION

The specific activity in the expired CO_2 from carp injected with either G-1-C^{14} or G-6-C^{14} is shown in figure 1. The general nature of the curves is the same regardless of which specifically labeled glucose was administered, although there were some differences between fish, particularly several hours after injection. Probably of most significance is the fact that the initial rates of production of labeled CO_2 were approximately the same regardless of whether G-1-C^{14} or G-6-C^{14} was the compound injected. If the pentose cycle contributed to any extent to glucose oxidation then the rate of production of labeled CO_2 should be substantially greater after administration of G-1-C^{14} than after G-6-C^{14} (Black et al., '57; Jolley et al., '58). Calculations based on the total amount of labeled respired CO_2 indicated that about 30% of the injected glucose radioactivity appeared in the CO_2 within 48 hours.

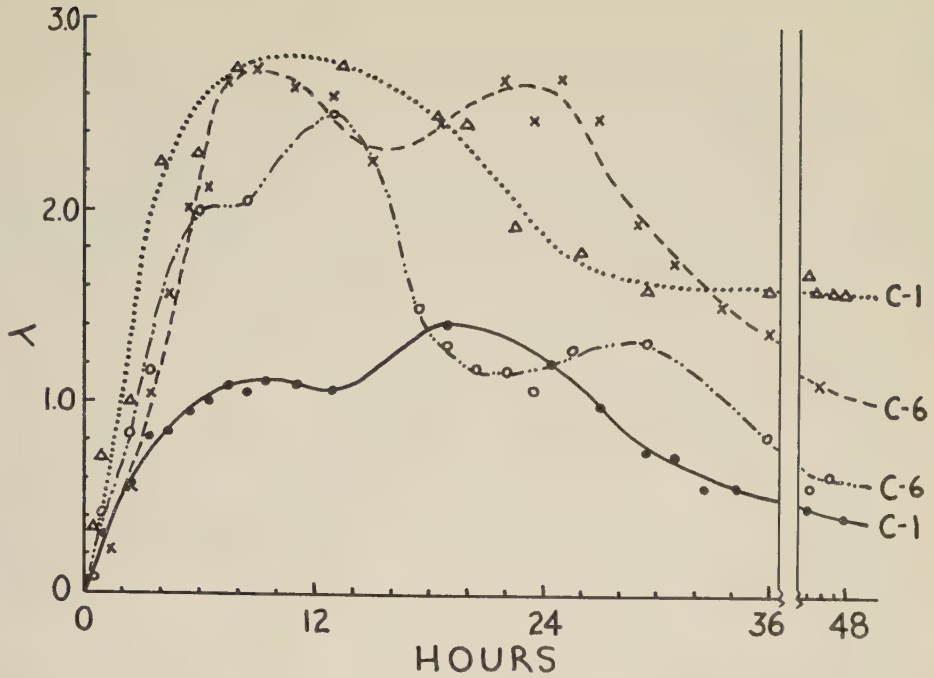

Fig. 1 Activity of respired CO_2 from carp injected with labeled glucose. Legend on graph: C-1 indicates glucose-1-C^{14} injected; C-6 indicates glucose-6-C^{14} injected. λ, microcuries per mole CO_2 per microcurie injected per kilogram of body weight.

TABLE 1

Specific activities of liver lipid fractions after injection of glucose-C^{14} [1]

Compound injected	Total lipids	Triglycerides			Phospholipids
		Total	Fatty acids	Glycerol	
	Sampled 48 hours after injection				
Glucose-1-C^{14}	2020	616	185	725	5580
Glucose-6-C^{14}	1760	536	300	340	4880
	Sampled two hours after injection				
Glucose-1-C^{14}	3380	435	150	350	3740
Gluocse-6-C^{14}	2270	1080	300	680	3170

[1] Values are in counts per minute, corrected to infinite thickness, and are averages of duplicates for the 48-hour samples, single values for the two-hour samples.

Specific activities of various fractions of the lipids isolated from livers of the experimental fish are shown in table 1. It would be expected that any major contribution to glucose oxidation by the pentose cycle would particularly affect the amount of C-1 of glucose entering into glycerol since this carbon atom would be lost as CO_2. Hence the fact that the specific activity of glycerol was higher in the 48 hour samples after injection of glucose-1-C^{14} than after glucose-6-C^{14} is evidence for the absence of participation of pentose cycle in glucose oxidation in these fish. Results opposite to these were obtained with the two-hour samples and suggest some involvement of the pentose cycle. However the amounts of material involved in these various fractions were small, particularly in the final fatty acid and glycerol fractions from the triglycerides; furthermore the separation of the fractions on the basis of solubility as used is not highly critical.

TABLE 2

Specific activities of amino acids of liver protein after injection of glucose-C^{14} [1]

Compound injected	Glutamic acid·HCl	Glutamic acid	Alanine
Glucose-1-C^{14}	104	72	49
Glucose-6-C^{14}	92	85	18

[1] Values are in counts per minute at infinite thickness. The glutamic acid values are averages of two runs each and are from liver samples taken 48 hours after injection of labeled glucose. The alanine values are from single runs and from samples taken two hours after injection; alanine was isolated and counted as the phenylazobenzene-*p*-sulfonic acid salt.

TABLE 3

Assay of pentose cycle enzymes in carp liver[1]

Assay	Amount of enzyme	Glucose 6-phosphate dehydrogenase activity	6-Phosphogluconate dehydrogenase activity
	ml		
1	0.02	0.4	
	0.05	0.4	0.1
2	0.10	0.4	0.3

[1] Units are 1.00 absorbancy change at 340 mμ per min. per ml. enzyme solution, corrected for substrate-less blank. Amount of enzyme indicates milliliters of a 1:6 isotonic sucrose homogenate of carp liver.

The specific activities of glutamic acid and alanine salts isolated from hydrolyzed protein fractions of livers of the experimental fish are shown in table 2. These results show that the levels of glutamic acid activity are very similar regardless of which labeled glucose was injected. Any operation of the pentose cycle should have the effect of lowering the specific activity of glutamic acid synthesized after administration of glucose-1-C^{14} because C-1 would be removed as CO_2 and hence not be found in glutamic acid. Since the specific activities are the same after G-1-C^{14}, it appears that the pentose cycle makes no major contribution to glucose oxidation. The results for the alanine salt may be similarly interpreted. It should be noted that the glutamic acid salt was isolated in substantially greater yield from the protein hydrolyzate than was the alanine salt; additionally the values for the glutamic acid activities are from duplicate runs.

Results from the assays for glucose-6-phosphate dehydrogenase and 6-phosphogluconate activities are presented in table 3. The results demonstrate that both enzymes are present in carp liver. The measured activities are, however, quite low.

The limited amount of information previously available concerning specific metabolic pathways in fishes and other aquatic animals has suggested that there are no major differences between these organisms and mammals, except for general, and expected, observations that the rates of enzymatic activity are lower in fish. For example, a recent study indicated that the rates of oxidation of fatty acids by carp liver mitochondrial enzymes were lower than the rates usually obtained from mammalian systems studied under similar conditions (Brown and Tappel, '59). The results of the present study indicate that the rate of CO_2 production by these fish is lower than usually reported rates from mammals; furthermore the activities of two enzymes of the pentose cycle were quite low. This lower level of metabolism is to be expected from the poikilothermic nature of these animals.

SUMMARY

Carp were injected with either glucose-1-C^{14} or glucose-6-C^{14} and the rates of production of radioactivity in the respired CO_2 were measured. The recovery of C^{14} in the respired CO_2 was approximately the same

regardless of which specifically-labeled glucose species was injected. Similarly the specific activities of various liver lipid fractions as well as glutamic acid and alanine isolated from liver protein fractions were also approximately the same. These results indicate that the oxidation of glucose in carp takes place primarily through the Embden-Meyerhof pathway with little participation by the pentose cycle.

Two pentose cycle enzymes, glucose-6-phosphate dehydrogenase and 6-phosphogluconate dehydrogenase, had demonstrable, but low, activities in carp liver homogenates.

LITERATURE CITED

Black, A. L., M. Kleiber, E. M. Butterworth, G. B. Brubacher and J. J. Kaneko 1957 The pentose cycle as a pathway for glucose metabolism in intact lactating dairy cows. J. Biol. Chem., 227: 537.

Brown, W. D., and A. L. Tappel 1959 Fatty acid oxidation by carp liver mitochondria. Arch. Biochem. Biophys., 85: 149.

Gumbmann, M., W. D. Brown and A. L. Tappel 1958 Intermediary metabolism of fishes and other aquatic animals. U. S. Fish Wildlife Serv. Spec. Sci. Rep., Fisheries Sec. No. 288.

Jolley, R. L., V. H. Cheldelin and R. W. Newburgh 1958 Glucose catabolism in fetal and adult heart. J. Biol. Chem., 233: 1289.

Kelly, P. B., R. Reiser and D. W. Hood 1958 The origin and metabolism of marine fatty acids: The effect of diet on the depot fats of *Mugil cephalus* (the common mullet). J. Am. Oil Chem. Soc., 35: 189.

——— 1958b The effect of diet on the fatty acid composition of several species of fresh water fish. Ibid., 35: 503.

Kornberg, A., B. L. Horecker and P. Z. Smyrniotis 1955 Assay of glucose-6-phosphate dehydrogenase and 6-phosphogluconic dehydrogenase. In: Methods of Enzymology, S. P. Colowick and N. Kaplan, I: 323. Academic Press Inc., New York.

Kruse, P. F., Jr., M. K. Patterson, Jr. and J. A. McCoy 1957 The isolation of glycine, alanine, leucine, arginine, and glutamic acid for radiometric assay in tracer experiments. Arch. Biochem. Biophys., 66: 146.

Tarr, H. L. A. 1958 Biochemistry of fishes. Ann. Rev. Biochem., 27: 223.

Effects of Temperature and Body Size upon Heart Rate and Oxygen Consumption in Turtles[1]

KENNETH E. HUTTON,[2] DON R. BOYER,[3] JAMES C. WILLIAMS[4] AND PETER M. CAMPBELL[5]
Department of Zoology, Tulane University, New Orleans, La.

Numerous scattered reports have given data on effects of temperature upon heart rates in reptiles. Reports have also been made on rates of oxygen consumption at different temperatures. However, few (with the exception of Adolph, '51) have attempted to correlate these phenomena even though Benedict, in his extensive study of reptile physiology ('32), has stated he believed that ". . . the heart rate of the tortoise may furnish a significant hint as to its metabolic activity." Also, the size of the animals has usually not been considered in interpreting the data reported.

It was the purpose of this investigation to attempt to determine the effects of temperature and body size upon heart rate and metabolic rate in two species of turtles, and to determine if a correlation exists between heart rate and metabolic rate in these animals.

MATERIALS AND METHODS

Six specimens of the Mobile cooter turtle, *Pseudemys floridana mobilensis*, were collected in the region of Lake Concordia, Louisiana, in May, 1957. Heart rates were taken of these animals of varying size at different temperatures between 10.5° and 35°C. The animals were initially cooled in a refrigerator and then gradually warmed to room temperature and heated under an incandescent lamp. Heart rates were recorded on a Sanborn Twin-Viso, Model 60, electrocardiograph. Channel 3 or, at times, channel 2 was found to give the best recordings. Leads were attached by means of copper alligator clamps to the plastron and epidermis ventral to the limbs. Electrode paste was liberally used. The animals were held immobile during the recording by strapping them with cord to a wooden platform. Results are given in figure 1.

More extensive studies were done on specimens of the red-eared turtle, *Pseudemys scripta elegans*. These animals were collected in the region of Schriever, Louisiana, a short time previous to each study in which they were used. In July of 1957 heart rates were taken on a group of 10 animals varying in weight between 300 and 800 gm. Rates were recorded at 5 degree intervals ranging from 15° to 35°C. The method of recording rates was similar to that used with the cooter turtles. However, body temperatures were achieved in a slightly different manner: the animals were placed in a water bath at the desired temperature for several hours previous to having the heart rates taken. Results are given in figure 2.

During March of 1958 oxygen consumption and heart rates at 10°, 20°, and 30°C were determined in a series of 11 red-eared turtles ranging between 233 and 1,805 gm. Oxygen consumption was measured by placing the animal in a sealed desiccator which, in turn, was placed in a constant-temperature water bath. Soda lime within the desiccator absorbed CO_2. Each desiccator was connected by tubing to a gravity-type water spirometer containing O_2. After one to two hours to allow the animal to become accustomed to its new surroundings, measurement was begun. Oxygen consumption was determined for a 20- to 22-hour period, and volume of oxygen con-

[1] This investigation conducted at the Dept. of Zoology, Tulane University, New Orleans, La., under grants from the National Institutes of Health and the Louisiana Heart Association.

[2] Now at the Dept. of Biological Sciences, San Jose State College, San Jose, Calif.

[3] Now at the Dept. of Biology, Washburn University of Topeka, Topeka, Kansas.

[4] Now at the Dept. of Veterinary Science, Louisiana State University, Baton Rouge, La.

[5] Now a student at the School of Medicine, Tulane University, New Orleans, La.

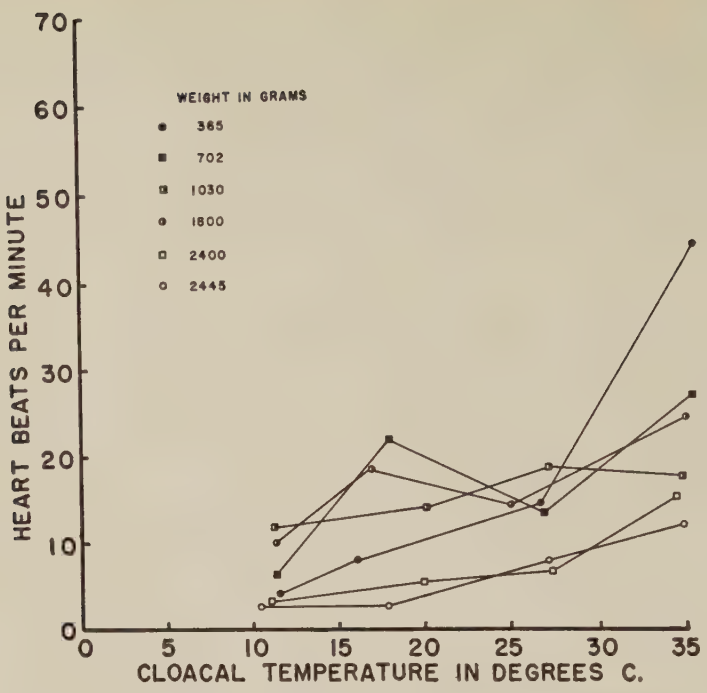

Fig. 1 Minimum heart rates at various temperatures in 6 specimens of *Pseudemys floridana mobilensis* of various body weights.

sumed was recorded after being converted to standard temperature and pressure. Just previous to placing the animal in the desiccator and just after removal, the heart rate was recorded. Previous to being placed in the desiccator, each animal had been maintained at the desired temperature for three days by having been kept in a water bath at 20° or 30°C, or in a refrigerator at 10 ± 1°C. No animal had eaten for one week previous to having its oxygen consumption determined, although the animals were kept in water-filled washtubs at room temperature and were fed whitefish and lettuce between the determinations at the different temperatures. Results are given in figure 3 and are summarized in figure 4.

In order to determine to what extent variations in heart rates at high temperatures were due to general excitement of the animals, heart rates in the series of 11 animals were determined at 25°C previous to and after cardiac injection of tubocurarine chloride. Doses two to three times that recommended for humans (2–3 × 1 mg per 10 lb. body wt.) were necessary to quiet the animals. Results will be discussed later.

Standard statistical procedures were used. Where suitable, lines of regression have been fitted to the heart rates and oxygen consumptions as compared to the weights using the method of least squares. Correlation coefficients have been computed and their significance evaluated using the Fisher z-transformation (as described by Mode, '51).

RESULTS AND DISCUSSION

Effects of temperature upon heart rate. It was not surprising to find that heart rate increased with temperature. This was true in all animals studied. In the group of 10 red-eared turtles in which heart rate was determined at different temperatures in July, the weights ranged between 300 and 800 gm. This is a relatively small weight range and no consistent differences due to weight were noticeable. For practical purposes, the variations in heart rates within this group may be considered as being due to temperature differences alone.

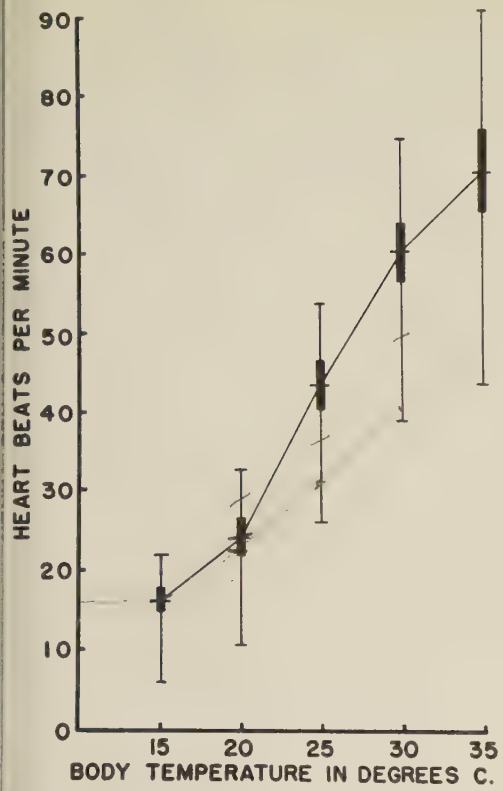

Fig. 2 Mean, standard error of the mean, and range of average heart rates at 5°C temperature intervals in 10 specimens of *Pseudemys scripta elegans* of essentially similar body weights (300–800 gm). The average heart rate at each temperature was determined in each of the 10 animals and these average rates used in the data above.

The average heart rate of each turtle at the different temperatures was determined. There was very little fluctuation within each individual of this group. Figure 2 shows the results. The mean change in heart rates and the Q_{10} of this change for each temperature increment are as follows:

°C	Beats	Q_{10}
15–20	9.0	2.53
20–25	19.3	3.24
25–30	17.1	1.92
30–35	10.2	1.37

The changes are statistically significant at the 1% level except for that between 30°–35°C which is not significant at even the 5% level. In short, the change in rate is most rapid in the center of the temperature range and falls off at the upper and lower limits. Figure 2 indicates that the higher the temperature, the wider the range of heart rates in different animals, while at lower temperatures the range is smaller. Figures 1 and 4 also indicate this tendency for heart rates to converge and fall less rapidly at lower temperatures—even considering weight differences. No sex differences were noted in any of the experiments.

Wilber and Lieb ('50) found the heart beat in the painted turtle, *Chrysemys picta*, varied from 28–35 per minute at 27°C to 93 per minute at 38°C. Kaplan and Taylor ('57) reported the heart rate in *Pseudemys sp.* was 15.3 ± 9.0 at 20°C. These rates are within the ranges found in this study. A brief review of earlier physiological studies on turtle hearts was given by Woodbury ('41) who reported gradually increasing heart rates in 6 turtles (unidentified) rising from two beats per minute at 0°C to 70 beats at 30°C. This increase in rate was accompanied by increasing systolic and diastolic pressures, indicating increasing cardiac output and vasodilation. Rodbard and Feldman ('46), in their work with *Pseudemys scripta elegans*, found the heart rate, systolic and diastolic pressures varied directly with body temperature between 3° and 38°C—although at higher temperatures these values fell. It is probable that in the present study the heart rates would not have gone much higher before starting to fall. It is at least apparent that the rate of increase is less between 30° and 35° than between the previous 5° increments of temperature. Rodbard et al. ('50) have later reported that the turtle brain, particularly the region of the third ventricle, is sensitive to temperature changes and controls thermally induced blood pressure changes. It is doubtful if intrinsic heart rhythms, as found by Loomis et al. ('30) in excised hearts of *Chrysemys picta* and *Pseudemys rubiventris*, play a significant role in the intact animal.

Effect of body size upon heart rate. Figure 1 indicates that in the Mobile cooter turtle at temperatures between 11° and 35°C, the heart rate is inversely related to the size of the animal. Weight in these 6 animals ranged between 365 and 2,445 gm.

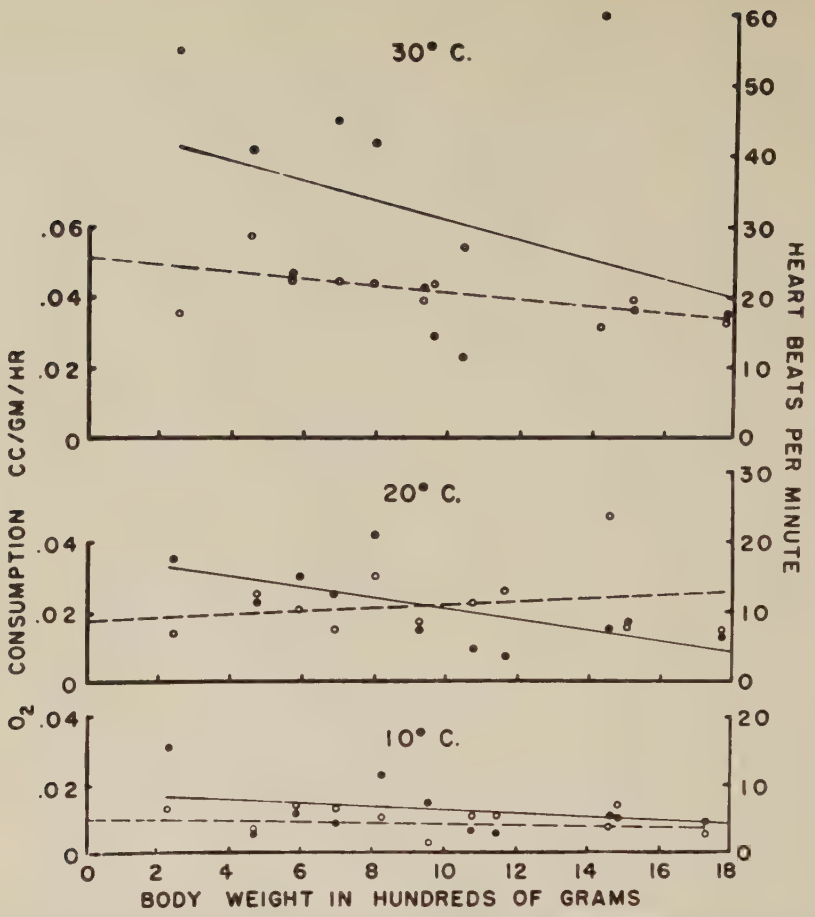

Fig. 3 Oxygen consumption (open dots) and minimum heart rates (solid dots) at 10°, 20°, and 30°C in 11 specimens of *Pseudemys scripta elegans* of various body weights. Lines of regression for oxygen consumption (broken line) to body weight and for minimum heart rate (solid line) to body weight at each temperature have been plotted using the method of least squares.

At a given temperature, the heart rate, in general, is slower the larger the animal. This is particularly true at the higher temperatures, but is less noteworthy at the lower temperatures where the differences between rates are less.

The red-eared turtle does not grow to be as large as the Mobile cooter. However, figure 3 indicates how the heart rates varied at 10°, 20°, and 30°C in 11 animals ranging in size from 233 to 1,805 gm. At 10°C the line of regression between minimum heart rates and weights slopes very gently downward with a correlation ratio of −0.313. A Fisher z-transformation of 0.907 indicates that this is not statistically significant. At 20°C the slope is more pronounced; the correlation ratio is −0.648 with a z value of 2.189, which is significant at the 5% level. There appears to be a definite inverse correlation between heart rate and body size at this temperature. At 30°C the correlation ratio is −0.380 with a z value of 1.130, which is not significant. The regression line at this temperature shows a definite slope, but there is a great deal of individual variation. We believe that the variation at this higher temperature is due to varying degrees of excitement displayed by the animals. This group of animals studied in March was more excitable than animals worked upon at

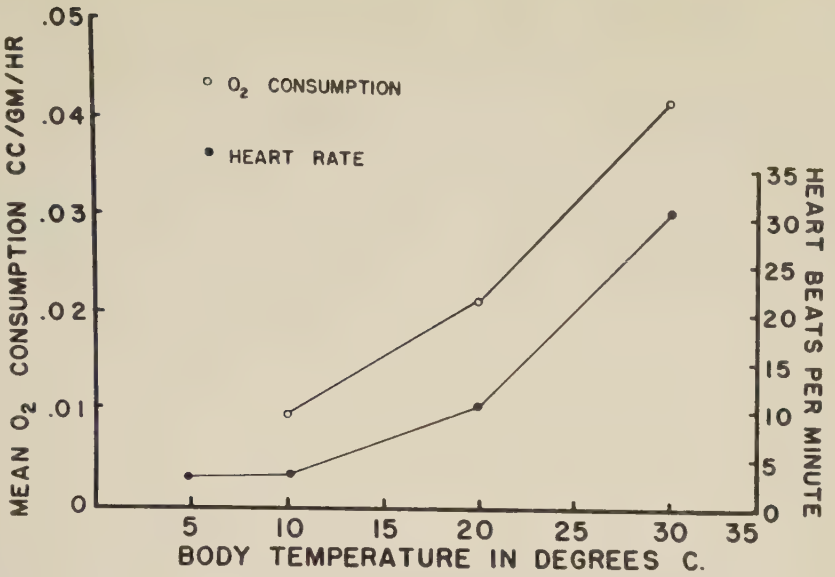

Fig. 4 Mean oxygen consumption and mean minimum heart rate for the group of 11 *Pseudemys scripta elegans* at 10°, 20°, and 30°C. Heart rates were also detremined at 5°C.

other times of the year in this and other studies. Work now in progress may indicate that this is a cyclic variation correlated with the mating season. This increased excitability plus a high temperature may account for the erratic results—although a negative correlation between heart rate and size still is indicated.

In an attempt to determine to what extent excitement affected the results, heart rates in this series of 11 animals were studied at 25°C before and after injection of tubocurarine chloride. Before injection heart rates ranged from 90 to 5 beats per minute with a correlation coefficient with weight of −0.299. After injection, the rates ranged from 40 to 5 beats per minute with a correlation coefficient of −0.553. The effect of tubocurarine chloride was not as successful or as consistent as had been hoped for, and neither coefficient may be considered statistically significant. However, perhaps some support is given to the concept that excitement is an important factor in this group of animals at a high temperature.

In summary, it may be said that there is a consistent negative correlation between body size and heart rate. This is most noticeable in the medium range of temperature. At lower temperatures this is less pronounced as all heart rates become slower; at higher temperatures it may be partially obscured by other factors. To our knowledge this relationship of heart rate to body size in reptiles has not been reported upon previously. It is not known if these differences in heart rate with size are compensated for by variation in cardiac output, arterial pressures, or other internal adjustments.

Effect of body size upon metabolic rate. In the oxygen consumption experiments done upon the red-eared turtles at 10°, 20°, and 30°C (fig. 3) there were no consistent or significant variations of oxygen consumption with size. Correlation coefficients were, respectively, −0.221, 0.347, and −0.052. Size appears to have no effect upon metabolic rate in these animals.

This agrees with the work of Baldwin, who, in his work with turtles ('26) and snakes ('30), could find no causal relationship between size or surface area and oxygen consumption. Benedict ('32), in his extensive studies on reptiles, found that, if anything, larger turtles had a higher metabolic rate per unit of body weight than did the smaller ones if entire body weight was considered. If body weight minus shell weight was considered, metabolism

per unit body weight was consistent in tortoises of all sizes. Shell weight does not appear to be a factor in the present investigation. In a previous study one of the authors (Hutton, manuscript in preparation) found that shell weight of the red-eared turtle did not vary significantly in percentage of body weight but varied between 24% and 33%, with a mean of 29% (although blood volume proportionately decreased with increasing size!). We are forced to the same conclusion as Benedict, namely, that comparison of the metabolism of tortoises and turtles with reference to surface area and body weight is of no significance whatsoever.

No attempt will be made to fit this lack of correlation between body size and/or surface area with metabolic rate in turtles into any broad picture concerning effects of these upon the animal kingdom in general. However, this lack of correlation appears strange, particularly when it has been reported in other reptiles—notably lizards (see Cook, '49; Dawson and Bartholomew, '56).

Effect of temperature upon metabolic rate. It is not surprising to find that metabolic rate is positively correlated with temperature in these poikilotherms. Figure 4 summarizes the finding concerning effects of temperature upon oxygen consumption in the red-eared turtle. The increases in oxygen consumption between 10°–20°C and 20°–30°C are statistically significant at the 1% level; the Q_{10}'s are, respectively, 2.22 and 1.93.

Hall ('24) has reported increasing rates of O_2 consumption in the midland painted turtle, *Chrysemys picta.* He also noted a lower respiratory quotient at lower temperatures. Rapatz and Musacchia ('57) noted comparable results in their work with the same species.

Relationship between heart rate and oxygen consumption. Figure 3 does not indicate any correlation between heart rate and oxygen consumption in individual turtles. Where oxygen consumption may be above the mean, heart rate may be low, or vice versa. And, of course, heart rate is generally lower in larger animals even though their metabolic rate may not differ from smaller ones. In figure 4, however, when the mean rates of oxygen consumption are compared to the mean minimum heart rates (size differences being ignored), both appear to follow a similar positive relationship to temperature and, therefore, possibly to each other.

Adolph ('51) has noted a proportionality between heart rate, oxygen consumption, and breathing rate in cold-blooded vertebrates. In the human, limited data has shown a correlation between heart rate and oxygen consumption in sleeping subjects (Hoffman, '56) and in exercising individuals (Le Blanc, '57). Considering the present turtles as a group, as in figure 4, this proportionality also appears to hold true. It is unfortunate that oxygen consumption and heart rate could not be measured simultaneously in this study. Until this can be done, a more precise statement regarding the relationship between heart rate and metabolic rate can not be made.

LITERATURE CITED

Adolph, E. F. 1951 Some differences in response to low temperatures between warm and cold-blooded vertebrates. Am. J. Physiol., *166:* 92–103.

Baldwin, F. M. 1926 Notes on oxygen consumption in turtles, *Chrysemys marginata* and *Chelydra serpentina* Linne. Proc. Iowa Acad. Sci., *33:* 315–323.

——— 1930 Oxygen consumption at 20° in certain snakes (*Pituophis sayi* and *Lampropeltis getulus holbrooki*), with some notes on size and seasonal differences. Ibid., *35:* 313–318.

Benedict, F. G. 1932 The Physiology of Large Reptiles. Carnegie Inst. of Washington, Publication No. 425, 539 pp.

Cook, S. F. 1949 Respiratory metabolism of certain reptiles and amphibians. Univ. Calif. Publ. Zool., *53:* 367–376.

Dawson, W. R., and G. A. Bartholomew 1956 Relation of oxygen consumption to body weight, temperature, and temperature acclimation in lizards *Uta stansburiana* and *Sceloporus occidentalis.* Physiol. Zool., *29:* 40–51.

Hall, F. G. 1924 The respiratory exchange in turtles. J. Metabolic Res., *6:* 393–401.

Hoffman, B. F., E. E. Suckling, C. McC. Brooks, E. H. Koening, K. S. Coleman and H. J. Treumann 1956 Quantitative evaluation of sleep. J. Appl. Physiol., *8:* 361–368.

Hutton, K. E. Effect of body size upon shell weight, blood volume, and corpuscular constants in the red-eared turtle. (Manuscript in preparation.)

Kaplan, H. M., and R. Taylor 1957 Anesthesia in turtles. Herpetologica, *13:* 43–45.

LeBlanc, J. A. 1957 Use of heart rate as an index of work output. J. Appl. Physiol., *10:* 275–280.

Loomis, A. L., E. N. Harvey and C. Mac Rae 1930 The intrinsic rhythm of the turtle's heart studied with a new type of chronograph together with the effect of some drugs and hormones. J. Gen. Physiol., *14:* 105–115.

Mode, E. B. 1951 Elements of Statistics, 2nd ed. Prentice-Hall, New York, 377 pp.

Rapatz, G. L., and X. J. Musacchia 1957 Metabolism of *Chrysemys picta* during fasting and during cold torpor. Am. J. Physiol., *188:* 456–460.

Rodbard, S., and D. Feldman 1946 Relationship between body temperature and arterial pressure. Proc. Soc. Exp. Biol. Med., *63:* 43–44.

Rodbard, S., F. Samson and D. Ferguson 1950 Thermosensitivity of the turtle brain as manifested by blood pressure changes. Am. J. Physiol., *160:* 402–408.

Wilber, C. G., and J. Lieb 1950 The effects of increased environmental temperatures on the lipids in the blood of the turtle, *Chrysemys picta.* Saint Louis Univ. Studies, Series C, *1:* 1–20.

Woodbury, R. A. 1941 Studies on turtle hearts —the end of systole, the duration of the refactory period, the latent period of extrasystoles and the influence of heart rate on aortic blood pressure. Am. J. Physiol., *132:* 725–736.

On the Excitability Change During the Rhythmic Excitatory State of the Single Optic Nerve-ending of Horseshoe Crab

ICHIRO TANAKA[1]
Department of Physiology, Tokyo Women's Medical College, Tokyo, Japan

As the rhythmic response is a prominent characteristic of nerve-cell activity, its physiological origins have been studied extensively in isolated single axons (Fessard, '36; Arvanitaki, '39; Katz, '36; Erlanger and Blair, '36; Hodgkin, '48).

On the other hand, studies of electrical activity recorded intracellularly within ommatidia of the lateral eye of the horeshoe crab have recently been reported (Hartline et al., '52; MacNichol et al., '53; Tomita, '56; Tomita et al., '60). According to Tomita ('56; '57), the membrane of a certain cell generating a slow potential (ommatidial action potential) in response to illumination does not show any active response to electrical stimulus. When an ommatidium was illuminated, the nerve-ending connecting protoplasmically with the cell was fired repetitively by an outward current through the cell membrane, caused by the slow potential.

An attempt was made to study the rhythmic excitatory process of the nerve-ending with the aid of intracellular microelectrodes. This experiment was one of a series of investigations (Tomita et al., '60; Tanaka and Yamanaka, unpublished).

METHOD

Experimental animals used were horseshoe crabs from the Inland Sea of Japan (*Tachypleus tridentatus*). An excised lateral eye of the horseshoe crab was cut horizontally and immersed in physiological saline solution (Kikuchi and Tanaka, '57). The solution was composed of 400 mM of NaCl, 10 mM of KCl, 10 mM of $CaCl_2$ and 25 mM of $MgCl_2$. The experimental arrangement is shown schematically in figure 1. A glass microelectrode (Ling and Gerard, '49; Nastuk and Hodgkin, '50) containing 3 M KCl was inserted into the cell within an ommatidium. Repetitive stimulating current pulses lasting 5 msec. were sent into the cell through a 200 megohm resistor and the microelectrode.

The intracellular potential changes were recorded by a cathode-ray oscillograph via pre-amplifier and a D.C. amplifier (Tomita et al., '60).

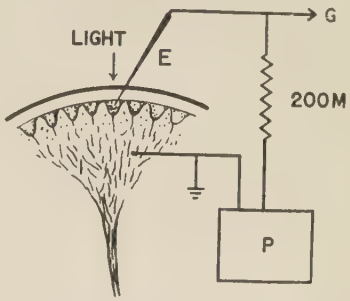

Fig. 1 Experimental arrangement for recording and stimulus. G, grid; E, microelectrode; P, square pulse generator.

Repetitive current pulses at various rates and intensities were sent into the cell for the determination of threshold at different stimulus rates. The minimum intensity at which the cell fired in response to each pulse defined the threshold for that stimulus rate.

The experiment was conducted at 23–24°C.

RESULTS

In many cases, a spontaneous discharge appeared after the resting potential has been observed. This may be due to an injury-depolarization caused by electrode insertion (Tomita, '56).

[1] Present address: Department of Physiology and Biophysics, School of Medicine, University of Washington, Seattle, Washington

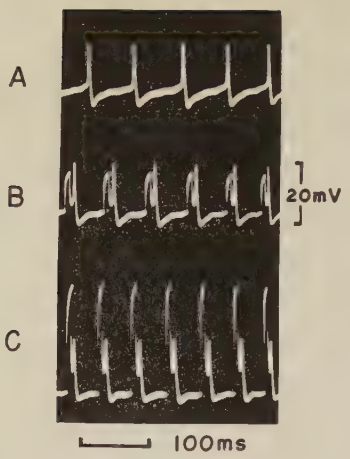

Fig. 2 Spontaneous discharge (A) and discharges evoked by repetitive current pulses of threshold intensity (B and C). First deflection of each pair is stimulus artifact; second is action potential.

The spontaneous discharge is shown in A of figure 2, and two examples of discharges evoked by repetitive current pulses of the same intensity but of different intervals in a series of experiments are shown in B and C. Intervals between the spontaneous discharges were approximately equal and about 67 msec.

Figure 3 illustrates the threshold at different stimulus intervals. As this figure shows, the threshold decreased exponentially as the stimulus interval was increased, reaching zero at the interval of the spontaneous discharge.

When the nerve-ending was depolarized by a background illumination, the same relation was found. The discharge interval caused by the illumination was 48 msec.

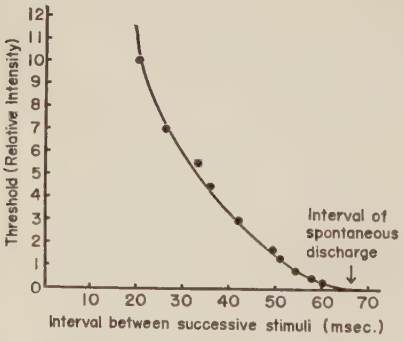

Fig. 3 Threshold intensity at different stimulus intervals.

The thresholds at each stimulus interval were less than those obtained without illumination, and became zero at the interval of 48 msec.

These results indicate that the threshold in the rhythmic excitatory state decreased exponentially as the stimulus interval decreased and fell to zero at the discharge interval of the initial rhythmic excitatory state.

DISCUSSION

From these results and previous experiments (Tomita et al., '60), it is concluded that the discharge interval at a repetitive excitatory state depends on both the time-course of excitability after each spike and the intensity of a steady depolarizing current on the nerve-ending. This phenomenon is similar to that explained by the "recovery cycle hypothesis" presented by Adrian ('28; '30).

The relationship between the discharge interval (i.e., the interval between impulses in a train of elicited discharges) and the intensity of a depolarizing direct current was plotted from the data of the experiment by Tomita et al. ('60) and is shown in figure 4. Using the data of figures 3 and 4 and taking into consideration the temperature differences of the experiments, the intensity of the repetitive current pulse which elicits a given discharge interval (fig. 3) can be related to the intensity of the depolarizing direct current eliciting a train of impulses having the same discharge interval (fig. 4).

The curve in figure 3 differs a little from the recovery curve of excitability after a spike, and it is more convenient than the recovery curve to compare with the relation shown in figure 4. The relation in figure 4 can thus apparently be explained by the excitability properties of the nerve-ending as demonstrated with repeated pulses in the experiment.

On the other hand, there were slowly depolarizing local potentials between each spike when the ending was in the repetitive excitatory state (see A of fig. 2). As the discharge interval was decreased by stronger depolarizing currents, the rate of rise of this local potential increased. The discharge interval appeared to be determined by how soon the local potential reached the critical firing level of the nerve-ending

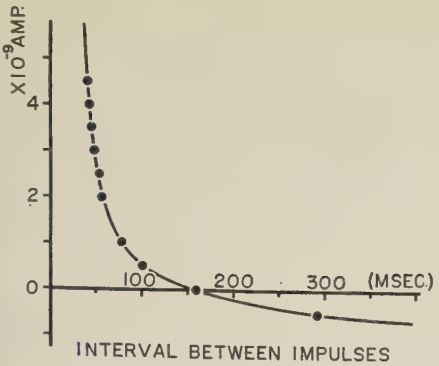

Fig. 4 Relation between continuous polarizing current and the interval between impulses in a train of elicited discharges, 15°C (Tomita et al.).

(Tomita et al., '60). This relation is similar to the phenomenon reported by Hodgkin ('48) in the crab giant axon. It seems that the relation between excitability and the local potential is important, but cannot be discussed fully from the data of this experiment.

SUMMARY

Thresholds during the rhythmic excitatory state of the optic nerve-ending of lateral eye of the horseshoe crab were investigated at various repetitive stimulus current rates by means of intracellular microelectrodes.

As the stimulus interval increased, the threshold decreased. This relation was exponential, and the threshold fell to zero when the stimulus interval had just become equal to the discharge interval with no applied current pulse.

From the results of this and previous experiments, it seems that the threshold-interval relation of the optic nerve-ending during its rhythmic excitatory state can be explained by the recovery cycle hypothesis.

ACKNOWLEDGMENTS

I wish to express my thanks to Dr. Tsuneo Tomita at Keio University, Tokyo, for his criticism, and to Mr. Robert E. Smith at the University of Washington, Seattle, for his help in preparing this paper.

LITERATURE CITED

Adrian, E. D. 1928 A Basis of Sensation. London.

——— 1930 The effects of injury on mammalian nerve fibers. Proc. Roy. Soc., B., 596.

Arvanitaki, A. 1939 Recherches sur la reponse oscillatoire locale de l'axone geant isolé de Sepia. Arch. Int. Physiol., *49:* 209.

Erlanger, J., and E. A. Blair 1936 Observations on repetitive responses in axon. Am. J. Physiol., *114:* 328.

Fessard, A. 1936 L'active rhythmique des nerfs isolés. Paris.

Hartline, H. K., H. G. Wagner and E. F. MacNichol 1952 The peripheral origin of nervous activity in the visual system. Cold Spr. Harb. Symp. Quant. Biol., *17:* 125.

Hodgkin, A. L. 1948 The local electric changes associated with repetitive action in non-medullated axon. J. Physiol., *107:* 165.

Katz, B. 1936 Multiple response to constant current in frog's medullated nerve. Ibid., *88:* 239.

Kikuchi, R., and I. Tanaka 1957 Physiological saline solution for Japanese horseshoe crab, *Tachypleus tridentatus.* Annot. Zool. Jap., *30:* 177.

Ling, G., and R. W. Gerard 1949 The normal membrane potential of frog sartorius fibers. J. Cell. and Comp. Physiol., *34:* 383.

MacNichol, E. F., H. G. Wagner and H. K. Hartline 1953 Electrical activity recorded within single ommatidia of eye of Limulus, Proc. XIX Int. Physiol. Conger., Montreal, p. 582.

Nastuk, W. L., and A. L. Hodgkin 1950 The electrical activity of single muscle fibers. J. Cell. and Comp. Physiol., *35:* 39.

Tanaka, I., and T. Yamanaka Effects of linearly increasing and decreasing current on the optic nerve discharge in the lateral eye of horseshoe crab. (In preparation).

Tomita, T. 1956 The nature of action potentials in the lateral eye of horseshoe crab as revealed by simultaneous intra- and extracellular recording. Jap. J. Physiol., *6:* 327.

——— 1957 Peripheral mechanism of nervous activity in lateral eye of horseshoe crab. J. Neurophysiol., *20:* 245.

Tomita, T., R. Kikuchi and I. Tanaka 1960 Excitation and inhibition in lateral eye of horseshoe crab. In: Electrical Activity of Single Cells. Tokyo.

Circadian[1] Activity Rhythms in Cockroaches

I. THE FREE-RUNNING RHYTHM IN STEADY-STATE[2]

SHEPHERD K. DE F. ROBERTS
Biology Department, Princeton University, Princeton, N. J.

The universality of daily rhythms in organisms has been adequately documented in several recent reviews (Pittendrigh and Bruce, '57; Aschoff, '58; Bünning, '58; and Harker, '58). In the majority of cases studied these rhythms, which include locomotion, insect eclosion, pigment-cell migration, phototaxis and many other activities, have been found to persist under conditions of constant darkness (or light) and constant temperature.

The majority of investigators agree that the persistence of rhythms under constant laboratory conditions reflects their endogenous nature, although this persistence does not, in itself, provide a rigorous proof for their endogenous origin. However, Aschoff ('58) and Pittendrigh ('58) have noted what is surely the crucial observation that provides the needed proof in this matter. They point out that the period of most rhythms is rarely, if ever, precisely that of a solar day. This observation rules out the hypothesis (Brown, '57) that persistent rhythms are being exogenously driven by any known or unknown environmental variables whose periodicity depends upon the earth's rotation. The fact that the period of persistent rhythms is generally only an approximation to a day has led to the adoption of the term *Circadian* (*circa*, about; *diem*, day) rhythm as more appropriate than the usual "24-hour," "Daily," or "Diurnal" designations.

Interest in this field currently focusses on the problem of what physiological systems are responsible for the endogenous, circadian rhythms of living organisms. As pointed out in several earlier papers from this laboratory (Bruce and Pittendrigh, '57; Pittendrigh and Bruce, '57; and Pittendrigh, '58) the search for a causal explanation will probably be facilitated by a preliminary comparative study of the formal properties of circadian rhythms in a diversity of organisms. The work summarized in the present series of papers on circadian activity rhythms in cockroaches is part of the comparative study this laboratory has undertaken in organisms ranging from protists to mammals.

The present paper deals specifically with the steady-state properties of the *free-running* (i.e., not entrained by external signals) rhythms of locomotion in cockroaches. These studies include estimates of the free-running periods of individual cockroaches under conditions of constant dark; constant light (several intensities); and constant temperature (several levels). Later papers will be devoted to the transient (as opposed to steady-state) behavior of cockroach rhythms (e.g., phase-shifting) in response to changes in the experimentally controlled light or temperature regime; and to the nature and action of *Zeitgebers* or entraining agents.

Throughout the paper the following commonly accepted abbreviations are used: LD signifies conditions of alternating light and dark; LD (23:1) more specifically denotes a regime in which 23 hours of light alternate with one hour of darkness; DD means constant dark, and LL constant light. As indicated above, the term free-running rhythm is used to signify one in which there is no control of period by an external periodic signal such as, for example, LD.

MATERIALS AND METHODS

Three different species of cockroaches have been used in the experiments: *Leu-*

[1] The term *circadian* was suggested (unpublished) by Dr. Franz Halberg (Minnesota). It derives from the Latin "circa-diem"—about a day.

[2] This first paper of a series is part of a thesis presented to the Department of Biology of Princeton University (unpublished) in partial fulfillment of the requirements for the degree of Doctor of Philosophy.

cophaea maderae (Fabricus); *Byrsotria fumigata* (Guèrin); and *Periplaneta americana* (Linnaeus). They have all been successfully cultured in 5 gallon tanks with a bedding of wood-chips and numerous cardboard tubes for shelter. Their nutritional requirements are simple; they grow satisfactorily on a diet of Purina Laboratory Chow, water, and apples. The cultures have been kept in a room maintained at 25°C on a clock-controlled light cycle—on at 0900 and off at 2100 hours E.S.T. Initial experiments (not included here) indicated that the activity patterns in female cockroaches were generally more erratic than those in males and consequently males were studied exclusively.

Various kinds of actographs were designed in order to record the locomotor activity of the roaches. The most suitable design proved to be the light-weight running-wheel cage illustrated in figure 1. The framework of the wheel is constructed of balsa wood and is covered with nylon netting. The wheel, mounted on a delicate bearing, is sufficiently well balanced so that the weight of the roach rotates the whole assembly with ease. An hexagonal nut on the rotating axle activates a microswitch which is connected to one of 20 channels on an Esterline-Angus operations recorder. Each switching operation produces a short lateral deflection of a pen writing on a moving strip of paper.

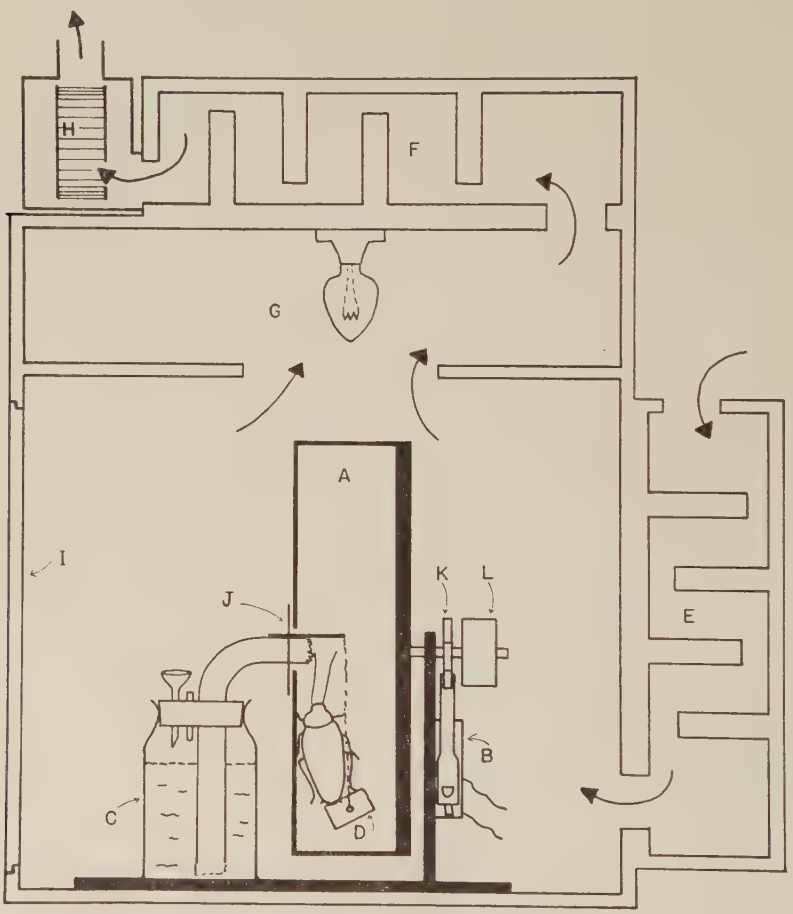

Fig. 1 Actograph assembly and light-tight housing described in text: A, Running-wheel cage; B, microswitch; C, water reservoir; D, food; E, intake light baffle; F, exhaust light baffle; G, "attic" space and lamp; H, location of exhaust fan (arrows indicate direction of air-flow); I, light-tight access door; J, roach baffle; K, hex-nut to activate micro-switch; L, counterweight.

A refinement of the switching device in some actographs has permitted the study of extremely small roaches including very young nymphs. The limiting factor in the use of the standard actograph is the friction inherent in its mechanical switch. This problem has been resolved by a frictionless electronic switch circuit that capitalizes on the peculiar property of ferrite materials to change the inductance of a coil. A compact electronic oscillator was designed so that the coil of the circuit could be placed near the wheel-cage. Ferrite rods were arranged in a radial fashion on the axle of the wheel so that its rotation would periodically bring the ferrites into proximity with the coil of the oscillator. The circuit was adjusted in such a way that oscillation ceased when a ferrite rod passed through the flux of the coil. The difference between the plate currents in the oscillating and non-oscillating conditions is sufficient to operate a sensitive relay which in turn is connected to the operations recorder.

The cockroach lives permanently in the running-wheel cage. Watering and feeding is accomplished as follows. A ½-pint water reservoir stands outside the cage. A plastic tube, containing a cotton wick, is led from the reservoir to the wheel cage which it enters, without contact, through a 3/4-inch hole in the side opposite the bearing and axle. A baffle mounted on the plastic tube prevents the roach from escaping through the gap between the wick-tube and the hole in the side of the wheel. The lip of the wick-tube inside the cage also serves to suspend a piece of Purina Chow on a thread. The roaches quickly learn to climb straight up the side of the wheel to drink from the cotton wick. The entire assembly can be left undisturbed for about a month after which time the water bottle usually requires refilling.

During the course of the experiments a total of 20 actographs were placed into individual boxes. These were individually ventilated with small fans, and carefully insulated from light leaks. Each box was fitted with an incandescent lamp which was located in an "attic" space above the actograph. The flow of fresh air through the box and out of the attic space kept the lower section (with actograph) at a constant temperature regardless of whether the lamp was on or not. These boxes were kept in a constant temperature room maintained at 25°C ± ½°.

The technique of handling the activity records was as follows. Twenty different roaches were simultaneously recorded on the 20-channel operations recorder. Each day's record for the animals was removed and the chart cut so as to separate the individual record of each animal. Each one of these record strips was then transferred to large poster-boards where one day's record was pasted down in chronological order directly below that of the preceding day. In this form the record of an individual's activity for many weeks can be expressed as a whole.

Interpretation of the data requires the adoption of some characteristic statistic of the locomotor pattern. The most regular feature of the activity rhythm is the time of the onset of running, and this has accordingly been chosen. The onsets of running activity over a period of several weeks are connected by solid black lines, which represent the best "eye-fit" to the data. The slopes of the lines are graphic representations of the periods of the rhythms. Due to the fact that the roach has no unequivocal onset of running, there is some subjective error involved in such a procedure. To obtain an estimate of this error, the "best eye-fit" procedure was repeated on a typical roach record by 12 different people. For 30 days of data, 12 individual estimates of period were remarkably similar, differing from the mean by less than ±½ minute per day. The accuracy of period estimates derived in this way will vary depending on the number of days analyzed, the discreteness of the onsets of activity, and perhaps some variable subjective factors. Recognizing these shortcomings, we can nevertheless be confident that for the majority of cases the estimate of period is reliable within ±2 minutes.

RESULTS

A. Rhythm in constant darkness

As an introduction to the results presented here it should be noted that under conditions of constant temperature the *phase* (time of onset of running) and *period* (interval between successive on-

sets) of the cockroach activity rhythm can be controlled by a periodic light regime (Roberts, '59). In an artificial regime where 12 hours of light alternate with 12 hours of dark (*LD 12*:12) the roach attains a steady-state rhythm whose period is 24 hours and whose phase is always such that activity begins at, or shortly after the light to dark transition. Similar entrainment of the phase and period of the

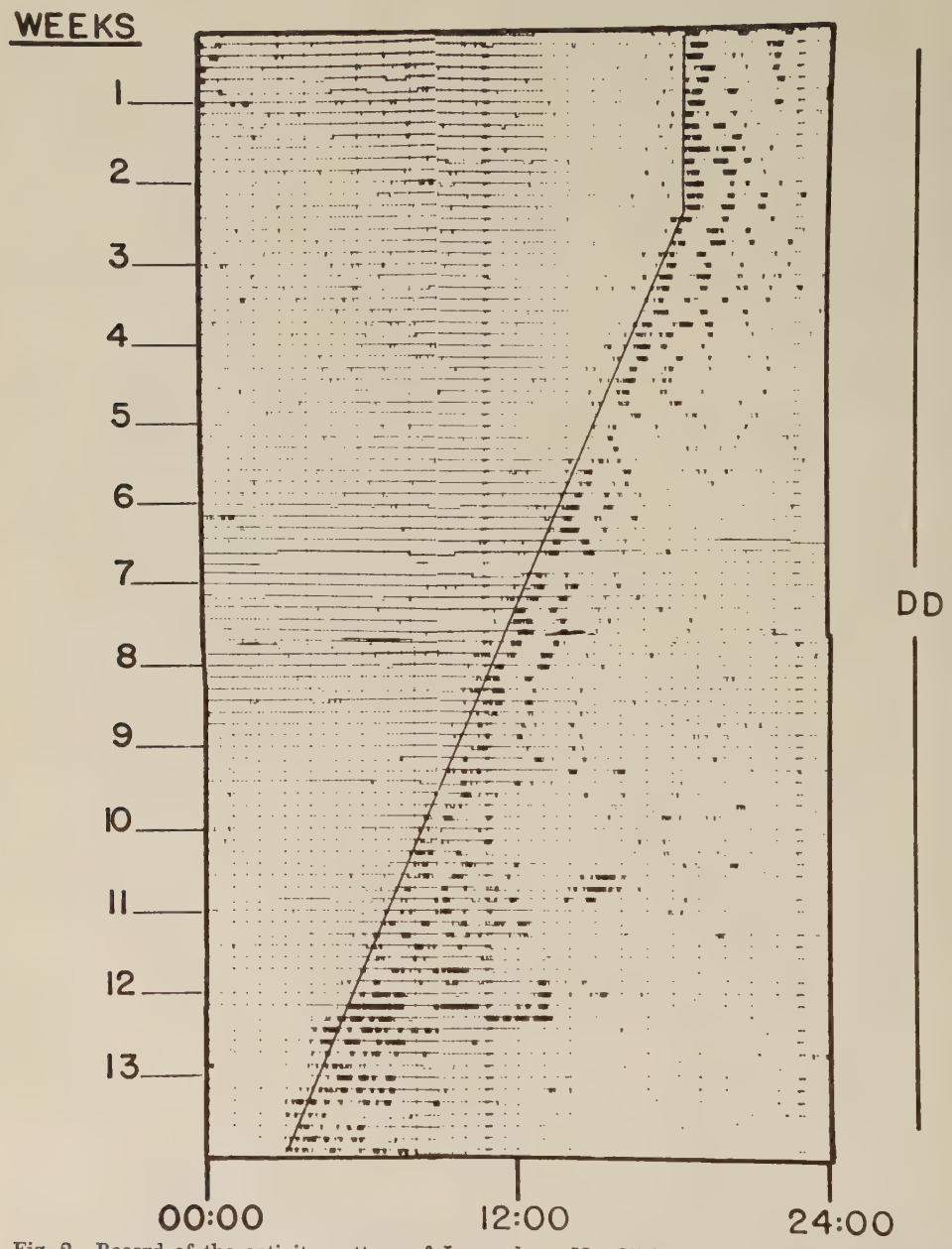

Fig. 2 Record of the activity pattern of *Leucophaea* No. 25 in constant darkness for 13 consecutive weeks (horizontal scale represents 24 hours). The period of the rhythm (derived from the slope of the eye-fitted line) is initially 24 hours, but changes spontaneously in an abrupt way during the third week to 23 hours, 48 minutes.

roach rhythm can be effected in constant darkness by a 24-hour periodic temperature fluctuation (Roberts, '59). Under these conditions (when the temperature is artificially fluctuated between 20°C and 30°C) activity begins about one hour before the time of maximum temperature.

1. Persistence of rhythm in DD. In the absence of such periodic light or temperature regimes the cockroach rhythm persists for at least three months in DD (see figs. 2 and 3). There is no indication of a gradual loss of the rhythm in the two illustrated cases, nor for that matter in any of the 20 tested roaches, and it is presumed, therefore, that these rhythms would continue until the death of the animals. The indefinite persistence of the rhythm in DD is a striking empirical result that merits emphasis.

2. The circadian period. The results of this study clearly demonstrate that the activity rhythm of the roach is typically circadian; that is, the rhythmic nature of the activity persists indefinitely in constant conditions of light and temperature with a period that is only a close *approximation* to 24 hours. For example, note in figures 2 and 3 that the periods of the rhythms are significantly different from 24 hours;

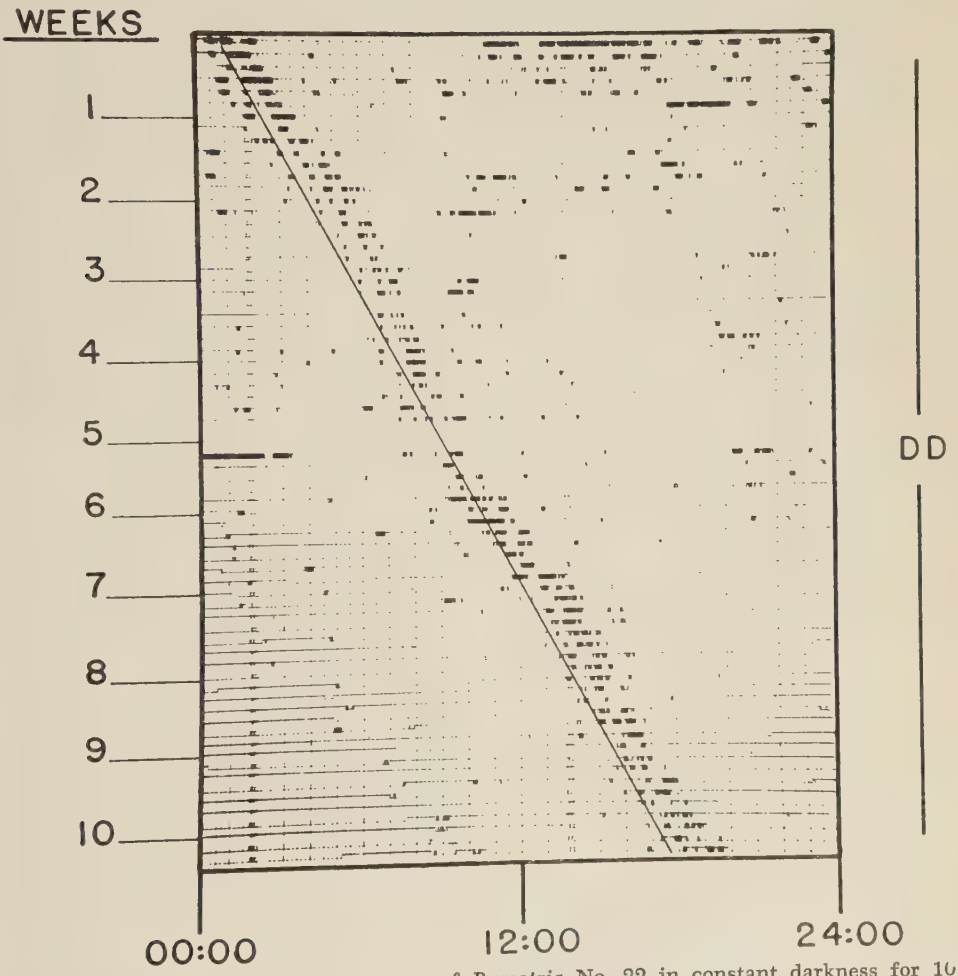

Fig. 3 Record of the activity pattern of *Byrsotria* No. 22 in constant darkness for 10 consecutive weeks (horizontal scale represents 24 hours). Note that in contrast to figure 2, the period of the rhythm illustrated here is significantly longer than 24 hours (estimated to be 24 hours, 14 minutes).

the former being approximately 23 hours, 48 minutes, and the latter 24 hours, 14 minutes.

3. *Lability of the period.* In general the cockroaches studied exhibited periods in DD within the range between 23½ to 24½ hours. It has also become apparent that a given roach has no single DD period that uniquely characterizes its rhythm. In practice, the recording of the activity rhythm of individual roaches continued for many months under various environmental conditions. The continuity of DD conditions was often experimentally interrupted every two or three weeks by environmental perturbations such as changes in the light or temperature regime. Measurements of an individual's DD period before and after these perturbations indicated a lability of the period. The magnitude of this lability for a given animal is expressed by the range of its observed DD periods (summarized in fig. 4).

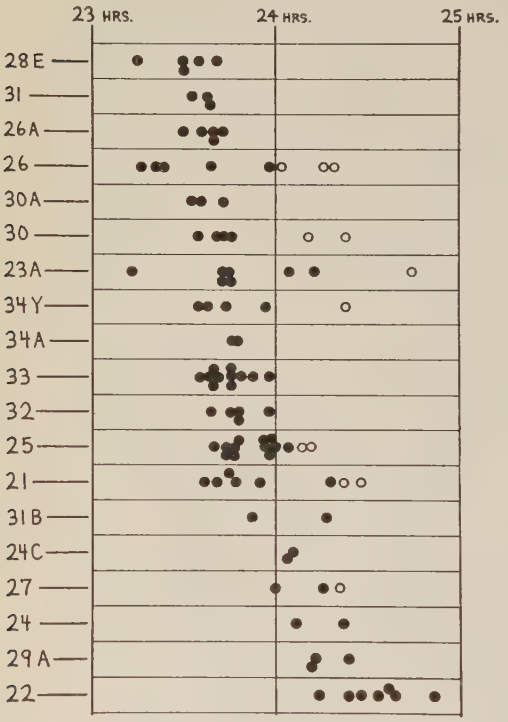

Fig. 4 Range of observed periods in 19 individual cockroaches at a constant 25°C. Solid circles are individual estimates of period in constant dark; open circles are periods in constant light. On the average the period estimates are based on runs of 25 days duration. Roaches Nos. 21, 22, 24C are *Byrsotria;* 34A is *Periplaneta;* and all the rest are *Leucophaea.*

Although the period of an individual's activity rhythm usually remains fixed under constant conditions of light and temperature, it may change abruptly in an apparently spontaneous fashion as illustrated in figure 2, or it can be *induced* to change in a predictable way in response to a perturbation of the environmental regime (or in LL as discussed below). A more complete presentation of induced period changes is deferred to a later publication. The significance of *differences* between the *ranges* of DD periods realized by individual animals in figure 4 is considered in the concluding discussion.

B. Rhythm in constant light

Previous investigations on the activity rhythms of cockroaches, for example *Blatta* (Gunn, '40) and *Periplaneta* (Harker, '56), have indicated a loss of the rhythm after a few days in continuous light. However, in three species of roaches used in these experiments the rhythm was *not* lost under such conditions. Figure 5 illustrates the persistence of the rhythm of *Leucophaea* in LL for up to 20 days with no indication of a loss of that rhythm. The LL rhythm of *Byrsotria* No. 21 (indicated in fig. 4) persisted for 7 weeks at 20 F.C., and more recently individual *Periplaneta* were maintained in LL with no apparent loss of a rhythm (see fig. 6).

1. *Change of period in LL.* The period of the rhythm is, however, markedly changed in LL. As first shown by Johnson ('39) for the deer-mouse and subsequently documented in many other nocturnal animals (Aschoff, '58), the period of the rhythm lengthens in continuous light. All of the observed period lengthenings in the roach rhythm were of an order of magnitude of about 20 minutes to one hour at intensities up to 25 F.C. (see table 1 and fig. 5). The data do not permit a critical analysis of intensity effects, although there is an indication that, within the experimental range of intensities used here, there is no obvious correlation between the LL intensity and the degree of period lengthening. For example, immeasurably low intensity LL will evoke a lengthening of period commensurate with those at much

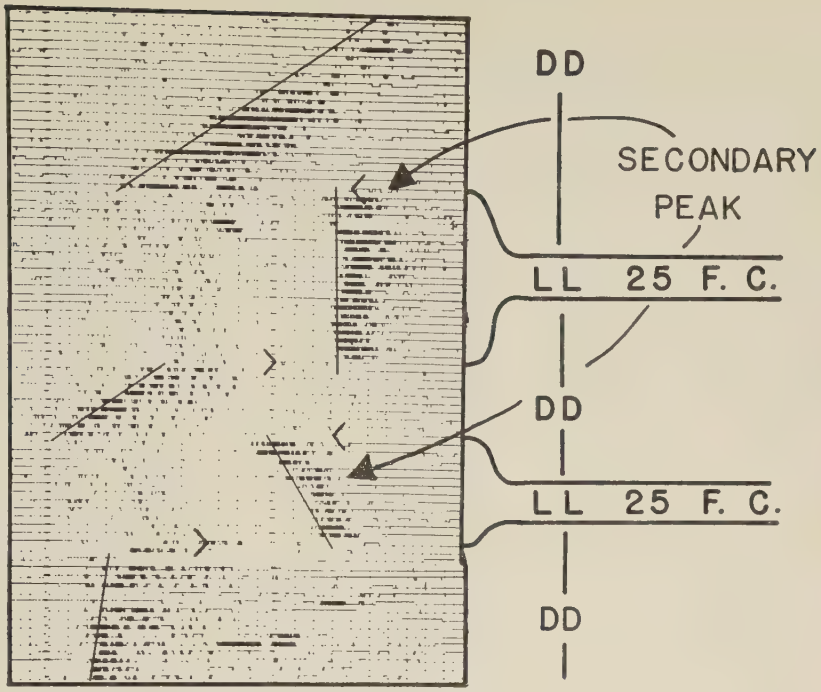

Fig. 5 Activity record of the roach *Leucophaea* No. 26 in constant dark (DD) and constant light (LL, 25 F.C.) demonstrating the following: (1) the lengthening of the period in LL; (2) the appearance of a secondary activity peak in LL; and (3) the lability of the free-running period—the period differs in two successive 25 F.C. runs. Horizontal scale is 24 hours as in figures 2 and 3.

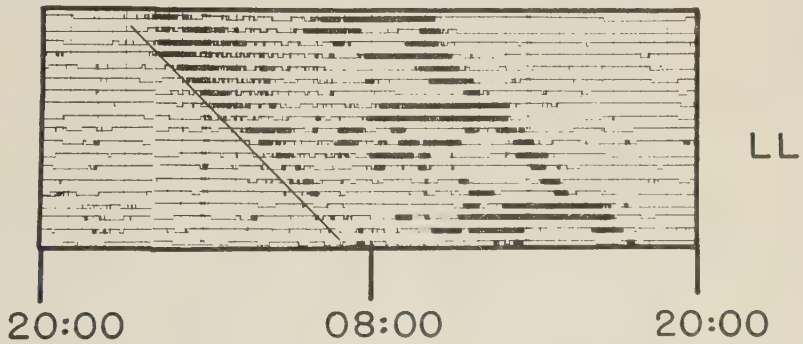

Fig. 6 Persistent rhythm of activity of *Periplaneta* in constant light (LL) at 1 F.C. for 19 days. Two other *Periplaneta* tested in LL (not shown) had similarly persistent rhythms under identical conditions. Note the secondary peak of activity—its onset is not as clear here as in figure 5.

greater illuminations. This remarkable fact was discovered quite by accident when it was noticed that the period of *Byrsotria* 22, running in DD, abruptly lengthened for about a week and subsequently reverted to its previous value. An investigation revealed that the roach in the adjacent "light-tight" box had been subjected to constant light for the corresponding interval of time. The circumstances were experimentally repeated, exposing the roach in the adjacent cabinet to LL for one week, and once again the period of *Byrsotria* 22 lengthened for 7 days. Subsequently these

TABLE 1

Lengthening of period in constant light

Periods in constant light (LL) are estimated for individual cockroaches following a prior run in constant dark (DD). The bracketed numbers indicate the duration of the runs in DD and LL by which the periods were estimated.

Animal number	DD period	No. of days	LL period	No. of days	Period change	LL intensity
					min.	
Leucophaea no. 23A	23h, 45m	(38)	24h, 45m	(26)	+60	0.7 F.C.
Leucophaea no. 25	23h, 42m	(8)	24h, 10m	(13)	+28	25 F.C.
Leucophaea no. 25	23h, 47m	(7)	24h, 11m	(13)	+24	0.1 F.C.
Leucophaea[1] no. 26	23h, 16m	(21)	24h, 02m	(20)	+46	25 F.C.
Leucophaea[1] no. 26	23h, 20m	(10)	24h, 16m	(12)	+56	25 F.C.
Leucophaea no. 26	23h, 56m	(18)	24h, 19m	(10)	+23	25 F.C.
Leucophaea no. 27	24h, 00m	(28)	24h, 21m	(17)	+21	25 F.C.
Leucophaea no. 30	23h, 41m	(22)	24h, 10m	(16)	+29	25 F.C.
Leucophaea no. 30	23h, 45m	(14)	24h, 25m	(20)	+40	25 W Red Safelight
Leucophaea no. 34Y	23h, 44m	(11)	24h, 23m	(18)	+39	25 F.C.
Byrsotria no. 21	23h, 56m	(34)	24h, 28m	(50)	+32	25 F.C.
Byrsotria no. 22	24h, 14m	(74)	25h, 30m	(7)	+76	Immeasurably low intensity[2]
Byrsotria no. 22	24h, 24m	(16)	25h, 24m	(7)	+60	Immeasurably low intensity[2]

[1] Illustrated in figure 5.
[2] See text for explanation.

adjacent cabinets were found to have a light leak between them, but in order to see this light the observer's eye had to be dark-adapted for 10 minutes! It was therefore evident that *Byrsotria* 22 had lengthened its period in response to "immeasurably" low intensity LL (see table 1).

These facts indicate that the period lengthening in LL either saturates at a very low level, or is an "all-or-none" phenomenon in the cockroach.

2. Secondary activity peak in LL. Besides the modification of the period of the rhythm in LL, we have found a previously unreported change in the pattern of activity. This change involves the appearance of a second peak of intense activity, the phase of which, like the primary onset of activity, can be reliably determined. The onset of this secondary activity occurs on the average about 10 hours after the onset of the primary peak. Figure 5 demonstrates the generation of the secondary activity peak when the roach is exposed to LL following a DD regime. After the DD to LL transition the secondary activity in this individual begins about 11 hours after the last primary onset in DD, and persists rhythmically for about three weeks until the resumption of DD conditions. At this time the primary onset of activity, which was markedly suppressed in LL, again becomes the dominant feature of the activity pattern, while the secondary peak abruptly disappears.

It should be emphasized that there is a relatively fixed phase relationship between the primary and secondary activity peaks; the latter usually occurring between 8 and 12 hours after the primary peak in 10 individuals tested. The further observation that the secondary peak often occurs with this same phase relationship in LD regimes (see fig. 7) indicates that this peak is not exclusively the result of LL conditions per se, but rather appears when the animal is subjected to light during a particular phase of its activity cycle. In one sense, therefore, the animal is more sensitive to light during that fraction of its rhythm.

C. Temperature compensation of the free-running period

The virtual insensitivity to temperature change of the period of circadian rhythms was first noted by Wahl ('32) in the honeybee; Welsh ('38) and Brown and Webb ('48) subsequently reported similar temperature independence of period in *Crustacea*. The *Drosophila* eclosion rhythm

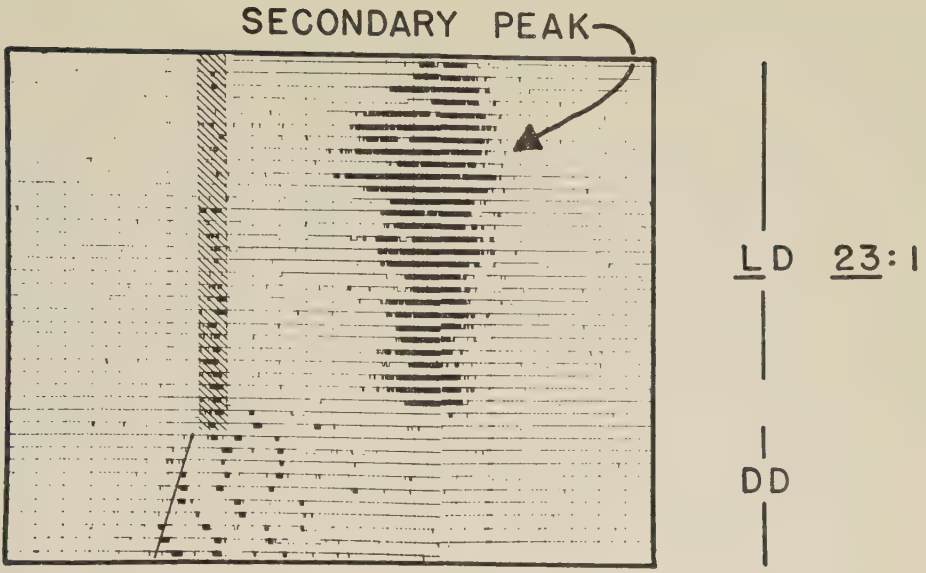

Fig. 7 Activity record of an individual *Leucophaea* showing the characteristic secondary peak in LD 23:1 regime. Shading indicates darkness, and the horizontal scale is 24 hours as in figures 2 and 3.

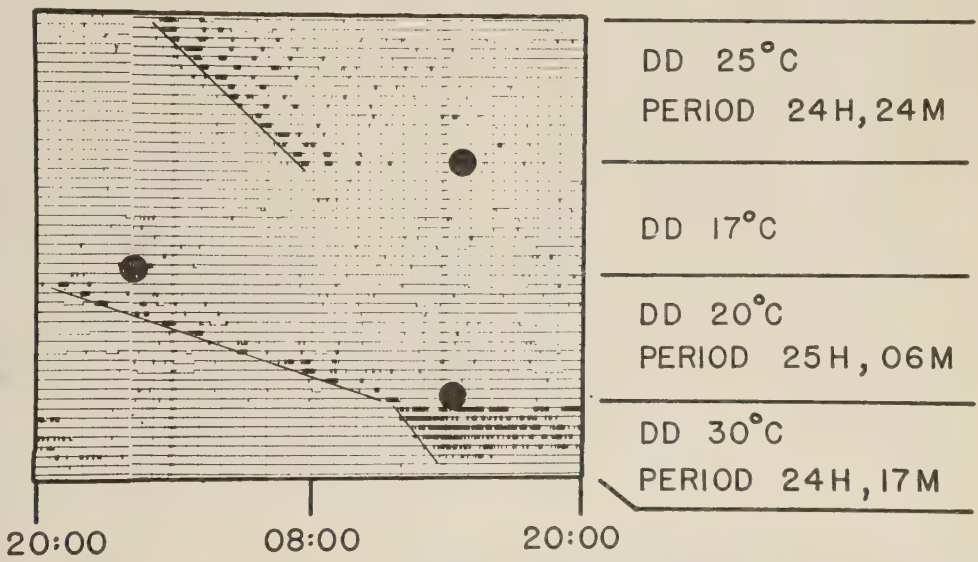

Fig. 8 Temperature compensation of the free-running period in an individual *Leucophaea*, No. 29A. The significance of the estimated periods at three different temperatures is discussed in the text. The activity of this roach was assayed in a precision cabinet which maintained the temperature to ±½°C. The time of a temperature change is indicated by solid black dots and the rate of change was uniformly 10°C per hour.

No estimate of period was made at 17°C because there is no well-defined rhythm at that temperature. According to Bünning ('58a) clear activity rhythms in *Periplaneta* are also lost below 18°C.

was also found to be temperature compensated (Pittendrigh, '54) and more recent work by other investigators documents the phenomenon in many other organisms (see Pittendrigh and Bruce, '57). The anticipation of temperature compensation in the roach rhythm led this writer to look for it early in this study. It was promptly found, as described below, and subsequently and independently discovered and reported by Bünning ('58a). As illustrated for *Leucophaea* 29A, figure 8, DD periods for 20, 25 and 30°C were determined. A Q_{10} calculated for periods at 20°C and 25°C was 1.06, and for the periods at 25°C and 30°C the Q_{10} was 1.03.

The previously demonstrated lability of the free-running period in the roach raises obvious obstacles to a simple computation of a temperature coefficient. Thus while the 20°C period of *Leucophaea* 29A was certainly 25 hours, 6 minutes prior to the temperature step-up to 30°C, the period is known to vary in this animal between 24 hours, 13 minutes, and 24 hours, 24 minutes at a constant 25°C. We would anticipate that sufficient study at 30°C would uncover a similar range of possible periods at that temperature. Taken at face value the shortening of the period caused by a 10°C temperature rise in this case indicated a Q_{10} of 1.03. Taking into consideration the range of observed periods for this animal, as indicated in figure 4, the Q_{10} could not be much greater than 1.04. The range of periods at 25°C in *Leucophaea* 29A was 24 hours, 13 minutes to 24 hours, 24 minutes or ± 5 minutes from the median of 24 hours, 18 minutes. On the basis of this observed lability we have estimated the greatest allowable error in the calculation of a Q_{10} by *adding* 5 minutes to the observed period at 20°C and *subtracting* 5 minutes from the observed period at 30°C. This gives us the maximum allowable difference between the measured periods at the two temperatures, or in other words, we have increased the difference by 10 minutes. Assuming this degree of error the calculated Q_{10} becomes 1.04 instead of 1.03. This extremely low estimated value of the Q_{10} reveals that virtual independence of temperature which gives the circadian rhythm its functional significance as a time measuring system.

DISCUSSION

The experimental results presented above justify the following conclusions about the free-running, steady-state locomotor rhythm in cockroaches: (1) it is persistent in both constant dark and constant light for months at least and probably indefinitely; (2) it is characterized by a circadian period which is stable for long intervals of time but (3) is subject to both induced and spontaneous change; (4) the range of periods realized by an animal differs from individual to individual; (5) the period—as well as the form of the rhythm—is altered by constant light; and (6) the rhythm is temperature compensated at least in the range 20°–30°C. Some of these results merit concluding comment.

The persistence of the rhythms in these studies is noteworthy for two reasons: (1) earlier investigators (Gunn, '40; Harker, '56) of cockroach rhythms have reported that the rhythms are lost after a few days in constant dark or light; and (2) the generalization of Pittendrigh and Bruce ('57) that circadian rhythms are, formally self-sustaining oscillations (which, by definition, are non-damped) predicts the persistent rhythms documented here for the roach. In discussing the persistence or loss of rhythms under so-called "constant" laboratory conditions it would be of prime importance to discriminate between, for example, the loss of the overt activity rhythm and the disruption of the underlying endogenous pacemaking system. Although the distinction can not be made at this time it is clearly possible that reports of the loss of rhythms may, in fact, represent only a temporary loss of the *overt* rhythm. Such arhythmicity might be due to the specific experimental conditions adopted to assay the locomotion. Thus it is possible that by tying the cockroach to a kymograph lever, as in Harker's published ('56) methods, one generates a frustrating restraint that promotes a breakdown of the rhythm in a few days. It may also be that the overt rhythm is obscured by frequent but irregular disturbance if the animal has to be fed and watered after short intervals. Whether or not the earlier claims of damping of roach rhythms can be explained in this way it is, nevertheless obvious that

certain advantages are to be gained in all rhythm studies by the long-term provisioning for the experimental animal.

Earlier work on the cockroaches *Blatta* (Gunn, '40) and *Periplaneta* (Harker, '56) indicated a loss of the activity rhythm in a few days in constant light of three and 25 foot-candles respectively. This arhythmicity should not, however, be construed as the direct result of constant light since the rhythms were likewise reported lost in constant darkness in a corresponding interval of time. Thus, these reports of damping in constant light might be explained in the same terms as enumerated above for the non-persistence of rhythms in constant dark. According to Bünning ('58a) the locomotor activity of *Periplaneta* is most clearly rhythmical in dim constant light (less than 25 foot-candles). Unfortunately his results do not indicate how long the rhythm persists in dim light as compared to constant dark. In the three species of roach used in this study an overt activity rhythm persists for at least several weeks in constant light up to 25 foot-candles.

The significance of the circadian period in excluding the hypothesis (Brown, '57) of external control of rhythms needs no further emphasis here.

We can not at this time draw any specific conclusions from the general facts that the period of the free-running, steady-state rhythm of the roach is remarkably stable over relatively long intervals of time, but is nevertheless subject to both spontaneous and induced change. However, it is noteworthy that similar period changes have been recorded in other organisms such as the laboratory mouse (Aschoff, '52); the hamster (Burchard, '56); and *Peromyscus* (Rawson, '56; Pittendrigh and Barth, '56). In these cases (and in cockroaches as well) the spontaneous change from one steady-state period to another is abrupt. The abrupt quality of the period change led Pittendrigh and Bruce ('57) to speculate on a system of high frequency internal physiological rhythms entraining and stabilizing by frequency demultiplication the overt circadian activity rhythm. Direct evidence for such a system awaits an examination of the prediction that the observed changes of period are all whole multiples of a common time interval.

It is clear from the study of 19 individual cockroaches that any given animal has no single free-running period that uniquely characterizes its endogenous rhythm in DD: the period is affected by immediately prior environmental perturbations, and on occasion by some as yet unknown spontaneous phenomenon. There is, on the other hand, equally clear evidence in figure 4 of *differences* between individual roaches in the *range* of periods that they can realize under the influence of prior experience. The significance of differences between the ranges of DD periods realized by individual animals invites speculation and further studies on the possibility that the individual's period range is genotypically fixed.

The temperature compensation of the free-running period of the cockroach rhythm was anticipated on the basis of earlier studies on other poikilothermic organisms. It was promptly found in the cockroach and Q_{10}'s calculated for periods at 20 and 25°C, and 25 and 30°C were 1.06 and 1.03 respectively. Although temperature compensation has been demonstrated in earlier experiments, it is relatively recently that the phenomenon has been explicitly recognized to be: (1) a functionally significant feature of a time measuring system (the rhythm functions as a clock . . . Pittendrigh, '54) and (2) a universal feature of circadian rhythms generally (Pittendrigh and Bruce, '57).

The effective lengthening of the roach's period in constant light can not, at this time, be explained in any concrete terms. There is, however, amongst many organisms studied (Aschoff, '58), a general correlation between the lengthening of the period in LL and nocturnalism; and shortening of the LL period in diurnal forms.

The appearance of the secondary peak of activity in LL and LD regimes suggests, as mentioned previously, a light-sensitive fraction in the activity rhythm. The fact that the phase of the secondary peak could closely coincide with "dawn" in the animal's natural environment, suggests a possible interpretation of the adaptive function of this light sensitivity. Thus the vigorous activity expressed in the secondary

peak might represent a kinesis reaction whereby the roach is stirred to activity by the dawn's light until it reaches an optimally dark refuge where its movements will cease.

SUMMARY

1. Under constant conditions of light and temperature the locomotor activity rhythm in cockroaches has been shown to persist for several months.

2. The rhythmic nature if this activity is characteristically *circadian,* that is, in constant darkness and constant temperature the period of the rhythm is significantly different from 24 hours.

3. The period of the activity rhythm is labile: induced and spontaneous period changes are discussed.

4. The period of the rhythm is temperature compensated in the range 20–30°C.

5. The rhythm persists in constant light with the following modifications: (1) the period is characteristically lengthened; and (2) a secondary peak of activity, about 10 hours out of phase with the primary nocturnal peak, dominates the activity pattern.

ACKNOWLEDGMENTS

The author wishes to acknowledge the support of the Porter Fellowship (for 1958–59) of the American Physiological Society. This work was also supported by a grant from the National Science Foundation and by funds from the Eugene Higgins Trust allocated to Princeton University.

We are also deeply grateful to Dr. C. S. Pittendrigh and Dr. V. G. Bruce for constructive criticism and encouragement offered during the course of these experiments and in the preparation of this paper, and to Dr. W. van B. Roberts and Mr. S. G. Frantz for consultation on the design of the actograph equipment.

LITERATURE CITED

Aschoff, J. 1952 Aktivitätsperiodik von Mäusen im Dauerdunkel. Pfluger's Archiv., *255:* 189–196.

——— 1958 Tierische Periodik unter dem Einfluss von Zeitgebern. Z. Tierpsychol., *15:* 1–30.

Brown, F. A. 1957 Biological chronometry. Am. Nat., *91:* 129–135.

Brown, F. A., and H. M. Webb 1948 Temperature relations of an endogenous daily rhythmicity in the fiddler crab, *Uca.* Physiol. Zool., *21:* 371–381.

Bruce, V. G., and C. S. Pittendrigh 1957 Endogenous rhythms in insects and microorganisms. Am. Nat., *91:* 179–195.

Bünning, E. 1958 Die Physiologische Uhr. Springer-Verlag, Berlin. Gottingen. Heidelberg.

——— 1958a Über den Temperatureinfluss auf die endogene Tagesrhythmik, besonders bei *Periplaneta americana.* Biol. Zbl., *77:* 141–152.

Burchard, J. E. 1956 "Resetting" a biological clock. Ph.D. Thesis, Princeton University.

Gunn, D. L. 1940 The daily rhythm of activity of the cockroach, *Blatta Orientalis.* J. Exp. Biol., *17:* 267–277.

Harker, J. E. 1956 Factors controlling the diurnal rhythm of activity in *Periplaneta americana.* J. Exp. Biol., *33:* 224–234.

——— 1958 Diurnal rhythms in the Animal Kingdom. Biol. Rev., *33:* 1–52.

Johnson, M. S. 1939 Effect of continuous light on periodic spontaneous activity of white-footed mice. J. Exp. Zool., *52:* 315–328.

Pittendrigh, C. S. 1954 On temperature independence in the clock system controlling emergence time in *Drosophila.* Proc. Nat. Acad. Sci., *40:* 1018–1029.

——— 1958 Perspectives in the study of biological clocks. In: Perspectives in Marine Biology. Edited by A. A. Buzzati-Traverso. University of California Press: 239–268.

Pittendrigh, C. S., and R. H. Barth 1956 Unpublished experiments done in this laboratory.

Pittendrigh, C. S., and V. G. Bruce 1957 An oscillator model for biological clocks. In Rhythmic and Synthetic Processes in Growth. Edited by Dorothea Rudnick. Princeton University Press: 75–109.

Rawson, K. S. 1956 Homing behavior and endogenous rhythms. Ph.D. Thesis, Harvard University.

Roberts, S. K. de F. 1959 Circadian activity rhythms in cockroaches. Ph.D. Thesis, Princeton University.

Wahl, O. 1932 Neue Untersuchungen über das Zeitgedächtnis der Bienen. Zeit. vergl. Physiol., *16:* 529–589.

Welsh, J. A. 1938 Diurnal rhythms. Q. Rev. Biol., *13:* 123–129.

NOTICE TO CONTRIBUTORS

THE JOURNAL OF CELLULAR AND COMPARATIVE PHYSIOLOGY, appearing bimonthly, is intended as a medium for the publication of papers which embody the results of original research of a quantitative or analytical nature in general and comparative physiology, including both their physical and chemical aspects. Short preliminary notices are not desired and papers will not be accepted for simultaneous publication or which have been previously published elsewhere. While not specifically excluding any particular branch of physiology, contributors should recognize that excellent journals already exist for publication in the field of experimental and physiological zoology, dealing particularly with genetics, growth, behavior, developmental mechanics, sex determination, and hormonal interrelationships, and also for pure mammalian functional physiology and the physical chemistry of non-living systems. Preference will be given to analyses of fundamental physiological phenomena whether the material is vertebrate or invertebrate, plant or animal. Since the journal is restricted, it is not possible to publish more than a limited number of papers which must be short and concise.

It is recognized that prompt publication is essential, and the aim will be to issue papers within three months of acceptance.

Manuscripts and drawings should be sent to the Managing Editor, DR. ARTHUR K. PARPART, P.O. Box 704, Princeton University, Princeton, New Jersey.

The paper must be accompanied by an author's abstract not to exceed 225 words in length, which will be published in Biological Abstracts. Nothing can be done with the manuscript until the abstract is received.

Manuscripts should be typewritten in double spacing on one side of paper 8½ × 11 inches, and should be packed flat — not rolled or folded. The original, not carbon, copy should be sent. The original drawings, not photographs of drawings, should accompany the manuscript. Authors should indicate on the manuscript the approximate position of text figures.

Manuscripts and drawings should be submitted in complete and finished form with the author's complete address. All drawings should be marked with the author's name. The Wistar Institute reserves the privilege of returning to the author for revision approved manuscript and illustrations which are not in proper finished form for the printer. When the amount of tabular and illustrative material is judged to be excessive, or unusually expensive, authors may be requested to pay the excess cost.

The tables, quotations (extracts of over five lines), and all other subsidiary matter usually set in type smaller than the text, should be typewritten on separate sheets and placed with the text in correct sequence. Footnotes should not be in with the text (reference numbers only), but typewritten continuously on separate sheets, and numbered consecutively. Explanations of figures should be treated in the same manner, and, like footnotes, should be put at the end of the text copy. A condensed title for running page headlines, not to exceed thirty-five letters and spaces, should be given.

Figures should be drawn for reproduction as line or halftone engravings, unless the author is prepared to defray the additional cost of a more expensive form of illustration. All colored plates are printed separately and cost extra. In grouping the drawings it should be borne in mind that, after the reduction has been made, text figures should fit one column width (2⅝ inches) or two column widths (5½ inches). Single plates may be 5 × 7½ inches, or less, and double plates (folded in the middle), 11½ × 7½ inches. Avoid placing figures across the fold, if possible.

Figures should be numbered from 1 up, beginning with the text figures and continuing through the plates. The reduction desired should be clearly indicated on the margin of the drawing.

All drawings intended for photographic reproduction either as line engravings (black-ink pen lines and dots) or halftone plates (wash and brush work) should be made on white or blue-white paper or bristol board — not on cream-white or yellow-tone. Photographs intended for halftone reproduction should be securely mounted with colorless paste — never with glue, which discolors the photograph.

Galley proofs and engraver's proofs of figures are sent to the author. All corrections should be clearly marked thereon.

Reprints may be obtained according to rates shown on a reprint order blank which will be sent with the proof to the author.

JOURNAL OF

CELLULAR AND COMPARATIVE PHYSIOLOGY

VOL. 55 FEBRUARY 1960 No. 1

CONTENTS

PRESS OF
THE WISTAR INSTITUTE
OF ANATOMY AND BIOLOGY
PHILADELPHIA

Printed in the United States of America